FERMILAB-PUB-10-193-E

MAN/HEP/2010/1
June 8, 2010

arXiv:1006.1289v1 [hep-ph] 7 Jun 2010

Central Exclusive Particle Production at High Energy Hadron Colliders

M.G. Albrow[1]
Fermi National Accelerator Laboratory, USA.

T.D. Coughlin[2]
University College London, Gower Street, London, WC1E 6BT, UK.

J.R. Forshaw[3]
The University of Manchester, Oxford Road, Manchester M13 9PL, UK.

Abstract

We review the subject of central exclusive particle production at high energy hadron colliders. In particular we consider reactions of the type $A + B \to A + X + B$, where X is a fully specified system of particles that is well separated in rapidity from the outgoing beam particles. We focus on the case where the colliding particles are strongly interacting and mainly they will be protons (or antiprotons) as at the ISR, S$p\bar{p}$S, Tevatron and LHC. The data are surveyed and placed within the context of theoretical developments.

[1]albrow@fnal.gov; corresponding author
[2]coughlin@hep.ucl.ac.uk
[3]jeff.forshaw@manchester.ac.uk

Contents

1 Introduction **2**

2 The Pomeron **3**

3 QCD Models of Central Production **7**

3.1 Perturbative QCD 7

3.2 Other Models 13

4 CERN Intersecting Storage Rings (ISR) **15**

4.1 Searches for double pomeron exchange 16

4.2 Searches for glueballs 19

5 Fixed Target experiments **23**

6 CERN Proton-antiproton Collider ($Sp\bar{p}S$) **24**

7 Tevatron **25**

7.1 Introduction 25

7.2 Central exclusive production 27

8 The Large Hadron Collider **32**

8.1 Higgs: SM and MSSM 33

8.2 Higgs: NMSSM 39

8.3 Other new physics 42

8.4 Two photon collisions 43

8.5 γp collisions 50

9 Concluding remarks **51**

1 Introduction

Central exclusive particle production (CEP) is defined as the class of reactions $A+B \to A+X+B$, where the colliding particles A and B emerge intact and a produced state, X, is fully measured. We will review the particularly interesting case where the centre-of-mass energy $\sqrt{s}$ is large, such that one can have rapidity regions $\Delta y \gtrsim 3$ completely devoid of particles between X and the outgoing particles A and B (rapidity gaps). With this definition, only high energy colliders are relevant, and we shall focus on hadron colliders. The field of central production in nucleus-nucleus collisions at the Relativistic Heavy Ion Collider (RHIC) and at the Large Hadron Collider (LHC) merits a review in itself and we will not attempt to cover it. The first hadron collider was the CERN Intersecting Storage Rings (ISR), which carried out pp and $p\bar{p}$ collisions (also dd and $\alpha\alpha$). The $Sp\bar{p}S$ collider at CERN followed and, most recently, the Tevatron at Fermilab has examined $p\bar{p}$ collisions. In the near future, the LHC will furnish us with pp (and AA) collisions with much higher energy and luminosity than before. It opens up the exciting new possibility of producing heavy systems X, such as Higgs bosons, weak vector bosons, supersymmetric (SUSY) particles and other "Beyond the Standard Model" (BSM) particles.

Much of the renewed interest in central exclusive production comes from the higher mass reach that will be opened up at the LHC. Added to that are strong constraints that are unique to exclusive processes. In some cases these allow measurements of particle properties that can be obtained no other way. The "strong constraints" are both kinematic and dynamic. In an exclusive process such as $p+p \to p+X+p$, four-momentum conservation means that knowing the incoming proton momenta, and measuring the outgoing proton momenta (in high precision forward spectrometers), the mass M_X is determined [1]. This is expected to be possible with a resolution of $\sigma(M_X) \approx 2$ GeV/c^2 *per event* [2], independent of the decay of X, even if X decays with a large amount of missing energy, e.g. $X \to W^+W^- \to e^+\mu^-\nu\bar{\nu}$. With a precise calibration of the forward spectrometers (using the QED process $p+p \to p+\mu^+\mu^-+p$), the central mass can be found with a resolution improving as $\sigma(M_X)/\sqrt{N}$, and if (in the case of a resonance) the width Γ_X exceeds a few GeV, that too can be measured. In addition, the transverse momenta, p_T, of the scattered protons are typically $p_T \lesssim 1$ GeV/c and so $p_T(X)$ is small. In this case, dynamic constraints, discussed later, allow one to also determine the spin J, parity P and charge-parity C of any exclusively produced particle, such as a Higgs boson.

The possibility to instrument the LHC in order to measure the small angle protons produced in CEP has been explored through the FP420 R&D project (so named because the forward protons would be detected 420 m from the collision region)[1] involving a consortium of ATLAS and CMS physicists and theorists [2]. Suitable sub-detectors have now been proposed: AFP (ATLAS Forward Protons) in ATLAS and HPS (High Precision Spectrometers) in CMS. Precision tracking and timing detectors at 220/240 m and 420 m will measure the momenta of both protons.

In this review our attention will focus on CEP mainly through $I\!P I\!P \to X$ and $\gamma\gamma \to X$, although photoproduction, i.e. $\gamma I\!P \to X$, is briefly mentioned. We use the symbol "$I\!P$" to signify pomeron exchange (see Section 2). We will neglect contributions from odderon exchange and consider data that are not much contaminated by sub-leading Regge exchanges. In classifying the production this way we are making explicit the theoretical property that in both QED and in Regge theory the scattering amplitudes can often be factorized so as to separate the dependence on the beam particles

[1] There are also plans to install detectors at 220/240 m.

from the dependence on the production of the central system. However, it is not always the case that the scattering amplitudes factorize this way. In particular, the QCD production of high-mass, short-distance ($Q^2 \gg \Lambda^2_{QCD}$) systems can be computed in perturbation theory (at least up to soft rescattering corrections) and the amplitudes do not factorize in quite this manner. Generally, they do not factorize wherever the dominance of a single pomeron pole does not hold. Nevertheless, we shall still follow popular nomenclature and refer to the production of a central system via strong dynamics as $I\!P I\!P \to X$, but it is to be understood that this is more of a placeholder than a description of the underlying strong dynamics. It is our aim in the following sections to clarify these matters and to present the theory underpinning central exclusive particle production.

In the next section we introduce the relevant ideas in Regge theory and show how one may describe CEP in terms of pomeron exchange in the t-channel. References [3] and [4] are treatises on diffraction and the pomeron and our treatment here will be brief. In Section 3 we explain how one can use QCD perturbation theory to compute the CEP of high mass systems. While perturbative Quantum Chromodynamics (QCD) is the well established theory of high-Q^2 (short distance) strong interaction processes, diffractive processes almost always involve some low-Q^2 physics, where perturbation theory cannot be used and factorization theorems do not hold. We are thus still far from a complete understanding, and that makes for an interesting field, both for theory and for experiment.

We shall then move on to a survey of the experimental data, covering the published results from hadron colliders up to the end of 2009. We do not attempt to review CEP in e^+e^- or ep machines, and only briefly mention fixed target experiments. We end our review with a forward look to the LHC era.

Some conventions need stating. We will frequently use the term proton to mean p or $\bar{p}$ whenever the distinction is unimportant or obvious. In a reported cross section, such as $2.09 \pm 0.90 \pm 0.19$ pb, the first uncertainty is statistical and the second is systematic. Feynman-x, $x_F = p_z/p_{\rm beam}$, represents the ratio of longitudinal momentum to the beam momentum and $\xi = 1 - x_F$ denotes the fractional momentum loss of a beam particle (typically a p or $\bar{p}$). The rapidity of a particle is defined as $y = \frac{1}{2}\ln\left(\frac{E+p_z}{E-p_z}\right)$, and the pseudorapidity $\eta = -\ln(\tan\frac{\theta}{2})$ with θ the polar angle; $\eta = y$ for massless particles.

2 The Pomeron

A detailed treatment of Regge theory is beyond the scope of this review and we refer instead to Refs. [3, 4, 5, 6, 7]. Here we provide a very basic introduction. Pomeron phenomenology was developed originally to describe the behaviour of total hadronic cross sections and diffractive/elastic scattering at high energies. Most recently, it has been taken to a new level by experiments conducted mainly at the HERA ep collider (see Refs. [8, 9] and references therein) and the Tevatron $p\bar{p}$ collider (see Section 7).

When the CERN ISR came into operation in 1971, the quark model had been formulated but not yet QCD [10]; asymptotic freedom was uncovered in 1973. At that time, strong interaction physics tended to focus on total cross sections, elastic scattering and few-body reactions (e.g. $\pi^- + p \to \pi^0 + n$). General methods, based on the unitarity, analyticity and crossing symmetry of the

scattering matrix provided the foundations, with Regge theory providing the principal tool. With the advent of QCD the emphasis shifted to the investigation of scattering processes at short distances for which the strong coupling is small and perturbative methods can be exploited. However, soft diffraction and elastic scattering processes cannot be described by perturbative QCD, and Regge theory remains an important tool. In Regge theory these process are described as the t-channel exchange of "reggeons" ($I\!R$), which correspond to a sum of mesons (ρ^0, ω^0, etc.) with the same quantum numbers. The contribution of the reggeons to the elastic scattering cross section falls with increasing centre-of-mass energy as $s^{\alpha_{I\!R}(0)-1} \sim 1/\sqrt{s}$, where $\alpha_{I\!R}(t)$ is the reggeon trajectory which is a function of the Mandelstam four-momentum transfer squared, t. By the Optical Theorem, the reggeon contribution to total cross sections likewise falls as the centre-of-mass energy increases. The observed rise of total hadronic cross sections therefore mandated the emergence of a new reggeon, with intercept $\alpha_{I\!P}(0) > 1.0$. To generate a non-falling total cross section, the exchange must have isospin zero and even charge parity, C $= +1$, i.e. it has the quantum numbers of the vacuum. The new reggeon was dubbed the pomeron ($I\!P$) after Pomeranchuk, who had previously studied the behaviour of vacuum exchange in Regge theory.

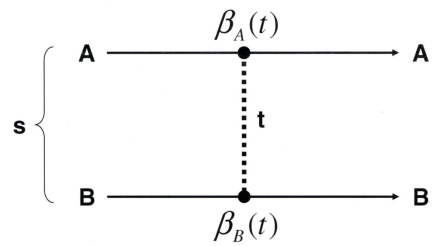

Figure 1: Elastic scattering between two hadrons A and B, at centre-of-mass energy $\sqrt{s}$. The four-momentum transfer squared is t.

At high enough centre-of-mass energy, if one assumes the dominance of a single Regge pole, the elastic scattering of strongly interacting particles may be described by pomeron exchange, see Fig. 1. The elastic scattering amplitude for $AB \to AB$ is thus approximated by

$$\frac{A(s,t)}{s} = \beta_A(t)\beta_B(t)\,\eta(t)\left(\frac{s}{s_0}\right)^{\alpha_{I\!P}(t)-1} \tag{2.1}$$

where

$$\eta(t) = i - \cot\left(\frac{\pi\alpha_{I\!P}(t)}{2}\right) \tag{2.2}$$

is the signature factor, $\alpha_{I\!P}(t)$ is the pomeron trajectory, $\beta_{A,B}(t)$ fixes the coupling of the pomeron to the external particles and s_0 is a constant. The Optical Theorem then relates the total cross section for $AB \to X$, σ_T, to the imaginary part of the forward ($t = 0$) scattering amplitude via

$$\mathrm{Im}A(s,0) = s\,\sigma_T(s) \tag{2.3}$$

and so

$$\sigma_T(s) = \beta_A(0)\beta_B(0)\left(\frac{s}{s_0}\right)^{\alpha_{I\!P}(0)-1} . \tag{2.4}$$

Thus we see that if the pomeron intercept $\alpha_{I\!P}(0) > 1$ the total cross section rises with energy, in accord with the data. Conversely, the contributions of any Regge poles with $\alpha_{I\!R}(0) < 1$ (such as those containing the ρ and π) become negligible at sufficiently high energy.

One might hope that the properties of Regge poles, i.e. their intercepts and couplings, would emerge from calculations based on QCD. To an extent that is what happens. For example, the gluon is known to "reggeize" to a simple Regge pole in perturbative QCD after re-summing to all orders in $\alpha_s \ln(s)$ (see for example Ref. [3] and references therein). However, calculations are generally plagued by the need to focus on processes at short distances, where perturbation theory is valid, and total hadronic cross sections certainly do not fall into that class. It is also far from clear that amplitudes are dominated by a single Regge pole at high energies, although there is some indication that this is so in the case of hadron-hadron elastic scattering at small (but not too small) values of t [11, 12]. In that case, fits to data suggest the existence of a pomeron with intercept

$$\alpha_{I\!P}(t) \approx \alpha_{I\!P}(0) + \alpha'_{I\!P}\, t \approx 1.08 + (0.25\ \mathrm{GeV}^{-2})\, t. \tag{2.5}$$

More recent analyses suggest that a global fit to all soft data from the ISR, S$p\bar{p}$S and Tevatron may require a pomeron with a higher intercept and substantial screening corrections (see for example Refs. [13, 14, 15] and references therein).

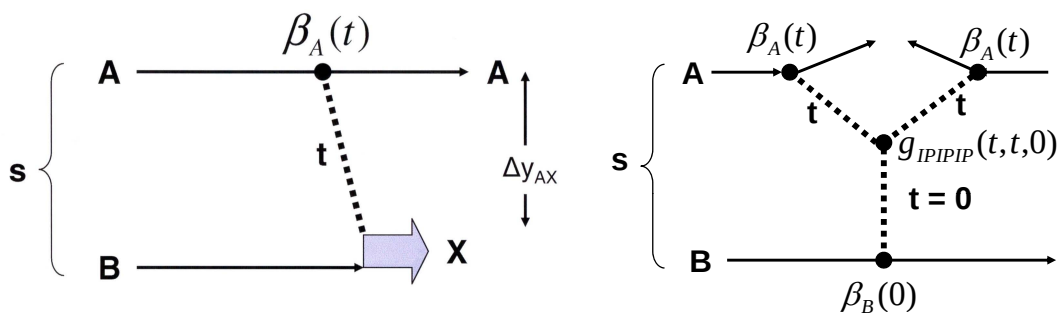

Figure 2: (a) Diffractive excitation of particle B to a state of mass M_X by pomeron exchange. (b) The corresponding cut diagram in the limit of large M_X.

Regge theory is not restricted to the consideration of elastic scattering amplitudes. A reggeon calculus can be developed, and used to tackle processes such as those illustrated in Fig. 2(a) and Fig. 3(a). Again the dotted lines represent pomerons, and pomeron dominance is presumed to pertain if the relevant sub-energies are large enough, i.e. $\Delta y_{AX} \gtrsim 3$ in Fig. 2(a) and $\Delta y_{AX}, \Delta y_{BX} \gtrsim 3$ in Fig. 3(a), where Δy_{AX} is the rapidity interval between A and X (and similarly for Δy_{BX}). For the single diffractive dissociation process represented in Fig. 2(a) one may write [16, 17]

$$M_X^2 \frac{\mathrm{d}\sigma}{\mathrm{d}t\, \mathrm{d}M_X^2} = \beta_A(t)^2\, |\eta(t)|^2 \left(\frac{s}{M_X^2}\right)^{2\alpha_{I\!P}(t)-2} \sigma_{BI\!P}(M_X^2, t) \tag{2.6}$$

and we are invited to think of $\sigma_{BI\!P}(M_X^2, t)$ as the total cross section for $BI\!P$ scattering at energy M_X. It is to be noted that the normalization of $\sigma_{BI\!P}(M_X^2, t)$ is a matter of convention. Provided M_X is sufficiently large, we expect that it is itself driven by pomeron exchange and $\sigma_{BI\!P}(M_X^2, t) \propto$

$(M_X^2)^{\alpha_{I\!P}(0)-1}$. This is shown in Fig. 2(b) which illustrates the M_X^2 discontinuity in the relevant three-body amplitude. We should stress that the pomeron is not a real particle and pomeron-induced cross sections are not directly measurable; however they are useful constructs. Going one step further, we can rewrite Eq. (2.6) as

$$\frac{\mathrm{d}\sigma}{\mathrm{d}t\,\mathrm{d}\xi} = f_{I\!P/A}(\xi,t)\,\sigma_{BI\!P}(M_X^2,t) \tag{2.7}$$

where we define a pomeron "flux"

$$f_{I\!P/A}(\xi,t) = \beta_A(t)^2\,|\eta(t)|^2\left(\frac{1}{\xi}\right)^{2\alpha_{I\!P}(t)-1} \tag{2.8}$$

and ξ is the fractional energy lost by the beam particle A, i.e. $M_X^2 = \xi s$. This approach describes very well the HERA data on single diffraction dissociation, albeit with a pomeron trajectory that differs from that in Eq. (2.5). In particular the t-dependence is consistent with a flat trajectory [9].

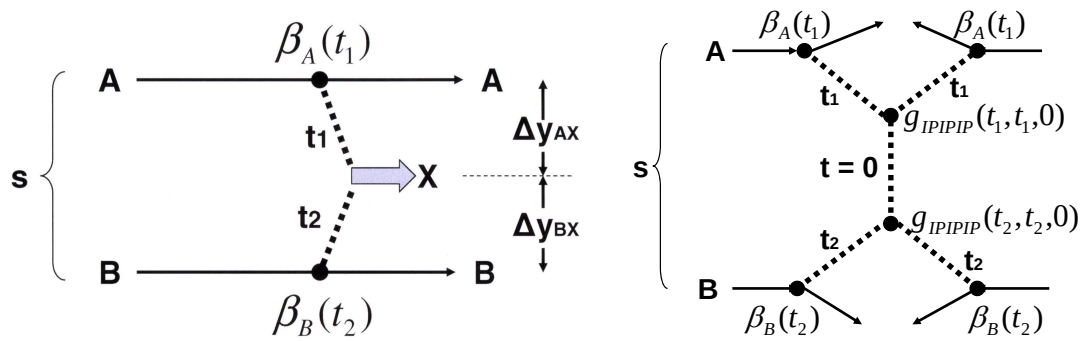

Figure 3: (a) Diagram for double pomeron exchange. (b) The corresponding cut diagram in the limit of large M_X.

The study of double pomeron exchange ($DI\!PE$), illustrated in Fig. 3, has a long history [6, 7, 18, 19, 20, 21, 22, 23, 24, 25, 26, 27]. In the Regge framework, such exchanges are responsible for the CEP process, and we may write the cross section for $A+B \to A+X+B$ in terms of the total cross section for two pomerons to fuse, producing the central system X, $\sigma_{I\!P I\!P}$:

$$\frac{\mathrm{d}\sigma}{\mathrm{d}t_1\mathrm{d}t_2\,\mathrm{d}\xi_1\,\mathrm{d}\xi_2} = f_{I\!P/A}(\xi_1,t_1)f_{I\!P/B}(\xi_2,t_2)\,\sigma_{I\!P I\!P}(M_X^2,t_1,t_2)\ . \tag{2.9}$$

Again, the ξ_i are the fractional energy losses, and kinematics fixes $M_X^2 = \xi_1\xi_2 s$. We shall return to this formula for $DI\!PE$ in Sections 4–6.

Eq. (2.7) and Eq. (2.9) clearly exhibit Regge factorization and the similarity to the two-photon production case is striking - the pomeron flux playing the role of the Weiszäcker-Williams flux in the case of photons (e.g. see Ref. [28]). Unfortunately Regge theory does not tell us how to compute the cross section $\sigma_{I\!P I\!P}(M_X,t_1,t_2)$, although it does predict the behaviour for large M_X. So, although we have a model for the rapidity dependence of the central system, we are not able to predict the overall production rate without further model dependence. Furthermore, we should

bear in mind that there is no *a priori* reason why more sophisticated pomeron diagrams should not be relevant.

It is time now to turn our attention to a rather different approach to CEP, namely an approach based firmly within perturbative QCD. As we shall see, it does not give rise to Regge factorization and leads to essentially different predictions for the CEP of systems for which $M_X \gg \Lambda_{\rm QCD}$. Furthermore, it is an approach that has recently had some striking success in predicting the CEP rate of χ_{c0} and dijets at the Tevatron.

3 QCD Models of Central Production

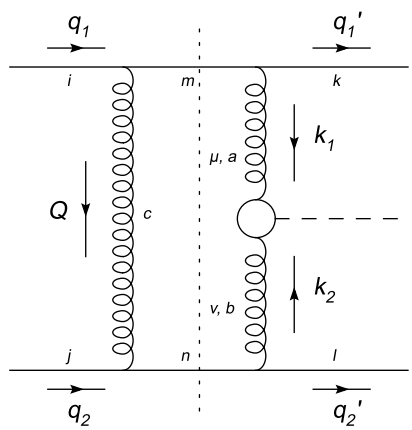

Figure 4: The relevant lowest order Feynman diagram for $qq \to q + H + q$.

3.1 Perturbative QCD

The perturbative approach to CEP was originally developed in Refs. [29, 30, 31, 32, 33]. We shall refer to the approach presented in those papers as the Durham model, and it is our goal in this subsection to review the calculation and comment upon its uncertainties. Our present focus is on the central exclusive production of a Higgs, i.e. $pp \to p+H+p$, although the theory is not essentially different for other high mass systems provided they contain a suitable hard scale. In particular, we shall use the same framework when it comes to comparing to Tevatron data on CEP of dijets, diphotons and χ_c mesons. The calculation starts by considering the process $qq \to q + H + q$ at lowest order in perturbation theory, as shown in Fig. 4. The Higgs is produced via a top quark loop and a minimum of two gluons needs to be exchanged in order that no colour be transferred between the incoming and outgoing quarks. The outgoing quark momenta may be parametrised in terms of the momentum fraction each transfers to the Higgs, x_i, and their transverse momenta, q'_{iT}:

$$q_1'^{\mu} = (1-x_1)q_1^{\mu} + \frac{\mathbf{q}_{1T}'^{\mu}}{(1-x_1)s} q_2^{\mu} + q_{1T}'^{\mu} \tag{3.10}$$

$$q_2'^{\mu} = (1-x_2)q_2^{\mu} + \frac{\mathbf{q}_{2T}'^{\mu}}{(1-x_2)s} q_1^{\mu} + q_{2T}'^{\mu} \tag{3.11}$$

with s denoting the centre-of-mass energy squared. In the high energy limit the colour-singlet amplitude is dominated by its imaginary part, as expected from arguments based on Regge theory

(see for example Ref. [3]). It may therefore be computed by considering only the cut diagram of Fig. 4. Thus, for small x_i and with the colour-singlet exchange contribution projected out, the amplitude is given by

$$\Im\mathrm{m}A \approx \frac{C_F^2}{N^2-1}\int \frac{\mathrm{d}^4Q}{(2\pi)^2}\delta_{(+)}((q_1-Q)^2)\delta_{(+)}((q_2+Q)^2) \times \frac{2gq_1^\alpha 2gq_{2\alpha}}{Q^2}\frac{2gq_1^\mu}{k_1^2}\frac{2gq_2^\nu}{k_2^2}V_{\mu\nu} \ . \tag{3.12}$$

In the Standard Model, the Higgs production vertex is

$$V_{\mu\nu} = \left(g_{\mu\nu} - \frac{k_{2\mu}k_{1\nu}}{k_1\cdot k_2}\right)V \ , \tag{3.13}$$

where $V = m_H^2\alpha_s/(4\pi v)F(m_H^2/m_t^2)$, v is the Higgs vacuum expectation value and $F \approx 2/3$ provided the Higgs is not too heavy [34, 35, 36]. The Durham group also include a next-to-leading order K-factor correction to this vertex [31], though this is extracted from calculations of inclusive Higgs production [37, 38] and not from an explicit calculation of the next-to-leading order corrections in CEP.

To proceed further, we parametrise the loop momentum in terms of Sudakov variables, $Q = \alpha q_1 + \beta q_2 + Q_T$; the δ-functions which fix the cut quark lines on-shell then set $\alpha \approx -\beta \approx \mathbf{Q}_T^2/s \ll 1$ and $Q^2 \approx Q_T^2 = -\mathbf{Q}_T^2$. As always, we neglect terms that are suppressed in s, such as the product $\alpha\beta$.

We can compute the contraction $q_1^\mu V_{\mu\nu}^{ab} q_2^\nu$ either directly or by utilising gauge invariance, which requires that $k_1^\mu V_{\mu\nu}^{ab} = k_2^\nu V_{\mu\nu}^{ab} = 0$. Writing[2] $k_i = x_i q_i + k_{iT}$ yields

$$q_1^\mu V_{\mu\nu}^{ab} q_2^\nu \approx \frac{k_{1T}^\mu}{x_1}\frac{k_{2T}^\nu}{x_2}V_{\mu\nu}^{ab} \approx \frac{s}{m_H^2}k_{1T}^\mu k_{2T}^\nu V_{\mu\nu}^{ab} \tag{3.14}$$

since $2k_1\cdot k_2 \approx x_1x_2s \approx m_H^2$. Note that it is as if the gluons which fuse to produce the Higgs are transversely polarized, i.e. we have for their polarisation vectors: $\epsilon_i \sim k_{iT}$. Moreover, in the limiting case that the outgoing quarks carry no transverse momentum $Q_T = -k_{1T} = k_{2T}$ and so $\epsilon_1 = -\epsilon_2$. This is an important result; it generalizes to the statement that the centrally produced system must have a vanishing z-component of angular momentum in the limit that the protons scatter through zero angle (i.e. $q_{iT}'^2 \ll Q_T^2$) [29]. Since we are interested in very small angle scattering this selection rule is effective. One immediate consequence is that the Higgs decay to b-quarks may now be detectable. This is because, for massless quarks, the lowest order $q\bar{q}$ background vanishes identically (it does not vanish at next-to-leading order). The leading order exclusive $b\bar{b}$ dijet background is therefore suppressed by a factor $\sim m_b^2/m_H^2$. The dominant background thus becomes CEP production of gg-dijets, which can be reduced by b-tagging both jets.

Returning to the task in hand, the differential cross section is given by

$$\frac{\partial\sigma}{\partial^2\mathbf{q}_{1T}'\partial^2\mathbf{q}_{2T}'\partial y} \approx \left(\frac{N_c^2-1}{N_c^2}\right)^2\frac{\alpha_s^6}{(2\pi)^5}\frac{G_F}{\sqrt{2}}\times\left[\int\frac{\mathrm{d}^2\mathbf{Q}_T}{2\pi}\frac{\mathbf{k}_{1T}\cdot\mathbf{k}_{2T}}{\mathbf{Q}_T^2\mathbf{k}_{1T}^2\mathbf{k}_{2T}^2}\frac{2}{3}\right]^2 \ , \tag{3.15}$$

[2] We can do this because $x_i \sim m_H/\sqrt{s}$ whilst the other Sudakov components are $\sim Q_T^2/s$.

with y the rapidity of the Higgs. We are mainly interested in the forward scattering limit whence

$$\frac{\mathbf{k}_{1T}\cdot\mathbf{k}_{2T}}{\mathbf{Q}_T^2\mathbf{k}_{1T}^2\mathbf{k}_{2T}^2}\approx-\frac{1}{\mathbf{Q}_T^4}. \tag{3.16}$$

As it stands, the integral over $\mathbf{Q}_T$ diverges. However, this is because the lowest perturbative order is insufficient for this process. Not only must we include a convolution with non-perturbative parton distribution functions (PDFs) but, due to the exclusive nature of the process, the perturbative contribution to the amplitude is enhanced at each order in α_s by large logarithms in the ratio $m_H^2/\mathbf{Q}_T^2$. These terms are due to virtual corrections involving soft gluons or partons that travel collinear to the incoming hadrons. They must be summed to all orders in order to give a reliable prediction.

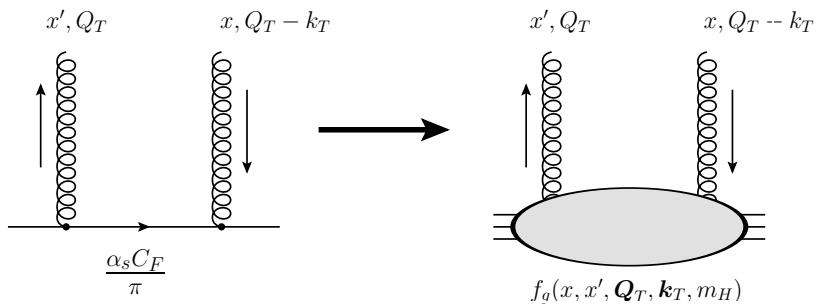

Figure 5: The recipe for replacing the quark line (left) by a proton line (right).

The Durham prescription to account for these effects is shown in Fig. 5. They replace $\alpha_s C_F/\pi$, at the quark level, with a skewed, unintegrated, gluon PDF, $f_g(x, x', \mathbf{Q}_T, \mathbf{k}_T, m_H)$. The amplitude is dominated by the region $x \gg x'$, $\mathbf{Q}_T^2 \gg \mathbf{k}_T^2$ and in this limit one may relate the f_g distribution to the standard, integrated, gluon distribution, $g(x, \mathbf{Q}_T^2)$ [31, 39]:

$$f_g(x, x', \mathbf{Q}_T, \mathbf{k}_T, m_H) \approx e^{-b\mathbf{k}_T^2/2} R_g \frac{\partial}{\partial \ln \mathbf{Q}_T^2}\left(\sqrt{T(\mathbf{Q}_T, m_H)}\, x g(x, \mathbf{Q}_T^2)\right). \tag{3.17}$$

The $\mathbf{k}_T$ dependence of the scattered proton is assumed to follow a Gaussian distribution, with slope parameter, $b \approx 4$ GeV^{-2}, fixed by a fit to soft hadronic data [40] and cross-checked against the $\mathbf{k}_T$-dependence of diffractive J/ψ production at HERA [41]. The factor R_g is given by

$$R_g = \frac{H_g\left(\frac{x}{2}, \frac{x}{2}; \mathbf{Q}_T^2\right)}{x g(x, \mathbf{Q}_T^2)} \tag{3.18}$$

and accounts for the skewed effect ($x \neq x'$). Here H_g is the skewed gluon distribution (see for example Ref. [42]). In [43] R_g was shown to be given approximately by

$$R_g \approx \frac{2^{2\lambda+3}}{\sqrt{\pi}} \frac{\Gamma(\lambda + 5/2)}{\Gamma(\lambda + 4)} \tag{3.19}$$

if one assumes a simple power-law behaviour for the gluon density, $x g(x, \mathbf{Q}_T^2) \sim x^{-\lambda}$. For the production of a 120 GeV/c^2 Higgs at the LHC, $R_g \approx 1.2$ [30]; the off-diagonality therefore provides an enhancement of $(1.2)^4 \approx 2$ to the cross section. Clearly the current lack of knowledge of the off-diagonal gluon is one source of uncertainty in the calculation.

Equation (3.17) also includes a Sudakov suppression factor, $T(\mathbf{Q}_T, m_H)$. This is present because real emission from the process is forbidden[3]. It is the Sudakov factor that collects terms in the perturbation series enhanced by logarithms in $m_H^2/\mathbf{Q}_T^2$. Taking into account the leading and next-to-leading logarithms, i.e. all terms of order $\alpha_s^n \ln^m(m_H^2/\mathbf{Q}_T^2)$ with $m = 2n, 2n-1$, the Sudakov factor has the form [31, 44, 45]

$$T(\mathbf{Q}_T, m_H) = \exp\left(-\int_{\mathbf{Q}_T^2}^{m_H^2/4} \frac{\mathrm{d}\mathbf{q}_T^2}{\mathbf{q}_T^2} \frac{\alpha_s(\mathbf{q}_T^2)}{2\pi} \int_0^{1-|\mathbf{q}_T|/m_H} \mathrm{d}z \left[zP_{gg}(z) + n_f P_{qg}(z)\right]\right) \tag{3.20}$$

where P_{ij} are the usual DGLAP splitting functions [46, 47, 48]. It is worth noting that, in order for this expression to collect the next-to-leading logarithms, the lower limit on the $\mathbf{q}_T^2$-integral and the upper limit on the z-integral must be specified precisely. The upper $\mathbf{q}_T^2$ limit in contrast, may be multiplied by any $\mathcal{O}(1)$ number without changing the leading or next-to-leading logarithms. This is because it corresponds to hard, non-collinear, emission and as such is not enhanced by a logarithm. The lower limit on the $\mathbf{q}_T^2$-integral can be understood as follows. For hard collinear emissions, $1 - z \sim \mathcal{O}(1)$, the region $\mathbf{q}_T^2 < \mathbf{Q}_T^2$ is already included in the PDFs (see the discussion below). On the other hand, for the soft region, $1 - z \sim \mathcal{O}(|\mathbf{q}_T|/m_H)$ (relevant for the $1/(1-z)$ piece of P_{gg}), emissions with $\mathbf{q}_T^2 < \mathbf{Q}_T^2$ cannot resolve the exchanged colour-singlet system (the size of which is of order $1/|\mathbf{Q}_T|$) and so do not contribute.

The form of Eq. (3.20) is somewhat different from that appearing in much of the literature. In particular, in Ref. [33] the upper limit on the z-integral was determined to be $|\mathbf{q}_T|/(|\mathbf{q}_T|+0.62m_H)$. It was shown recently that this determination is incorrect and Eq. (3.20) is in fact the correct form of the Sudakov factor [45]. At the present time, the extent to which this modification alters previous predictions has not been fully assessed. However, it has been estimated to give approximately a factor two reduction in the cross section for Higgs masses in the range 100–500 GeV/c^2, with the suppression increasing(decreasing) for larger(smaller) Higgs masses [45]. As we shall see, this uncertainty still lies within the range of the other uncertainties in the calculation.

The Sudakov factor solves the $Q_T \to 0$ divergence problem we encountered in the lowest order calculation; the cross section, integrated over final state hadron momenta, is now given by

$$\frac{\partial\sigma}{\partial y} \approx \frac{1}{256\pi b^2} \frac{\alpha_s G_F \sqrt{2}}{9} \left(\int \frac{\mathrm{d}^2\mathbf{Q}_T}{\mathbf{Q}_T^4} \frac{\partial}{\partial \ln \mathbf{Q}_T^2} \left(\sqrt{T} x_1 g(x_1, \mathbf{Q}_T^2)\right) \frac{\partial}{\partial \ln \mathbf{Q}_T^2} \left(\sqrt{T} x_2 g(x_2, \mathbf{Q}_T^2)\right)\right)^2 \tag{3.21}$$

and since the exponential Sudakov factor vanishes faster than any power of Q_T as $Q_T \to 0$, this integral is finite. Furthermore, for a 120 GeV/c^2 Higgs, the typical $Q_T \sim 2$ GeV/c [49], justifying, *a posteriori*, the use of perturbation theory. Note that the parton momentum fractions are, to a very good approximation, equal to the fractional momentum losses of the incident protons, i.e. $x_i \approx \xi_i$ and $y_X = \frac{1}{2}\ln(\xi_1/\xi_2)$.

Returning to Eq. (3.17), the derivative structure can be understood as follows (see Ref. [45] for more details). Transverse momentum ordered ladder diagrams, as shown schematically in Fig. 6, are enhanced[4] by logarithms of $\mathbf{Q}_T^2$. Summing up these contributions evolves the parton distributions

[3]Note that, for a colour-singlet central system, a single real emission is forbidden regardless of experimental cuts, since it violates colour conservation.

[4]In a physical gauge the large logarithmic corrections are organised into ladders on a diagram-by-diagram basis. In contrast, the ladder structure only emerges in a covariant gauge after a sum over diagrams and application of the Ward identity (see for example Ref. [50]).

associated with the upper and lower hadrons to the scale $\mathbf{Q}_T^2$. The central hard process however, is sensitive to the transverse momenta of the final rung in each ladder. If the final rung has an energy much larger than its transverse momentum, $E \gg |\mathbf{Q}_T|$, then it is included in the PDF and so we require the gluon PDF unintegrated over transverse momentum, $\partial g(x, \mathbf{Q}_T^2)/\partial \mathbf{Q}_T^2$. If, on the other hand, the final rung is soft, $E \sim |\mathbf{Q}_T|$, then it may not be included in the PDF. This contribution is accounted for by the derivative of the Sudakov factor. Shown also in Fig. 6 (by the blob labelled T) are the corrections making up the Sudakov factor. These are virtual corrections to the $gg \to H$ sub-process with larger transverse momenta than the final ladder rungs.

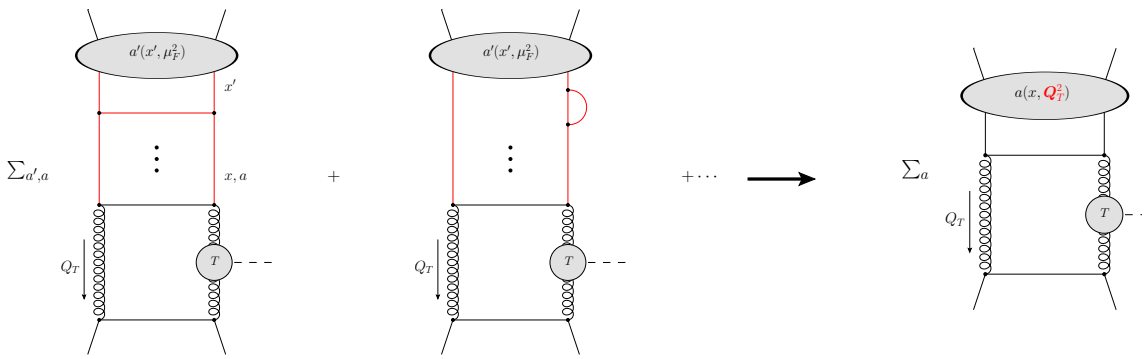

Figure 6: Schematic diagram of the transverse momentum ordered ladder corrections which evolve the PDFs to the scale $\mathbf{Q}_T^2$. Solid lines denote either quarks or gluons.

So far we have only discussed the Higgs production case, however the general features of the calculation are expected to remain the same for other central systems. The differential cross section for the production of a central system X, of invariant mass $\sqrt{\hat{s}}$, may therefore be written as

$$\frac{\partial \sigma}{\partial \hat{s} \partial y \partial \mathbf{q}_{1T}'^2 \partial \mathbf{q}_{2T}'^2} = \frac{\partial \mathcal{L}}{\partial \hat{s} \partial y \partial \mathbf{q}_{1T}'^2 \partial \mathbf{q}_{2T}'^2} \mathrm{d}\hat{\sigma}(gg \to X) \,. \tag{3.22}$$

The partonic cross section, $\hat{\sigma}$, is related to the matrix element for two on-shell gluons to produce the central system as

$$\mathrm{d}\hat{\sigma}(gg \to X) = \frac{1}{2\hat{s}} \left| \bar{\mathcal{M}}(gg \to X) \right|^2 \mathrm{dPS}_X \tag{3.23}$$

where dPS_X is the phase-space of the final-state, X and

$$\bar{\mathcal{M}}(gg \to X) = \frac{1}{2} \frac{1}{N^2 - 1} \sum_{a_1 a_2} \sum_{\lambda_1 \lambda_2} \delta_{a_1 a_2} \delta_{\lambda_1 \lambda_2} \mathcal{M}_{\lambda_1 \lambda_2}^{a_1 a_2}(gg \to X) \tag{3.24}$$

with $\mathcal{M}_{\lambda_1 \lambda_2}^{a_1 a_2}$ the amplitude for two on-shell gluons, with colours a_i and helicities λ_i, to fuse to produce X. Finally, the effective luminosity is given by

$$\frac{\partial \mathcal{L}}{\partial \hat{s} \partial y \partial \mathbf{q}_{1T}'^2 \partial \mathbf{q}_{2T}'^2} = \frac{1}{\hat{s}} \left(\frac{\pi}{N^2 - 1} \int \frac{\mathrm{d}\mathbf{Q}_T^2}{\mathbf{Q}_T^4} f_g(x_1, x_1', \mathbf{Q}_T, \mathbf{q}_{1T}', \sqrt{\hat{s}}) f_g(x_2, x_2', \mathbf{Q}_T, \mathbf{q}_{2T}', \sqrt{\hat{s}}) \right)^2 . \tag{3.25}$$

Returning to Higgs production, before we can compute the cross section we need to introduce the idea of rapidity gap survival. The Sudakov factor has allowed us to ensure that the exclusive

nature of the final state is not spoilt by perturbative emission off the hard process. What about non-perturbative particle production? The protons can in principle interact independently of the perturbative process discussed above, and this interaction will lead to the production of additional particles. We need to account for the probability that such emission does not occur. Provided the hard process leading to the production of the Higgs occurs on a short enough timescale, we may suppose that the physics which generates extra particle production (including additional parton-parton interactions) factorizes, and that its effect can be accounted for by an overall factor multiplying the cross section we just calculated. This is the "gap survival factor", S^2, introduced in Ref. [51] (see also [52]). It is defined by

$$\mathrm{d}\sigma(p + H + p|\text{no soft emission}) = \mathrm{d}\sigma(p + H + p) \times S^2 \ , \tag{3.26}$$

where $\mathrm{d}\sigma(p + H + p)$ is the differential cross section computed above. The task is to estimate S^2. Clearly this is not straightforward since we cannot utilize QCD perturbation theory. However data on a variety of processes observed at HERA, the Tevatron and the LHC can help improve our understanding of rapidity gap survival. We expect that $S^2 \sim 3\%$ for CEP at the LHC (see for example [53] for an overview). Early measurements at the LHC of rapidity gap processes will provide valuable information on S^2. Note that the gap survival probability has some process dependence: it will be higher for large impact parameter, r, interactions. Thus we expect that $S^2(\gamma\gamma) > S^2(\gamma I\!P) > S^2(I\!P I\!P)$.

The issue of gap survival is frustrating to theorists. The spacetime structure of the collision suggests that it may approximately factorize. Possible non-factorizing contributions have been examined in Ref. [54], although their importance has been questioned in Refs. [55, 56, 57]. Assuming it to factorize, we may use data to constrain it and accurate theoretical predictions are possible. Here we shall present a simple model of gap survival which should provide a good starting point for understanding the more sophisticated treatments in Refs. [14, 55, 57, 58, 59, 60].

Dynamically, one expects that the likelihood of extra particle production will be greater if the incoming protons collide at small r. The simplest model which is capable of capturing this feature is one which additionally assumes that there is a single soft particle production mechanism, let us call it a "rescattering event", and that rescattering events are independent of each other for a collision between two protons at transverse separation r. In such a model we can use Poisson statistics to model the distribution in the number of rescattering events per proton-proton interaction:

$$P_n(r) = \frac{\chi(r)^n}{n!} \exp(-\chi(r)) \ . \tag{3.27}$$

This is the probability of having n rescattering events where $\chi(r)$ is the mean number of such events for proton-proton collisions at transverse separation r. Clearly the important dynamics resides in $\chi(r)$; we expect it to fall monotonically as r increases and to be much smaller than unity for r much greater than the QCD radius of the proton. Let us for the moment assume we know $\chi(r)$, then we can determine S^2 via

$$S^2 = \frac{\int \mathrm{d}r \ \mathrm{d}\sigma(r) \ \exp(-\chi(r))}{\int \mathrm{d}r \ \mathrm{d}\sigma(r)} \tag{3.28}$$

where $\mathrm{d}\sigma(r)$ is the cross section for the hard process that produces the Higgs expressed in terms of the transverse separation of the protons. Everything except the r dependence of $\mathrm{d}\sigma$ cancels when computing S^2 and so we need focus only on the dependence of the hard process on the transverse

momenta of the scattered protons ($\mathbf{q}'_{iT}$), these being Fourier conjugate to the transverse position of the protons, i.e.

$$\begin{aligned} \mathrm{d}\sigma(r) &\propto [(\int \mathrm{d}^2\mathbf{q}'_{1T}\ e^{i\mathbf{q}'_{1T}\cdot\mathbf{r}/2}\ \exp(-b\mathbf{q}'^2_{1T}/2)) \times (\int \mathrm{d}^2\mathbf{q}'_{2T}\ e^{-i\mathbf{q}'_{2T}\cdot\mathbf{r}/2}\ \exp(-b\mathbf{q}'^2_{2T}/2))]^2 \\ &\propto \exp\left(-\frac{r^2}{2b}\right) . \end{aligned} \tag{3.29}$$

Notice that b here is the same as that which enters into the denominator of the expression for the total rate (Eq. (3.21)). There is thus a reduced sensitivity to b when one includes the soft survival factor, due to the fact that as b decreases so does S^2 (since the collisions are necessarily more central). Thus what matters is the ratio S^2/b^2.

It remains for us to determine the mean multiplicity $\chi(r)$. If there really is only one type of rescattering event[5] independent of the hard scattering, then the inelastic scattering cross section can be written

$$\sigma_{\text{inelastic}} = \int \mathrm{d}^2\mathbf{r}(1-\exp(-\chi(r))), \tag{3.30}$$

from which it follows that the elastic and total cross sections are

$$\sigma_{\text{elastic}} = \int \mathrm{d}^2\mathbf{r}(1-\exp(-\chi(r)/2))^2, \tag{3.31}$$

$$\sigma_{\text{total}} = 2\int \mathrm{d}^2\mathbf{r}(1-\exp(-\chi(r)/2)). \tag{3.32}$$

There is an abundance of data which we can use to test this model and we can proceed to perform a parametric fit to $\chi(r)$. This is essentially what is done in the literature, sometimes going beyond a single channel approach. Suffice to say that this approach works rather well. Moreover, it also underpins the models of the underlying event currently implemented in the PYTHIA [61, 62] and HERWIG [63, 64] Monte Carlo event generators which have so far been quite successful in describing many of the features of the underlying event, see Refs. [65, 66, 67, 68, 69, 70, 71]. Typically, models of gap survival predict S^2 to be a few percent at the LHC. Although data support the existing models of gap survival there is considerable room for improvement in testing them further, thereby gaining greater control of what is perhaps the major theoretical uncertainty in the computation of exclusive Higgs production. Early diffractive studies at the LHC should give valuable information on S^2 (see for example [72]) and comparisons between different CEP channels at both the Tevatron and LHC will further constrain the theory (see Ref. [73]).

3.2 Other Models

Bialas and Landshoff (BL) developed [74] a model inspired by a blend of QCD perturbation theory and Regge phenomenology to predict the rate of central Higgs production in $pp \to p + H + X + p$, i.e. central *inclusive* Higgs production. Although their calculation looks ostensibly as if it is valid for exclusive production, BL were careful to emphasise that "additional...interactions...will generate extra particles...Thus our calculation really is an inclusive one", but with both protons having

[5] Clearly this is not actually the case, but such a "single channel eikonal" model has the benefit of being simple.

$x_F > 0.95$. Inspired by this calculation, the Saclay group [75] attempted to compute the rate for $pp \to p + H + p$ under the assumption that the exclusive rate can be obtained, modulo an overall gap survival factor, from the calculation in Ref. [74]. We note in passing that the first attempt to compute the central inclusive Higgs cross section, for proton-proton collisions, appeared in [76]. This was followed by a similar analysis for nucleus-nucleus scattering in [77], where the first effort to estimate the exclusive Higgs cross section was made. Other early studies of central inclusive and exclusive Higgs production can be found in Refs. [78] and [79] respectively.

We can understand the BL calculation starting from Eq. (3.15). BL account for the coupling to the proton in a very simple manner: They multiply the quark level amplitude by a factor of 9 (which corresponds to assuming that there are three quarks in each proton able to scatter off each other). Exactly like the Durham group they employ a form factor, $\exp(-bq_{iT}'^2)$, for each proton (at the cross section level), with $b = 4$ GeV^{-2}. Since BL are not interested in suppressing radiation, they do have a potential infrared problem since there is no Sudakov factor. They dealt with this by following the earlier efforts of Landshoff and Nachtmann (LN) in replacing the perturbative gluon propagators with non-perturbative ones [80, 81]:

$$\frac{g^2}{k^2} \to A \exp(-k^2/\mu^2). \tag{3.33}$$

Rather arbitrarily, $g^2 = 4\pi$ was assumed, except for the coupling of the gluons to the top quark loop, where $\alpha_s = 0.1$ was used.

Following LN, μ and A are determined by assuming that the $p\bar{p}$ elastic scattering cross section at high energy can be approximated by the exchange of two of these non-perturbative gluons between the 3×3 constituent quarks. The imaginary part of this amplitude determines the total cross section for which there are data to which they can fit. To carry out this procedure successfully, one needs to recognize that a two-gluon exchange model is never going to yield the gentle rise with increasing centre-of-mass energy characteristic of the total cross section. BL therefore also include an additional "reggeization" factor of $s^{\alpha_{I\!P}(t)-1}$ in the elastic scattering amplitude, where the pomeron trajectory is given by Eq. (2.5). In this way the two-gluon system models pomeron exchange. They found that $\mu \approx 1$ GeV and $A \approx 30$ GeV^{-2} gave a good fit to the data. Similarly, the amplitude for central Higgs production picks up two reggeization factors.

The inclusive production of a Higgs in association with two final state protons is clearly much more infrared sensitive than the exclusive case where the Sudakov factor saves the day. Nevertheless, the Saclay model does not include the Sudakov suppression factor. Instead it relies on the behaviour of the non-perturbative gluon propagators to render the Q_T integral finite. As a result, the typical Q_T is much smaller than in the Durham case.

Putting everything together, the Saclay model of the cross section for $pp \to p + H + p$ gives

$$\begin{aligned} \frac{\partial\sigma}{\partial^2\mathbf{q}_{1T}'\partial^2\mathbf{q}_{2T}'\partial y} \approx\ & S^2 \left(\frac{N_c^2-1}{N_c^2}\right)^2 \frac{\alpha_s^2}{(2\pi)^5} \left(\frac{g^2}{4\pi}\right)^4 \frac{G_F}{\sqrt{2}} e^{-bq_{1T}'^2} e^{-bq_{2T}'^2} \\ & \times \xi_1^{2-2\alpha_{I\!P}(q_{1T}'^2)} \xi_2^{2-2\alpha_{I\!P}(q_{2T}'^2)} \left[9 \int \frac{\mathrm{d}^2\mathbf{Q}_T}{2\pi} \mathbf{Q}_T^2 \left(\frac{A}{g^2}\right)^3 \exp(-3\mathbf{Q}_T^2/\mu^2) \frac{2}{3}\right]^2 . \end{aligned} \tag{3.34}$$

The only difference between this and the original BL result is the factor of S^2. Integrating over the

final state transverse momenta and simplifying a little gives

$$\frac{\partial\sigma}{\partial y} \approx S^2 \frac{\pi}{b+2\alpha'\ln(1/\xi_1)} \frac{\pi}{b+2\alpha'\ln(1/\xi_2)} \times \left(\frac{N_c^2-1}{N_c^2}\right)^2 \frac{G_F}{\sqrt{2}} \frac{\alpha_s^2}{(2\pi)^5} \frac{1}{(4\pi)^4} \left(\frac{s}{m_H^2}\right)^{2\alpha_{I\!P}(0)-2} \frac{1}{g^4} \left[\frac{A^3\mu^4}{3}\right]^2 . \tag{3.35}$$

A very similar formula was also presented by Bzdak [82], with the important difference that the Sudakov factor was reinstated, i.e. the integral over $\mathbf{Q}_T$ in Eq. (3.34) is replaced as follows

$$\int \mathrm{d}^2\mathbf{Q}_T\ \mathbf{Q}_T^2\ \exp(-3\mathbf{Q}_T^2/\mu^2) \to \int \mathrm{d}^2\mathbf{Q}_T\ \mathbf{Q}_T^2\ \exp(-3\mathbf{Q}_T^2/\mu^2)\ T(\mathbf{Q}_T, m_H) \tag{3.36}$$

with $T(\mathbf{Q}_T, m_H)$ given in Eq. (3.20).

Not surprisingly, the Saclay and Bzdak approaches produce very different predictions: the Sudakov factor strongly suppresses the value of the predicted cross section. Broadly speaking, the Saclay prediction is similar to the Durham one for Higgs masses around 100 GeV/c^2 and (due to the absence of a Sudakov factor) overshoots it at higher masses. In contrast, the Bzdak calculation is typically much smaller than the Durham result. In both models, the choice of an exponentially falling gluon propagator means that there is little place for a perturbative component. However, as the Durham calculation shows, there does not seem to be any good reason for neglecting contributions from perturbatively large values of Q_T. In addition, neither calculation can lay claim to a systematic summation of the leading double and single logarithms, which is in contrast to the Durham calculation. As we shall see in Section 7.2, the CEP dijet data from CDF [83] appear to exclude the Saclay model in favour of the Durham one.

The perturbative Sudakov factor is also included in the approach of Refs. [84, 85, 86]. This latter approach also uses perturbative gluons throughout the calculation but Regge factors are included to determine the coupling of the gluons into the protons, rather than the unintegrated partons of the Durham model. The results are broadly consistent with those of the Durham model.

Finally, we mention the work of Szczurek and Lebiedowicz, which takes the Durham model as the basis for (part of) their predictions for $pp \to p + f_0(1500) + p$ [87] and $pp \to p + \chi_c + p$ [88].

In the following sections we shall survey existing results on CEP from experiments performed up to the end of 2009. The reader most interested in the LHC may skip Sections 4–6, but Section 7 remains relevant.

4 CERN Intersecting Storage Rings (ISR)

The ISR started in 1971, and provided pp and $p\bar{p}$ (also dd and $\alpha\alpha$) collisions from $\sqrt{s} = 23$ GeV to 63 GeV, greatly extending the energy range above the $\sqrt{s} = 7.6$ GeV of the CERN PS and Brookhaven AGS. The higher energies allowed for a more direct study of pomeron exchange. Ganguli and Roy gave an excellent review of Regge phenomenology as it stood after the first eight years of ISR operation [7] . Before discussing the data, a note on nomenclature is in order. We will, especially in this section, follow the historical terminology and use the term "double pomeron exchange" ($D\!I\!\!P\!E$) for inclusive studies of central particle production or for exclusive particle production when we wish

to emphasise its $I\!P + I\!P \to X$ component. At the low masses typical of the ISR, the central system will be dominated by production of $\pi^+\pi^-$ making it in effect exclusive. We shall aim to reserve "CEP" for strictly exclusive central systems. It is now accepted that the pomeron is predominantly gluonic, which means that $DI\!PE$ should be a good place to look for glueballs, and at the ISR (and even at the lower $\sqrt{s}$ of the SPS) this became a strong motivation to study such processes. This section provides some historical background, covering the ISR experiments that published results on $DI\!PE$ and CEP.

4.1 Searches for double pomeron exchange

At the start of the ISR era, light hadron spectroscopy was being studied intensively and it was "known" that the produced particles have low transverse momentum, p_T. Feynman had just invented the parton model and proposed that Lorentz-invariant inclusive particle production cross sections should "scale", i.e. $E\mathrm{d}^3\sigma/\mathrm{d}^3p(p_T, x_F, s)$ should become independent of s. Several single particle spectrometers tested this and scaling was found to be approximately true at small polar angles θ, but was dramatically broken at $p_T \gtrsim 2$ GeV/c due to hard scattering of partons, with the growing realisation that these are quarks and gluons, interacting according to the rules of QCD.

The ISR physics with which we are concerned in this review has two primary aspects: understanding the pomeron and looking for glueballs. A full understanding of strong interaction physics must necessarily include an understanding of the pomeron/glueball sector. Yet, even after almost 40 years of QCD, the physics of these objects is still not well understood. The ISR enabled for the first time the study of pomerons beyond simple elastic scattering and low mass diffractive excitation. One could study reactions such as $I\!P + p \to X$ for $M_X > 10$ GeV/c^2 and, our main concern here, $I\!P + I\!P \to X$. At the ISR, the state X could be separated in rapidity from both outgoing coherently scattered protons by large gaps $\Delta y \gtrsim 3$.

In colliding proton beams the total rapidity coverage is given by $\ln(s/m_p^2)$, which is 8.4 at the top ISR energy of $\sqrt{s} = 63$ GeV. It was found that single diffractive excitation, e.g. $p+p \to p+p^* \to p + (p\pi^+\pi^-)$ as studied at lower energies, now extended well above the resonance (N^*) region. The inclusive forward proton spectrum has a distinct peak [89] for $x_F = 1 - \xi > 0.95$, independent of $\sqrt{s}$ (Feynman scaling) and corresponding to $I\!P$ exchange. The diffractive mass calculated from $x_F = 1 - M_X^2/s$ extended up to 14 GeV/c^2, with this limit arising from the requirement of a rapidity gap adjacent to a leading proton of $\Delta y \geq 3$ units. For CEP, we similarly find that requiring both protons to have $x_F > 0.95$ (or equivalently two gaps of $\Delta y > 3$) one is restricted to $M_X \lesssim 3$ GeV/c^2.

Earlier searches for $DI\!PE$ in fixed target experiments, such as that by the France-Soviet Union (FSU) Collaboration at Serpukov [90], were only able to put upper limits on the cross section. FSU used a bubble chamber to study the exclusive reaction $p + p \to p + \pi^+\pi^- + p$ at $p_{\mathrm{beam}} = 69$ GeV/c, i.e. $\sqrt{s} = 11.5$ GeV. All the events were found to have both pions close in rapidity to one of the outgoing protons, consistent with single diffractive dissociation. A limit of $\sigma_{DI\!PE} \lesssim 20$ μb was determined for events with $M_{\pi^+\pi^-} \lesssim 0.7$ GeV/c^2 and $|y_{\pi^+} + y_{\pi^-}| < 1.6$, a factor ~ 20 less than the dominant single diffractive cross section $\sigma(p + p \to p + (p\pi^+\pi^-))$. At this low value of $\sqrt{s}$ the beam rapidity is only $y_{\mathrm{beam}} = 2.5$, too low for the distinctive kinematics of $DI\!PE$. Another bubble chamber experiment, at Fermilab [91], with the higher beam energy of $p_{\mathrm{beam}} = 205$ GeV/c ($\sqrt{s} =$ 19.7 GeV), placed an upper limit of 44 μb on the $DI\!PE$ cross section. It required the higher ISR

energy for the $D\mathbb{P}E$ signal to emerge.

Chew and Chew [23] made a prediction for the $D\mathbb{P}E$ signal, based on the single diffraction dissociation cross sections for $A + B \to A + X$ (σ^A) and $A + B \to B + X$ (σ^B) and an assumption of factorization, following Mueller [92]. They anticipated a differential $A + B \to A + X + B$ cross section given by

$$\frac{\mathrm{d}\sigma}{\mathrm{d}t_A \mathrm{d}t_B \mathrm{d}\xi_A \mathrm{d}\xi_B} = \frac{1}{\sigma_T(AB)} \frac{\mathrm{d}\sigma^A}{\mathrm{d}t_A \mathrm{d}\xi_A} \frac{\mathrm{d}\sigma^B}{\mathrm{d}t_B \mathrm{d}\xi_B}, \tag{4.37}$$

where $\xi_{A,B}$ are the fractional momentum losses of the colliding particles and $\sigma_T(AB)$ is the total AB cross section. Integrating over $t_{A,B}$ and over the $\xi_{A,B}$ range expected to be dominated by $D\mathbb{P}E$, they predicted $\sigma_{D\mathbb{P}E}(\pi^+\pi^-) \approx 65\ \mu$b at $\sqrt{s} = 63$ GeV, mostly with $M_X < 1$ GeV/c^2.

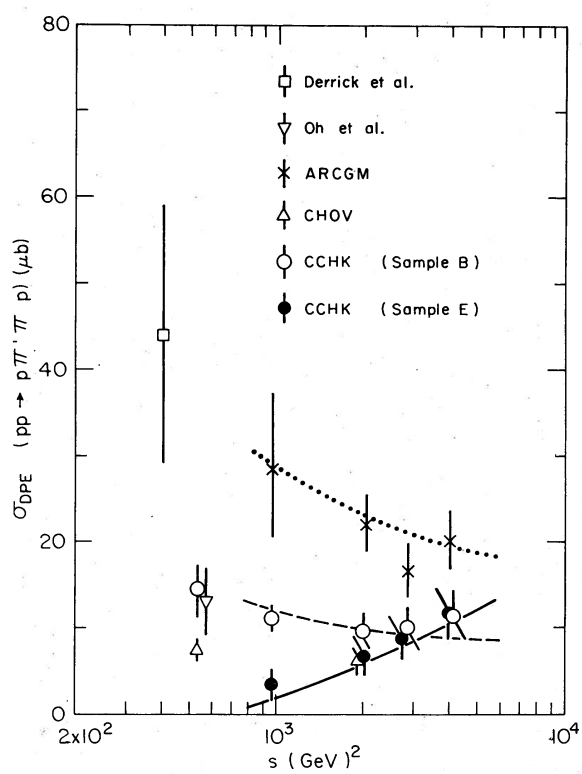

Figure 7: Experimental $D\mathbb{P}E$ cross sections (μb) versus s (GeV^2) at the ISR together with the Regge calculations of Ref [26]. The full circles and the rising solid line are for two gaps with $\Delta y > 3$. The dashed line is for $|y_\pi| < 1.0$ and the dotted line for $|y_\pi| < 1.5$. Figure from Ref. [26].

A more sophisticated calculation using Eq. (2.9), and illustrated in Fig. 3, was performed by Desai *et al.* [26] (see also Ref. [7]). To estimate $\sigma_{\mathbb{P}\mathbb{P}}$ they assumed pomeron dominance, i.e. they took

$$\gamma_A^2(t_1)\sigma_{\mathbb{P}\mathbb{P}}(M_X^2, t_1, t_2)\gamma_B^2(t_1) = \frac{g_{\mathbb{P}\mathbb{P}\mathbb{P}\mathbb{P}}(t_1) g_{\mathbb{P}\mathbb{P}\mathbb{P}\mathbb{P}}(t_2)}{\sigma_{\mathbb{P}}} (M_X^2)^{\alpha_{\mathbb{P}}(0)-1}, \tag{4.38}$$

where

$$\gamma_{A,B}^2(t) = \beta_{A,B}(t)^2 |\eta(t)|^2 \ ,$$

$g_{I\!P I\!P I\!P}(t)$ is the triple-pomeron coupling (e.g. see Fig. 3(b)) and $\sigma_{I\!P}$ is the pomeron contribution to the total cross section, i.e.

$$\sigma_T(AB) = \sigma_{I\!P}\left(\frac{s}{s_0}\right)^{\alpha_{I\!P}(0)-1} + \sigma_{I\!R}\left(\frac{s}{s_0}\right)^{\alpha_{I\!R}(0)-1} . \tag{4.39}$$

The values of $g_{I\!P I\!P I\!P}(t)$ and the Regge trajectory parameters were taken from the analysis of Field and Fox [93] and secondary ($I\!R$) exchanges were included as a correction (around 30–50% at the lowest values of s, falling to under 10% at the higher values). They calculated cross sections both for two gaps with $\Delta y > 3$ and for fixed ranges, $|y_\pi| < 1.0$ or $|y_\pi| < 1.5$, of the central pions, through the ISR energy range. The predictions are shown together with the ISR data in Fig. 7 and the agreement between the two is rather good. The predicted cross section for two gaps of fixed length rises with $\sqrt{s}$, while for a fixed $|y_\pi| < y_{max}$ cut the cross section falls with $\sqrt{s}$. The predictions also indicate that the two protons should each have an exponential t-slope with $b_{DI\!PE} \sim b_{\rm elastic}/2$ and they should be uncorrelated in azimuth and t. In the ISR energy range $b_{\rm elastic} \sim 13$ GeV^{-2}, with a small t-dependence, rising like $b(s) = c + d\ln(s)$. Note that, under the assumption that $\sigma_{I\!P I\!P}$ is independent of M_X^2, the Desai *et al.* approach is almost identical to that of Chew and Chew, the only substantive difference being the treatment of secondary exchanges.

Desai *et al.* also consider a pion exchange model for $\sigma_{I\!P I\!P}$, and in this context they point out that absorptive corrections may well be important. We refer to Ref. [26] and references therein for more detail. We shall now turn to discuss the data, and note that Fig. 7 contains the main results on the integrated cross section measurements. Table 1 summarises the ISR $DI\!PE$ cross section measurements.

The first experimental evidence for $DI\!PE$, at the ISR, was presented by the ARCGM Collaboration [94] which had forward proton tracking (but no momentum measurement) and full angular coverage with scintillation counters. Candidate events had two leading non-collinear proton tracks with polar angle $6 < \theta < 10$ mrad, and exactly two hits in a scintillation counter hodoscope covering $|\eta| < 1.5$. Approximately 100 events were found at each ISR $\sqrt{s}$ value. Setting $t_{A,B} = -(p_{\rm beam}\theta_{A,B})^2$ they found no evidence for any correlation between t_A and t_B, and writing $\mathrm{d}^2\sigma/\mathrm{d}t_A\mathrm{d}t_B = a\, e^{-b(t_A+t_B)}$ they measured a slope $b = (9.9 \pm 1.8)$ GeV^{-2}, not significantly changing with energy. This is somewhat higher than $b_{\rm elastic}/2$ but is consistent at the 2σ level. The cross section is also approximately constant, from $\sigma_{DI\!PE} = (28.4 \pm 8.1)\mu$b at $\sqrt{s} = 31$ GeV to $(20.2 \pm 3.3)\mu$b at $\sqrt{s} = 63$ GeV. These are expected characteristics of $DI\!PE$.

The Split Field Magnet (SFM) facility at the ISR had nearly full angular coverage for charged particle tracks using proportional chambers, with dipole fields in the forward directions to analyse the momenta of the scattered protons. The central field was complicated (a quadrupole) and central particles were not identified but were assumed to be pions. A study by the CCHK Collaboration [95] selected events with two leading positive tracks ($x_F > 0.9$) and forward rapidity gaps $\Delta y > 2$. They observed the $DI\!PE$ characteristics of no correlations in ϕ and t, and measured $b = (5.5 \pm 0.9)$ GeV^{-2}. Extrapolating in $|t|$ they found $\sigma_{DI\!PE} = (25 \pm 10)\mu$b, consistent with the subsequent Desai *et al.* calculation. The mass distribution (assuming the central particles to be pions) had mostly $M_{\pi^+\pi^-} < 1$ GeV/c^2 with no significant $\rho \to \pi^+\pi^-$ signal, indicating $DI\!PE$ dominance, as $I\!P I\!P \to \rho$ is forbidden by isospin. The authors point to the absence of an $f_0(980)$, but we will see later that it appears strongly in CEP as an edge, but not a peak. Au *et al.* [96]

later proposed that this is because the $\pi^+\pi^- \to \pi^+\pi^-$ cross section is already as large as allowed by unitarity up to $M_{\pi\pi} \sim 1$ GeV/c^2.

The CHOV Collaboration also studied $p + p \to p + \pi^+\pi^- + p$ at the SFM [97], selecting events with $x_F > 0.9$ for both protons and $|y_\pi| < 1.0$. After applying a four-constraint kinematic fit, the $\Delta\phi(pp)$ distribution showed two components, attributed to single diffraction and $D\mathbb{P}E$. The inclusive proton spectra showed a diffractive peak for $x_F \gtrsim 0.95$, while the region $0.90 < x_F < 0.95$ was dominated by non-diffraction (Reggeon $\mathbb{R}$ exchange). They claimed, for $|y_\pi| < 1.0$, $\sigma_{D\mathbb{P}E} = (7.1 \pm 1.0)\mu$b at 23 GeV and $(6.0 \pm 1.5)\mu$b at 45 GeV. Assuming the central particles to be pions, $M_{\pi^+\pi^-} < 1.5$ GeV/c^2.

The CCHK Collaboration then followed the CHOV analysis with a more detailed study using five ISR energies and much higher statistics [98]. A sample was obtained with $x_F > 0.9$, predominantly $M_{\pi^+\pi^-} \lesssim 1$ GeV/c^2, with no observed ρ resonance and with an indication of a dip around 1 GeV/c^2. The helicity angle, defined as the angle in the $\pi^+\pi^-$ centre-of-mass frame between the π^+ and the direction of the $\pi^+\pi^-$ system in the overall centre-of-mass frame, showed a flat distribution which suggests a dominantly $J = 0$ system. No correlation was seen in ϕ or t between the protons, and the slope was measured to be $b = 7.0\pm0.5(6.1\pm0.8)$ GeV^{-2} at $\sqrt{s} = 30.7(52.8)$ GeV. Extrapolating in $|t|$, requiring both protons to have $x_F > 0.9$ and to have both rapidity gaps $\Delta y > 3$, the cross section $\sigma_{D\mathbb{P}E}(\pi^+\pi^-)$ was found to rise from $(3.6\pm1.7)\mu$b to $(11.7\pm3.0)\mu$b as $\sqrt{s}$ increases from 30.7 to 62.3 GeV.

The CHM Collaboration [99] studied events with two leading protons, measured with single-arm magnetic spectrometers with $\sigma(p)/p \approx 0.6\%$, at $\theta \sim 30$ mrad (and excluding elastic scattering by acollinearity). A scintillation counter hodoscope covered 98% of the full solid angle and measured the directions of central charged particles, but without magnetic analysis. The mass and rapidity of the central hadronic system were determined entirely from the measured protons via

$$\frac{M_X^2}{s} \approx \xi_1\xi_2; \;\; y = \frac{1}{2}\ln\left(\frac{\xi_1}{\xi_2}\right) \; . \tag{4.40}$$

However, the study of centrally produced resonances was limited by the lack of tracking and the modest mass resolution of $\sigma_{M_X} \approx 200$ MeV at $\sqrt{s} = 30$ GeV.

Table 1 gives an at-a-glance summary of the above experiments; more details are given in the text and, of course, in the original publications.

4.2 Searches for glueballs

Glueballs (G) are gluon bound states that are widely anticipated in QCD. There is general agreement that the lightest glueball should be a scalar with mass in the range $1 - 2$ GeV/c^2, with pseudoscalar and tensor glueballs at higher mass. However, understanding the light scalars has proven to be experimentally and theoretically very challenging, and after thirty years of investigation the glueball sector is still not well understood, due in no small part to the likely mixing of any scalar glueball with $q\bar{q}$ (meson) bound states of the same quantum numbers. It is not our aim here to review the experimental status of glueballs; excellent recent reviews can be found in Refs. [102, 103]. Rather we will focus our attention on data collected in $D\mathbb{P}E$ that is of relevance to the search for glueballs. It

Expt.	Collaboration.	Ref.	$\sqrt{s}$ (GeV)	Forward p momenta	Central momenta/ID	Cuts: x_p^{min}, y_π^{max}	σ_{DIPE} (μb)
R602/4	ARCGM	[94]	31			–, 1.5	28.4±8.1
R602/4	ARCGM	[94]	45			–, 1.5	22.2±3.3
R602/4	ARCGM	[94]	53			–, 1.5	16.8±3.1
R602/4	ARCGM	[94]	62			–, 1.5	20.2±3.3
R407/8	CCHK/SFM	[95]	31	√	√	0.9, 1.5	25±10
R401	CHOV/SFM	[97]	23	√	√	0.90, 1.0	7.1±1.0
R401	CHOV/SFM	[97]	45	√	√	0.90, 1.0	6.0±1.5
R407/8	CCHK/SFM	[98]	23	√	√	0.9, 1.0	14.4±3.1
R407/8	CCHK/SFM	[98]	31	√	√	0.9, 1.0	11.0±1.2
R407/8	CCHK/SFM	[98]	45	√	√	0.9, 1.0	9.4±1.9
R407/8	CCHK/SFM	[98]	53	√	√	0.9, 1.0	10.2±2.1
R407/8	CCHK/SFM	[98]	62	√	√	0.9, 1.0	11.5±3.0
R407/8	CCHK/SFM	[98]	31	√	√	0.9, 1.0^d	3.6±1.7
R407/8	CCHK/SFM	[98]	45	√	√	0.9, 1.7^d	6.8±2.7
R407/8	CCHK/SFM	[98]	53	√	√	0.9, 2.1^d	8.8±2.8
R407/8	CCHK/SFM	[98]	63	√	√	0.9, 2.4^d	11.7±3.0
R807	AFS	[100, 101]	63		$\pi^+\pi^-$	0.95, 1.2	34±14^{a,c}
R807	AFS	[100, 101]	63		$\pi^+\pi^-$	0.95, 1.2	1.9±0.9^{b,c}
R807	AFS	[100, 101]	63		K^+K^-	0.95, 1.2	1.4±0.6^c
R807	AFS	[100, 101]	63		$p\bar{p}$	0.95, 1.2	0.035±0.02^c
R807	AFS	[100, 101]	63		$\pi^+\pi^-\pi^+\pi^-$	0.95, 1.2	2.8±1.4^c

Table 1: ISR experiments reporting $DIPE$ cross sections. See text and cited papers for details. The forward protons are always tracked, but their momenta were not always measured. Only the AFS experiment identified the central particles, otherwise pions were assumed. ^{a}For $M_{\pi\pi} < 1$ GeV/c^2. ^{b}For 1 GeV/$c^2 < M_{\pi\pi} < 2.3$ GeV/c^2. ^{c}Assuming slope $b = 6$ GeV^{-2}. ^{d}For $\Delta y > 3$.

was Robson [104] who, in 1977, first suggested that $D\mathbb{P}E$ should provide a gluon-dominated channel that favours central glueball production.

Glueball searches in CEP are not only favoured by the gluon-dominated nature of $\mathbb{P}$, but also the quantum numbers the central state must have: zero isospin, CP = ++ and even spin; it is thus a *quantum number filter*. The lightest known states satisfying these constraints are the very broad (and long controversial) $f_0(600)$ (or σ) and the $f_0(980)$, which lies at the $K\bar{K}$ threshold. Note that scalar glueballs cannot lie on the pomeron trajectory $\alpha_{\mathbb{P}}(t)$ specified by Eq. (2.5), which instead anticipates a $J = 2$ tensor glueball with $M_G \approx 2.1$ GeV/c^2.

Following Robson's suggestion, Waldi, Schubert and Winter examined the $p+\pi^+\pi^-+p$ data, taken by the CHOV Collaboration, for resonant structure [105]. They observed a bump between 1100 and 1500 MeV/c^2, which they incorrectly attributed to the $f_2(1270)$. Later the Axial Field Spectrometer (AFS) experiment (which we discuss in more detail in the next paragraph) showed that this bump, visible in Fig. 8, is predominantly S-wave and is broader than the $f_2(1270)$, with a small ($\lesssim 10\%$) D-wave contribution from the $f_2(1270)$ [101]. Since the $f_2(1270)$ is also seen in $e^+e^- \to e^+ + \pi^+\pi^- + e^-$ (two-photon) production with a cross section that favours a large $q\bar{q}$ composition, it is not now considered to be a glue-dominated state.

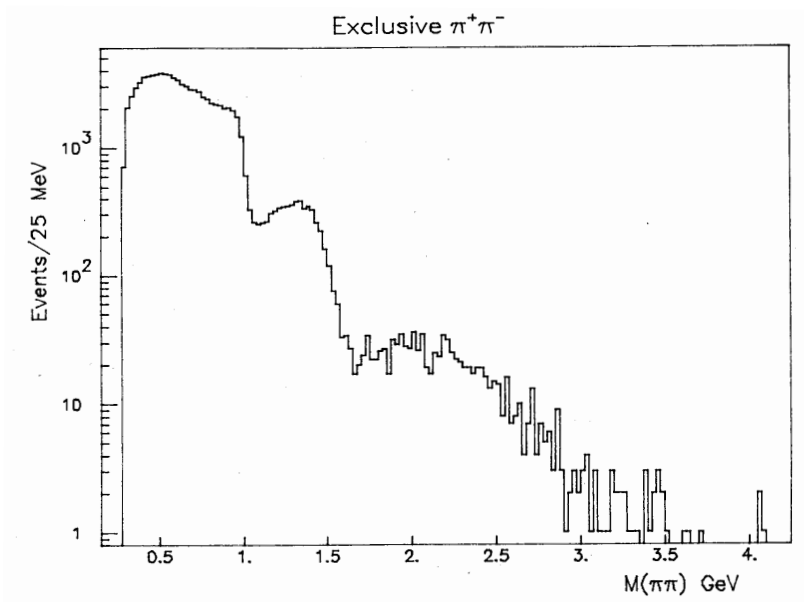

Figure 8: $M_{\pi^+\pi^-}$ spectrum in $D\mathbb{P}E$ at the ISR (Axial Field Spectrometer, R807 [100, 101]). Figure from Ref. [101].

Compared to the CHOV analysis, the AFS Collaboration benefitted from a factor 20 more statistics (89,000 exclusive events), better mass resolution, $\sigma_M = 10(25)$ MeV/c^2 at 1(2) GeV/c^2, and particle identification [100, 101]. Forward proton track detectors and rapidity gap detectors were added to the central spectrometer, and CEP processes with $X = \pi^+\pi^-, K^+K^-, p\bar{p}$, and $\pi^+\pi^-\pi^+\pi^-$ were measured. The two-pion mass spectrum $M_{\pi^+\pi^-}$ shown in Fig. 8 shows several interesting features. The cross section rises steeply from threshold and there is no sign of $\rho^0 \to \pi^+\pi^-$, which is forbidden in $D\mathbb{P}E$. There is however an order-of-magnitude sharp drop just below 1 GeV/c^2,

followed by another bump-dip structure. The absence of a ρ, which is prominent in lower energy $p+p \to p+\pi^+\pi^-+p$ experiments (e.g. at the SPS [106]), is a sign that $I\!R$ exchange is unimportant in the AFS data. Since photons can be exchanged across large rapidity gaps, they *could* give rise to a centrally photoproduced ρ via $\gamma + I\!P \to \rho$. However the cross section is much lower than for $DI\!PE$, and protons with $|t| < 0.01$ GeV^2 were not detected, which further diminishes the rate. Despite the absence of a ρ signal in the mass distribution, when the angular distributions were studied and a P-wave ($J = 1$) component was selected, a small ρ signal was seen, demonstrating the sensitivity of such distributions[6]. Conversely when the fixed-target experiment WA102 [106] projected out the S-wave their ρ peak disappeared and the $M_{\pi^+\pi^-}$ spectrum at $\sqrt{s} = 29$ GeV had a similar shape to the AFS spectrum. The partial wave analysis of the AFS group showed that the (J=0) S-wave dominates as far up as 1700 MeV/c^2 [101].

The striking drop at $M_{\pi^+\pi^-} \approx 1$ GeV/c^2 in Fig. 8 is the $f_0(980)$, the lowest mass narrow scalar state with full width $40-100$ MeV/c^2 [107]. According to Au *et al.* [96] the interaction can be understood as $I\!P + I\!P \to \pi\pi \to \pi^+\pi^-$ with the final state interaction phase shift dominating the structure. Coupled channels such as intermediate $K\bar{K}$ states contribute; similarly in the K^+K^- final state intermediate $\pi\pi$ states $I\!P + I\!P \to \pi\pi/KK \to K^+K^-$ need to be taken into account. Au *et al.* claimed that the coupled channel analysis could be interpreted as showing two narrow states near 1 GeV/c^2: a $K\bar{K}$ "molecule" and a glueball candidate. Narison [108] suggested from an analysis of widths and couplings that both $f_0(600)$ and $f_0(980)$ have about 50% (gg) and 50% $\frac{1}{\sqrt{2}}(\bar{u}u + \bar{d}d)$ in their wave functions. Mennesier, Minkowski, Narison and Ochs [109] analysed $\pi^+\pi^-$ scattering below 700 MeV/c^2 in an analytic K-matrix model. This is the region of the broad $f_0(600)$. They argue that the small direct coupling of this state to $\gamma\gamma$ is "hidden" by the $\pi\pi$, i.e. $f_0(600) \to \pi\pi \to \gamma\gamma$ and find that while $\Gamma(f_0(600) \to \gamma\gamma) \sim 3.9 \pm 0.6$ keV, large enough to suggest a $q\bar{q}$ nature, after taking into account the rescattering, the direct width is only $\Gamma(f_0(600) \to \gamma\gamma) \sim 0.13 \pm 0.05$ keV. This is considerably smaller than the width anticipated in the non-relativistic quark model for a $\frac{1}{\sqrt{2}}(u\bar{u} + d\bar{d})$ meson of similar mass. However, the interpretation of this state as a glueball is far from clear. For example, it is also commonly identified as the scalar partner of the pions under spontaneously broken chiral symmetry, especially in the context of NJL models [110].

Minkowski and Ochs in particular have interpreted the scalar $\pi\pi$ data from this and other experiments in terms of a single very broad state extending from 400 MeV/c^2 to about 1700 MeV/c^2, with the $f_0(980)$ and $f_0(1500)$ states superimposed, interfering destructively and therefore manifesting as dips in Fig. 8. They find that in this energy range, after the $f_0(980)$ and $f_0(1500)$ are subtracted, the $\pi\pi$ elastic amplitude describes a full loop in the Argand diagram. They take this broad object, which they call the "red dragon", to be the lightest scalar glueball [111]. This is a remarkable claim: The full $\pi^+\pi^-$ spectrum of Fig. 8 from threshold to ~ 1700 MeV/c^2 is one very broad scalar glueball. However any state with a width Γ exceeding a few hundred MeV decays within $\sim \hbar c/\Gamma < 1$ fm, and will not propagate beyond the interaction region as a free particle. The situation remains unclear however: Spanier, Tornqvist and Amsler reviewed the scalar mesons in the PDG [107] and concluded that "The I = 0, $J^{PC} = 0^{++}$ sector is the most complex one, both theoretically and experimentally." There is however something of a consensus that the scalar meson

[6]This method could in principle be applied to, e.g., exclusive $p+p \to p+\ W^+W^- + p$ (or $X = b\bar{b}$) at the LHC, if one had high enough statistics and good angular coverage. A scalar state (e.g. a Higgs) would show up only in the S-wave component.

sector does contain a scalar glueball degree of freedom; the challenge is to understand its mixing with the quark states [112].

The AFS experiment also measured central K^+K^- production [100, 101]. The cross section rises very steeply from threshold, probably due to $f_0(980)$, but with no sign of exclusive $\phi \to K^+K^-$, which is forbidden in $D\mathbb{P}E$. The cross section ratio $\sigma(K^+K^-)/\sigma(\pi^+\pi^-)$ even exceeds 1.0 above threshold, perhaps an indication of a gluonic component. Exclusive $p+(p\bar{p})+p$ with mass $M_{p\bar{p}}$ from threshold to 2.8 GeV/c^2 was also seen (64 events), but with no evident structures. An extrapolation in $|t|$ gives an estimate of the total $\sigma(p+p \to p+p\bar{p}+p) \approx 35$ nb (see Table 1). We are not aware of a prediction for exclusive baryon pairs. One could expect a similar cross section, but scaled by M^{-2}, for other baryon pairs, e.g. $\Lambda\bar{\Lambda}$, as the pomeron is flavour-blind. $D\mathbb{P}E$ production of hyperon pairs was not studied at the ISR, but it would be possible at the Tevatron and the LHC.

The ISR also provided $\alpha\alpha$ collisions with $\sqrt{s} = 126$ GeV. The forward drift chambers installed for the CEP measurements could distinguish charge $Q = 1$ and $Q = 2$ particles. The exclusive process $\alpha + \alpha \to \alpha + \pi^+\pi^- + \alpha$ was seen [101], with the $M_{\pi^+\pi^-}$ spectrum having the same shape as in pp collisions within limited statistics (395 events). The α-particles must have been coherently scattered, making this is a very clean channel for $D\mathbb{P}E$, but the statistics were too low for serious spectroscopy.

The ISR was terminated in 1983, after the $Sp\bar{p}S$ collider was turned on. From a CEP perspective, what had we learnt? Well, the existence of double pomeron exchange had been established and was in agreement with Regge predictions, but it had been a long struggle. While CEP with large rapidity gaps in hadron-hadron collisions can come from $\gamma\gamma, \gamma\mathbb{P}$, or $\mathbb{P}\mathbb{P}$ interactions, only the latter had been observed. There was no evidence for the odderon, the C $= -1$ partner to the $\mathbb{P}$, except for a small difference in pp and $p\bar{p}$ elastic scattering [113] at $t = -1.2$ GeV^2 (the dip region). The reach of CEP was up to $M_X \approx 3$ GeV/c^2, which was favorable for hadron spectroscopy and especially for glueball searches. The best detector for CEP, the AFS, was designed for high-p_T physics and added a CEP programme only in the final $2-3$ years of operation; the analysis was completed after the ISR was turned off. The spectra for $X = \pi^+\pi^-, K^+K^-, p\bar{p}$ and $\pi^+\pi^-\pi^+\pi^-$ showed structures (especially $\pi^+\pi^-$) but no unequivocal evidence for glueballs. The low mass scalar sector is still unsettled, and the whole $M_{\pi\pi}$ region from $400-1700$ MeV/c^2 may even be a very broad scalar glueball "cut" by the $f_0(980)$ and $f_0(1500)$.

5 Fixed Target experiments

After the ISR was closed in 1983, CEP of low multiplicity hadron states, for both hadron spectroscopy and for studies of production mechanisms, became an active field in fixed target experiments in the 1980s and 1990s. We shall restrict ourselves to a few brief comments since our focus is on high energy colliding beam experiments.

Thanks to high luminosities, dedicated experiments in multiparticle spectrometers, such as the Omega facility at the CERN SPS experiments (WA76, WA91 and WA102) and experiment E690 at the Fermilab Tevatron, were highly productive. In particular, the experiments using the Omega spectrometer [114, 115] confirmed the earlier observation by the SFM collaboration (at the ISR) [116] of a correlation between the properties of the central system and the directions of the outgoing

protons. Close & Kirk suggested that glueballs and $q\bar{q}$ mesons may have different dependencies on the difference in the transverse momenta of the outgoing protons [117, 118] but this idea remains unproven. Moreover, $\sqrt{s}$ was only 29 GeV and so $I\!R I\!R$ and $I\!R I\!P$ exchanges were certainly not negligible. Ref. [115] contains many relevant references to CEP at the Omega facility, with a large number of results that are of interest for meson spectroscopy.

Experiment NA22 at the European Hybrid Spectrometer (EHS) also extracted $D I\!P E$ cross sections in π^+p and K^+p collisions, although with $p_{\rm beam} = 250$ GeV/c ($\sqrt{s} = 21.7$ GeV) a large non-$D I\!P E$ background had to be subtracted [119]. They found an inclusive (but mostly $\pi^+\pi^-$) $D I\!P E$ cross section of $(39 \pm 5 \pm 8)\mu$b for K^+p and $(24 \pm 6 \pm 3)\mu$b for π^+p. Such a difference is qualitatively expected in Regge theory since $\sigma_T(K^+p) > \sigma_T(\pi^+p)$.

At $p_{\rm beam} = 800$ GeV/c, Fermilab Experiment E690 studied the $X = K^0_S K^0_S$ system, showing in particular a large $f_0(1500)$ peak [120].

6 CERN Proton-antiproton Collider ($Sp\bar{p}S$)

In 1981 the first $p\bar{p}$ collider, the $Sp\bar{p}S$, came into operation at CERN. It provided an increase in $\sqrt{s}$ from 63 GeV at the ISR up to 630 GeV, and even 900 GeV for some low luminosity "ramping runs". This step-up in energy enabled the discoveries of the W and Z bosons, and observations of dramatic high E_T jets. Diffractive physics took a back seat during this period, although experiment UA8, by adding forward Roman pots on both beam pipes to the central UA2 experiment, observed diffractively produced dijets [121] with E_T up to ~ 13 GeV. Ingelman and Schlein had earlier proposed to describe the pomeron in hard processes as having quark and gluon constituents, analogous to a hadron [122]. In this picture, the parton densities in the pomeron can be measured in high mass diffraction. The jet kinematics gives the scattering parton momenta and thus rather direct information on the parton distributions in the $I\!P$. This approach led directly to the subsequent very precise measurement of diffractive parton densities at the HERA collider (see for example Refs. [8, 9]).

Experiment UA8 measured $p/\bar{p}$ tracks after (low-β) quadrupole magnets, and they studied $p+X+\bar{p}$ with $X =$ "anything", using the UA2 central detector [123]. They selected 107 events in the $D I\!P E$-dominated region with $x_F > 0.95$ (i.e. gaps $\Delta\eta \gtrsim 3$ on both sides). Most of the events had $M_X < 8$ GeV/c^2 but no specific exclusive states X could be resolved, as central particle momenta were not measured (UA2 had no magnetic field) and the missing mass resolution was much worse than the mass derived using the calorimeter alone (which was $\sigma_M \sim 1$ GeV/c^2). UA8 extracted the $D I\!P E$ cross section, $\sigma_{I\!P I\!P}$, assuming the validity of Eq. (2.9) with a flux (see Eq. (2.8)) given by

$$f_{I\!P/p}(\xi, t) = \frac{K}{(1 - t/a)^4} e^{bt} \left(\frac{1}{\xi}\right)^{2\alpha_{I\!P}(t)-1} \tag{6.41}$$

and with parameters extracted from data on elastic scattering and single diffraction:

$$
\begin{aligned}
a &= 0.71 \text{ GeV}^2 \\
b &= 1.08 \text{ GeV}^{-2} \\
K &= 0.74 \text{ GeV}^{-2} \\
\alpha_{I\!P}(t) &= 1.035 + 0.165t + 0.059t^2 \ . \qquad (6.42)
\end{aligned}
$$

UA8 inferred that $\sigma_{I\!P I\!P} \approx 3$ mb for $2 \lesssim M_X \lesssim 8$ GeV/c^2, decreasing to $0.5 - 1.0$ mb for $10 \lesssim M_X \lesssim 25$ GeV/c^2. This is significantly larger than expected assuming the simple factorization formula presented in Eq. (4.37) at the same total energy. The UA8 paper also included a prediction for $\mathrm{d}\sigma_{DI\!PE}/\mathrm{d}M_X$ at the Tevatron and LHC assuming a constant $\sigma_{I\!P I\!P} = 1$ mb. They predicted about 0.4 μb/GeV/c^2 at $M_X = 100$ (200) GeV/c^2 at these colliders respectively.

The largest experiment at the $Sp\bar{p}S$, UA1, was designed to discover the W and Z, but it also performed a CEP study at $\sqrt{s} = 630$ GeV using forward rapidity gaps [124]. They required no energy in forward calorimeters with $3 < |\eta| < 6$ and some energy in the central calorimeters ($5^\circ < \theta < 175^\circ$). A localized energy deposition of $E_T > 1.5$ GeV and/or a "jet" with $E_T > 3$ GeV was required to trigger, which excluded the possibility of detecting low mass exclusive states. The data were compared to a non-diffractive sample, containing at least one charged particle with $1.5 < |\eta| < 5.5$ in each forward direction. The mass M_X of the central hadrons had a mean $\langle M_X \rangle \sim 36$ GeV/c^2 and extended a little above 63 GeV/c^2 (above which at least one scattered proton must have $x_F < 0.90$). At low M_X, the mean charged particle multiplicity $\langle n_{ch} \rangle$ was measured to be similar to that in pp or e^+e^- collisions at $\sqrt{s} \equiv M_X$, but it was found to rise faster and, by $M_X = 70$ GeV/c^2, it was a factor of two higher. This effect has not been quantitatively explained, and hopefully it will be checked at the Tevatron or LHC. Recall, however, that the final state in e^+e^- collisions producing dijets is $q\bar{q}$ and in $I\!P I\!P$ collisions it is predominantly gg, so one might expect $\langle n_{ch} \rangle_{I\!P I\!P} > \langle n_{ch} \rangle_{e^+e^-}$ as a result of the difference between quark and gluons jets, together with pomeron "remnants". With the UA1 jet algorithm it was found that 5% of the events have at least one jet with $E_T > 10$ GeV, but this fraction would probably be lower if the trigger had not required an energy deposition of $E_T > 1.5$ GeV. This class of central dijet events is expected be a dominant background to searches such as $p + H + p \to p + JJ + p$ at the LHC.

7 Tevatron

7.1 Introduction

Until the LHC began operation in December 2009, the Tevatron at Fermilab was the highest energy hadron collider, making proton-antiproton collisions at $\sqrt{s} = 1.96$ TeV. In Run I (1992-1996) it provided collisions at $\sqrt{s} = 546$ GeV, 630 GeV (to equal the CERN $Sp\bar{p}S$ collider) and 1800 GeV. The total delivered luminosity per experiment (CDF and DØ) was 110 pb^{-1}, compared to about 7000 pb^{-1} so far in Run II (2004-2009).

In the first (Run I) phase of diffractive studies, installation of Roman pots by CDF, with silicon and drift chamber track detectors along both beam pipes, allowed measurements of elastically

and diffractively scattered protons and antiprotons. Elastic scattering was measured at $\sqrt{s} = 546$ (1800) GeV for $-0.29 < t < -0.025$ GeV^2, where it was well described by an exponential slope with $b = 15.28 \pm 0.58$ (16.98 ± 0.25) GeV^{-2}, and the integrated elastic cross sections were $\sigma_{\rm el} = 12.9 \pm 0.3$ mb and 19.7 ± 0.9 mb, at the two energies [125]. By measuring the rates of elastic scattering and inelastic collisions simultaneously, CDF exploited the Optical Theorem to measure the total cross section, σ_T, independent of the luminosity [126]. They found $\sigma_T = 61.26 \pm 0.93$ (80.03 ± 2.24) mb, with $\sigma_{\rm el}/\sigma_{\rm tot}$ rising from 0.210 ± 0.002 to 0.246 ± 0.004 over this $\sqrt{s}$ range. Two other experiments, E710 [127] and E811 [128] found significantly ($\sim 2.5\sigma$) lower values for both $\sigma_{\rm el}$ and $\sigma_{\rm tot}$ (but with the same ratio) at $\sqrt{s} = 1800$ GeV. These results, together with LHC expectations, are discussed in [40] and [129]. CDF also measured the inelastic proton spectra for $x_F \gtrsim 0.88$ [130, 131], where they observed the expected dominance of the diffractive peak above $x_F \sim 0.95$. This corresponds to diffractive masses $M_X = 400$ GeV/c^2; indeed later Tevatron studies succeeded in observing W, Z and jets with E_T up to 80 GeV in single diffraction. Unfortunately the forward proton detectors were removed without having measured CEP with both protons detected.

The second stage of diffractive physics at the Tevatron took place in Run II, initially without any forward $p/\bar{p}$ measurements. CDF and DØ both studied hard single diffraction with forward rapidity gaps, after which CDF installed a new set of Roman pot detectors 50 m downstream to measure diffractive antiprotons. There were no detectors for forward protons, so $p + X + \bar{p}$ could not be studied with both the p and $\bar{p}$ tagged, however sets of scintillation counters with $\theta < 3^\circ$ were added along the beam pipes. These "beam shower counters" (BSC) acted as rapidity gap detectors, using showers produced in the beam pipe by secondaries with $5.4 < |\eta| < 7.4$. When combined with "miniplug calorimeters" covering $3.6 < |\eta| < 5.2$, gaps of $\Delta\eta > 3.8$ could be required on each side, with or without a measured antiproton. Later DØ also installed Roman pots with tracking on both sides, but has not yet presented any CEP results.

The single diffractive production of dijets [132, 133], W [134, 135] and Z [136] (preliminary) has been observed and the fraction of W, Z or dijets that are classed as diffractive, i.e. either with a high-x_F antiproton or a large forward gap, is around 1%. This is to be contrasted with ep collisions at HERA, where H1 and ZEUS found that the corresponding fraction of diffractive to non-diffractive events is $\sim 10\%$. This is in accord with the rough expectation that the gap survival probability S^2 is lower by about an order of magnitude in hadron-hadron collisions than in $\gamma^* p$ collisions.

CDF also studied the central production of dijet events containing both a leading $\bar{p}$ with $0.035 < \xi_{\bar{p}} < 0.095$ and a rapidity gap in the proton direction, corresponding to $0.01 < \xi_p < 0.03$ [137]. Although the proton is not observed, its ξ can be computed using

$$\xi_p = \frac{1}{\sqrt{s}} \sum_i E_T^i e^{\eta^i}, \tag{7.43}$$

where the sum is over all the observed particles in the detector. This constitutes an observation of $D\!\!\!\!\mathbb{P}E$ dijet production, and a comparison to the theoretical predictions has been carried out using pomeron parton densities extracted from the HERA data in Refs. [138, 139]. Again a gap survival factor of around 10% was needed to fit the data. Importantly, it was noted that the rate of $D\!\!\!\!\mathbb{P}E$ (two-gap) dijet events is approximately 10% of the rate of single diffractive (one-gap) dijet events , i.e. the price to pay for gap survival should not be applied twice. This was also observed in a CDF study [140] of *inclusive* $D\!\!\!\!\mathbb{P}E$, with a measured antiproton with $0.035 < \xi_{\bar{p}} < 0.095$ and a rapidity gap on the proton side.

7.2 Central exclusive production

The study of CEP at the Tevatron is a recent activity, largely motivated by the possibility of studying exclusive $p+p \to p+H+p$ and related processes at the LHC. In 2001 there was a very large spread in predictions for this exclusive cross section, some of which even suggested that a Higgs search may be possible at the Tevatron, and a Letter of Intent to perform such a search by measuring both final state protons was submitted to the Fermilab Program Advisory Committee [141]. It did not proceed to the proposal stage however, partly because of the large cross section uncertainty. Although the exclusive cross section is much smaller than the inclusive one, if the protons are measured precisely it was noted that the "missing mass" method can be used to give a very good measurement of the central state, independent of its nature [1][7]. Although it is now understood that the Higgs is not likely to be produced this way at the Tevatron, the measurement of other central systems, in particular those with the same quantum numbers as the Higgs (such as χ_{c0} and χ_{b0}) constrains the predictions for $\sigma(p+H+p)$. The diagrams for χ_{c0} and χ_{b0} production are similar to those for exclusive Higgs production, but with c- and b-quark loops instead of a top-quark loop. Of course the relevant scale is much lower for these lighter states and this renders the applicability of perturbative QCD more uncertain. The cleanest related process is $p+\gamma\gamma+\bar{p}$ (through $I\!P I\!P \to \gamma\gamma$) but the cross section is small for $E_T(\gamma) > 5$ GeV, where measurements were made. Exclusive dijet production has a much higher cross section but one must then compromise on not having such a clean final state.

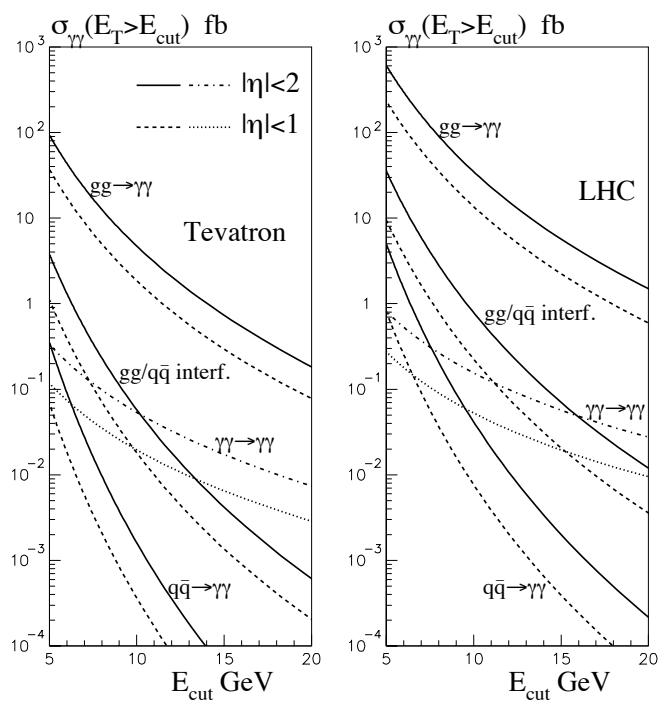

Figure 9: Predictions for CEP di-photon production at the Tevatron and the LHC. Figure from Ref. [142].

[7] Ref. [1] also pointed out that a measurement of the difference in the proton arrival times at the forward detectors could be used to greatly reduce the impact of pile-up background.

Nevertheless, CDF has succeeded in measuring exclusive $\gamma\gamma$, χ_c and dijet production, and we discuss each of these in turn. We also discuss exclusive $\gamma\gamma \to e^+e^-, \mu^+\mu^-$ and $\gamma I\!P \to J/\psi, \psi'(2S)$, which was recently seen for the first time in hadron-hadron collisions. Apart from the dijet study, the forward $\bar{p}$ could not be detected, as the Roman pots (only on the $\bar{p}$ side) did not have acceptance for low M_X. The analyses instead relied on finding events that contain just the state X in conjunction with an otherwise empty (i.e. consistent with noise levels) detector. The miniplug calorimeters and BSC counters, which have coverage out to $|\eta| = 7.4$, were crucial for this exclusivity requirement (the BSC was used as a veto in the trigger).

Firstly we shall discuss the exclusive $\gamma\gamma$ search [143], which was combined with a CEP e^+e^- search [144], as the trigger (and most of the analysis) is identical. Only in the final step was the central tracking used to separate 16 e^+e^- events from three with electromagnetic showers with $E_T > 5$ GeV and no tracks. In all cases the showers had $\Delta\phi \sim \pi$ and $\sum \vec{E_T}$ small, and the e^+e^- events agreed with the precise QED expectation, providing a good control for the $\gamma\gamma$ candidates. The gap survival probability is not an issue for the QED events; the impact parameter is large and $S^2 \sim 1$. Also, the balance in E_T and $\Delta\phi$ should make it possible to find QED events (especially $\mu^+\mu^-$) in the presence of pile-up; this is now being studied in CDF. Background, e.g. from $\pi^0\pi^0$ in the $\gamma\gamma$ candidate sample, could not be quantitively assessed *a priori*, but two of the events had narrow single showers on each side and were very unlikely to be background. The prediction using the Durham model [142] is shown in Fig. 9. The prediction of $36^{\times 3}_{\div 3}$ fb for $E_T(\gamma) > 5$ GeV and $|\eta(\gamma)| < 1$ would give $0.8^{+1.6}_{-0.5}$ events, and the CDF data are in good agreement with this. The two events correspond to $\sim 10^{-12} \times \sigma_{\rm inel}$, showing that it is possible to find even very rare exclusive events. More CDF data has been taken with a lower threshold $E_T(\gamma) > 2.5$ GeV, and there are plans to search for exclusive $\gamma\gamma$ events at the LHC.

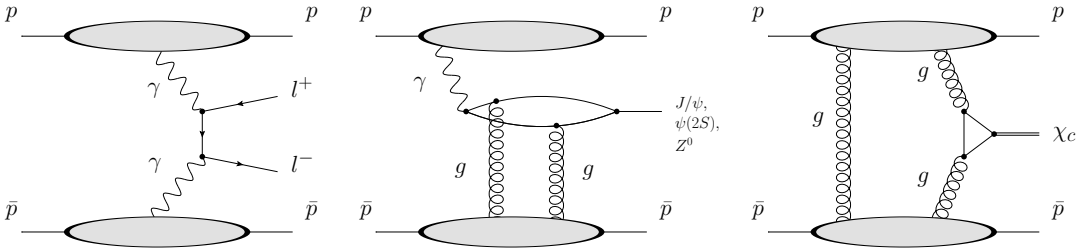

Figure 10: Feynman diagrams for processes contributing to the exclusive di-lepton signal. (a) $\gamma\gamma \to l^+l^-$, (b) $\gamma I\!P \to J/\psi, \psi(2S), Z^0$, and (c) $I\!P I\!P \to \chi_{c0}$.

In addition to the exclusive $\gamma\gamma$ search, CDF also studied the production of lepton pairs ($e^+e^-, \mu^+\mu^-$), either in association with no other particles or with one additional photon. Such exclusive leptons may be produced through several mechanisms, as shown in Fig. 10. We begin by discussing $\mu^+\mu^-$ production at low $M(\mu^+\mu^-)$, for which CDF used an exclusive di-muon trigger in the mass range $M(\mu^+\mu^-) \in [3.0, 4.0]$ GeV/c^2 and $|\eta_\mu| < 0.6$. The mass range was limited to $M(\mu^+\mu^-) > 3$ GeV/c^2, as below $p_T = 1.5$ GeV/c muons range out in the calorimeters.

Photoproduction of a vector meson, shown in Fig. 10(b), is one source of exclusive muon pairs in both ep and $pp(\bar{p})$ collisions. The predictions for the $p\bar{p}$ process are closely related to those for the ep process, bearing in mind the differing soft survival factors, $S^2(p\bar{p}) < S^2(ep)$. CDF recently

observed the production of J/ψ and $\psi(2S)$, with subsequent decay to $\mu^+\mu^-$, via this mechanism, the first such observation of vector meson photoproduction in hadron-hadron collisions [145]. Simply requiring rapidity gaps in conjunction with two central muons results in an extremely clean spectrum, and any non-exclusive background (mostly undetected proton dissociation) is at most a few percent, see Fig. 11. The cross sections agree with predictions [146, 147, 148]. Although these vector mesons cannot be produced in either $\gamma\gamma$- or $I\!P I\!P$-collisions, they could be produced in odderon-pomeron interactions. While the odderon is required in QCD [149], the couplings are expected to be suppressed compared to pomeron couplings and there is at present no direct evidence for it.

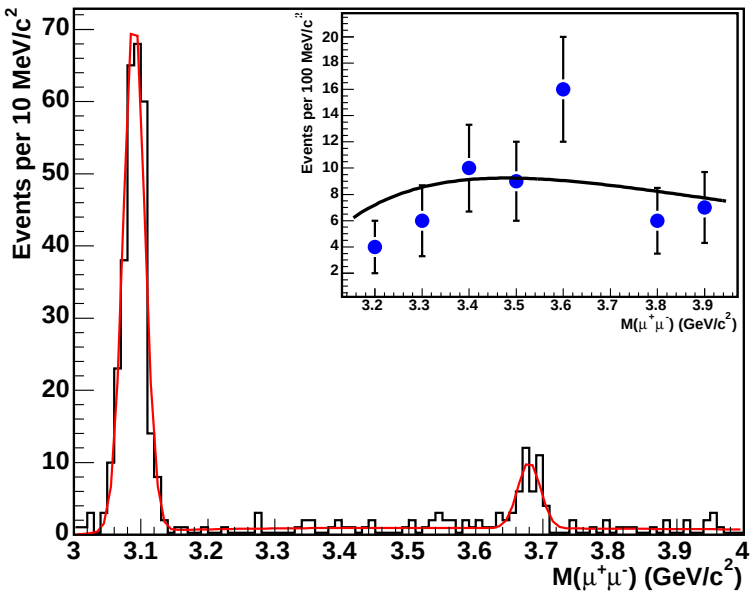

Figure 11: Di-muon mass distribution of exclusive $\mu^+\mu^-$ events in CDF, with no EM shower, (histogram) together with a fit to two Gaussians for J/ψ and $\psi(2S)$, and a QED continuum. Inset: Data above the J/ψ and excluding $3.65 < M(\mu^+\mu^-) < 3.75$ GeV/c^2 ($\psi(2S)$) with a fit to the QED spectrum. Figure from Ref. [145].

Another source of exclusive muon pairs, this time in association with a photon, is central exclusive χ_c production: $p + \bar{p} \to p + \chi_c + \bar{p}$, with subsequent decay: $\chi_c \to J/\psi + \gamma \to \mu^+\mu^- + \gamma$, see Fig. 10(c). This is a process much more closely related, at least theoretically, to CEP of a Higgs boson. Measurement of this at the Tevatron provides, together with exclusive dijets which we shall discuss shortly, a good test of the theory. CEP of $\gamma\gamma$ and χ_b are both superior theoretically, but unfortunately their cross sections are smaller. CDF has observed $p + (\chi_c \to J/\psi + \gamma) + \bar{p}$ events, with $\mathrm{d}\sigma/\mathrm{d}y|_{y=0}(\chi_c) = 76 \pm 10 \pm 10$ nb, assuming the χ_{c0} dominates [145] (CDF could not resolve different χ_c states). The theoretical predictions of the χ_{c0} cross section are in agreement with the measured value. Ref. [150] predicted $\mathrm{d}\sigma/\mathrm{d}y|_{y=0}(\chi_{c0}) = 130$ nb, however since that paper the PDG value of the χ_{c0} width was lowered by 45% [107], correcting their prediction to 90 nb and correcting Yuan's prediction [151] of 160 nb to 110 nb. Bzdak's prediction is 45 nb [152]. It should be noted however, that the assumed dominance of the χ_{c0} has been questioned. In Ref. [29] it was suggested that higher spin χ_c states may contribute to the cross section, with their smaller production rates being compensated by larger branching ratios. Indeed, a recent re-analysis has

been performed by the Durham group and collaborators, including the effects of non-factorising, "enhanced", contributions to the gap survival probability [153, 73]. Their studies suggest that the χ_{c0} production cross section is somewhat lower than previous determinations, but that the reduction to the total rate is compensated by the production of χ_{c1} and χ_{c2} states. They find for the total production of all three states, $\mathrm{d}\sigma/\mathrm{d}y|_{y=0}(\chi_c) = 65$ nb and the calculation has been implemented in the Monte Carlo SuperCHIC [154]. The agreement between theory and experiment is encouraging and indicates that the predictions for CEP Higgs production at the LHC are unlikely to be far off the mark.

Exclusive muon [145] (and electron [144]) pairs are also produced via the QED $\gamma\gamma$ fusion process, depicted in Fig. 10(a). This process generates a continuum in the $M(\mu^+\mu^-)$ distribution over the which the J/ψ and $\psi(2S)$ peaks are visible, as shown in Fig. 11. The continuum agrees in both shape and magnitude with the QED predictions. Also, since the exclusive $p + l^+l^- + p$ cross section is very well known (only Coulomb elastic scattering is as well known), it is a good candidate for measuring the absolute luminosity of the LHC, and thus for calibrating high-rate luminosity monitors. The limit to the precision ($\sim 1\% - 2\%$) with which this can be done will come from the knowledge of acceptances and efficiencies (favouring $\mu^+\mu^-$ over e^+e^-). One must do this in the presence of some pile-up, as the probability of vetoing on pile-up will depend on the unknown inelastic cross section. Another difficulty is that the protons may dissociate, e.g. $p \to p^* \to N\pi\pi$. The CDF BSCs, situated along both beam pipes, were efficient at detecting such dissociations, which create forward showers in the pipes and surrounding material. CMS and ATLAS do not yet have such counters, but there is a proposal to add them [155].

At high mass, lepton pairs may be produced in exclusive Z photoproduction, $\gamma I\!P \to Z$. A nearly real photon is radiated by one of the incoming beam particles, fluctuates into a $q\bar{q}$ pair, which then scatters by $I\!P$ exchange on the other proton, see Fig. 10(b). CDF performed a search for this reaction [156], however, the cross section is predicted to be only 0.21 fb [157] or 0.3 fb [147] at the Tevatron, far below the CDF sensitivity. In contrast, as we shall discuss in section 8.5, the cross section at the LHC is expected to be about 6 fb for $|y(Z)| < 2$ and the Z decaying to e^+e^- or $\mu^+\mu^-$ [147]. It would be very interesting to measure exclusive Z production, as BSM theories with additional particles in the $\gamma I\!P \to Z$ vertex loop change the cross section. For example, in White's theory of the pomeron there should be a "large" (but not quantified) increase, due to colour-sextet quark loops [158]. Exclusive $\gamma\gamma \to l^+l^-$ pairs have been seen with pair masses up to 75 GeV/c^2 and no observed Z candidates [156, 159].

Unlike exclusive lepton production, exclusive dijet production, $X = jj$, has the advantage of a relatively high cross section but, unlike $X = \gamma\gamma$ or χ_c, it is subject to the usual uncertainties associated with defining jets. CDF measured it from a sample of $DI\!PE$ dijet events, with a detected $\bar{p}$ together with a large gap on the p side [83]. They reconstructed the mass of the dijet system, M_{jj}, and the mass of all the particles in the central detectors, M_X. Exclusive dijets would have the ratio $R_{jj} = M_{jj}/M_X$, shown in Fig. 12, close to 1. Above $R_{jj} \sim 0.6$ the data show a significant excess over that expected from POMWIG, which is a Monte Carlo generator for diffractive processes, including an implementation of the Ingelman-Schlein model of $DI\!PE$ [160]. POMWIG is tuned to CDF and H1 data and does not include an exclusive component. After combination with a full CDF detector simulation, the excess is well described by the predictions for exclusive dijet production given by the ExHuME Monte Carlo generator [161], which implements the Durham model. Making such fits for several values of the minimum jet transverse energy, $E_T^{\min}$, CDF derived the exclusive

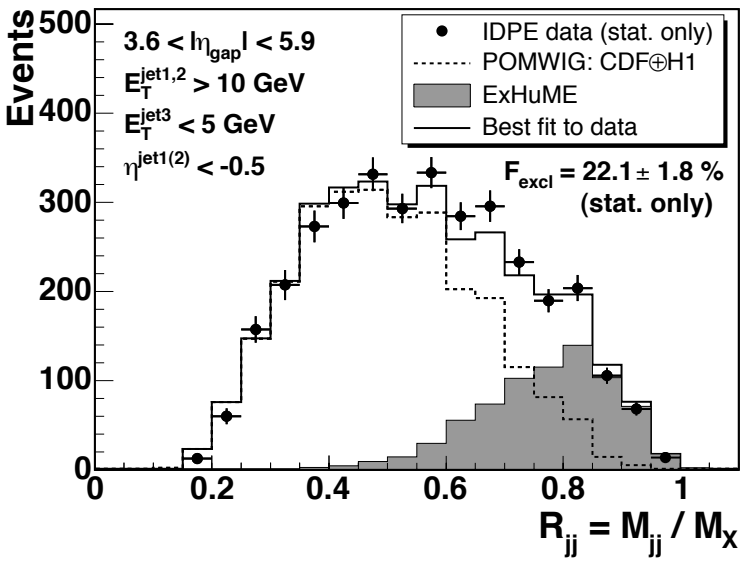

Figure 12: Dijet mass fraction for *DIPE* data (points) and best fit to the sum of two components: POMWIG *DIPE* + SD and ND background, and ExHuME (exclusive dijets). Figure from Ref. [83].

dijet cross section shown in Fig. 13. The data are far below the prediction of the DPEMC Monte Carlo generator [162], which implements the Saclay model discussed in Section 3.2, and although slightly below the ExHuME prediction the agreement is much better and certainly within the theoretical uncertainties[8].

Exclusive dijets are expected to come primarily from $gg \to gg$ since quark pair production, $gg \to q\bar{q}$, is suppressed due to the $J_z = 0$ rule, by a factor $\sim m_q^2/M_{jj}^2$ [29]. In particular (see for example [30])

$$\frac{\mathrm{d}\hat{\sigma}_{excl}}{\mathrm{d}t}(gg \to gg) = \frac{9}{4}\frac{\pi\alpha_s^2}{E_T^4} \tag{7.44}$$

and

$$\frac{\mathrm{d}\hat{\sigma}_{excl}}{\mathrm{d}t}(gg \to q\bar{q}) = \frac{\pi\alpha_s^2}{6E_T^4}\frac{m_q^2}{M_{jj}^2}\left(1 - \frac{4m_q^2}{M_{jj}^2}\right) \tag{7.45}$$

where these partonic cross sections are to be used in conjunction with Eq. (3.22). Light quark jets cannot easily be experimentally distinguished from gluon jets, but some c-jets and b-jets can be tagged by secondary vertices or displaced tracks. CDF found the that fraction of all exclusive dijets that are from c- or b-quark jets is suppressed at $R_{jj} > 0.5$ compared to lower R_{jj} values. This lends further support to the claim that the excess is due to CEP dijet production. Note that $q\bar{q}$ dijet suppression will be very important in reducing QCD backgrounds in exclusive $H \to b\bar{b}$ searches at the LHC, as we discuss in Section 8.1.

Tevatron luminosities are now (in 2009) too high, even at the end of a store, to study events with no pile-up. A search is being made in CDF [159] for exclusive $\Upsilon \to \mu^+\mu^-$ and high mass

[8]We note that better agreement between the Durham approach and the CDF dijet data was found in the analysis of Ref. [163].

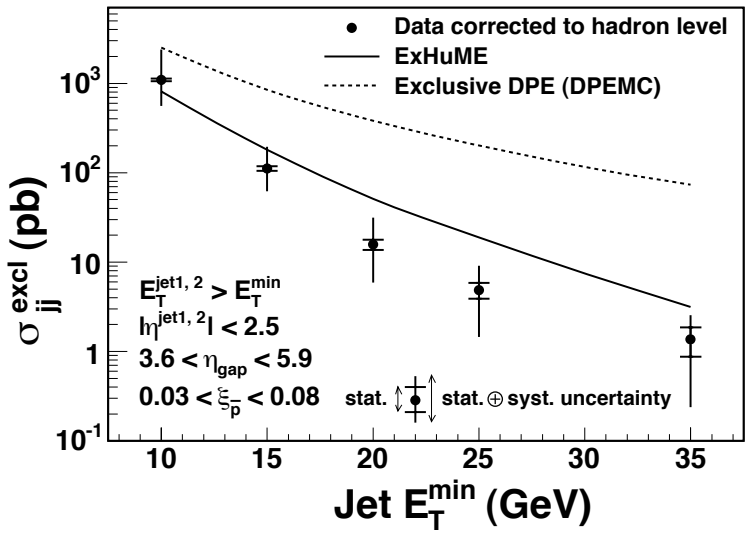

Figure 13: Exclusive dijet cross section *vs.* the minimum E_T of the two jets, compared to the DPEMC and ExHuME predictions. Figure from Ref. [83].

di-muons, with pile-up, based on their distinctive kinematics (and no associated tracks on the $\mu^+\mu^-$ vertex). Unfortunately $\chi_b \to \Upsilon + \gamma$ is not likely to be visible since the cross section is expected to be much smaller than that of the χ_c, and due to the difficulty in selecting the correct photon in events that are contaminated by pile-up.

8 The Large Hadron Collider

The idea to install detectors far from the interaction point at CMS and/or ATLAS with the capacity to detect protons scattered through small angles has gained a great deal of attention in recent years, and the report presented in Ref. [2] constitutes a significant milestone on the road to CEP physics at the LHC. Measurement of both protons by detectors located 420 m from the interaction point at ATLAS or CMS has the virtue that central systems with masses up to 200 GeV/c^2 can be measured with an event-by-event precision of $\sigma(M_X) \approx 2-3$ GeV/c^2. Adding detectors at 220–240 m extends the acceptance to much higher central system masses, with the limiting factor becoming the rate of the production process. Fig. 14 shows the forward detector acceptance as a function of central system mass for the case where both protons are detected at 420 m and when one is detected at 420 m and one at 220 m. The clean environment of CEP, combined with four-momentum constraints, makes for reduced backgrounds (even in the presence of significant amounts of pile-up), often aided by the fact that the centrally produced system is predominantly in a $J_z = 0$, C-even, P-even state [29, 164]. Of course having such a spin-parity filter also provides an excellent handle on the nature of any new physics. For little extra cost, forward detectors promise to significantly enhance the physics potential of the LHC.

That said, CEP is not without its challenges. As we have seen, the theory is difficult, triggering can be tricky, signal rates for new physics are often low, high precision tracking and

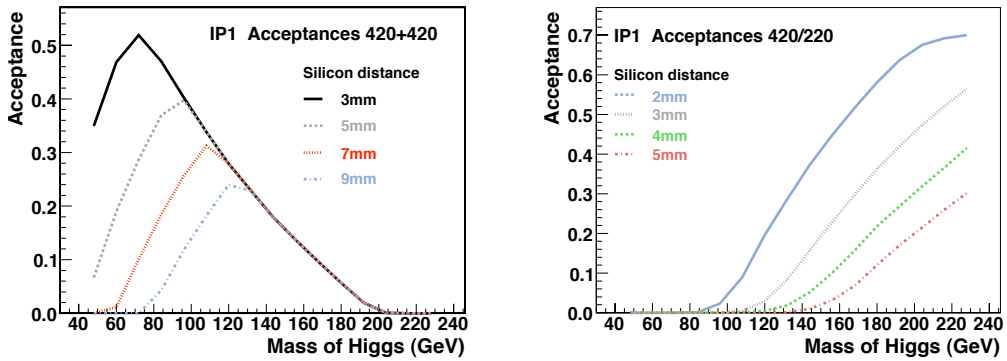

Figure 14: Forward proton detector acceptances, as a function of the Higgs mass (mass of the central system), in the case of two protons detected at 420 m (left) and in the case that one proton is detected at 420 m and one at 220 m (right). The different curves correspond to differing positions of the active edge of the tracking detector relative to the beam. Figure from Ref. [2].

timing detectors need building and installing and pile-up needs to be dealt with. As the last section showed, recent data on CEP from CDF at the Tevatron gives confidence in the theoretical modelling, and extensive studies have demonstrated that the other challenges can be met, e.g. see Ref. [2]. Both in ATLAS and CMS, detectors at 420 m are situated too far from the central detector to be included in the level 1 trigger, although this should be possible in a future upgrade of the data acquisition system. The data from the proton detectors are, of course, available for integration in a higher level trigger. Note that, unlike the 420 m detectors, those at 220–240 m could be included in the level 1 trigger.

8.1 Higgs: SM and MSSM

The possibility of observing central exclusive Higgs boson production, $p + p \to p + H + p$, is largely responsible for the current interest in exclusive processes at hadron colliders.

There are several important features of the CEP process which may allow one to extract, potentially unique, information on the structure of the Higgs sector. Firstly, precision measurements of the scattered proton momenta, in very forward detectors, offer the possibility of observing the Higgs as a bump in the missing mass distribution [2]. This is possible with a resolution $\sigma(M) \sim 2$ GeV/c^2 *per event*, regardless of the final state (provided one can trigger on the central system). The precise calibration of the forward detectors necessary to achieve such a measurement can be obtained from data, using another exclusive (QED) process: $p + p \to p + \mu^+\mu^- + p$. The muons can be measured very well in the central detector, and then both proton momenta are known with an uncertainty limited by the incoming beam momentum spread, $\Delta p/p \sim 10^{-4}$, i.e. $\Delta p \sim 700$ MeV. To get sufficient rate for calibration on a reasonable time scale (e.g. one day), one must use muon pairs with low mass, $M_{\mu^+\mu^-} \gtrsim 10$ GeV/c^2. This is too small to have any acceptance for detecting both protons but by selecting same-side-dimuon events with $|\eta_{\mu^\pm}| \geq 2$, one proton can have large enough momentum loss to be detected.

In addition to obtaining the mass and width (provided it exceeds a few GeV) of any observed Higgs, one can also probe its spin and CP properties, due to the $J^{PC} = 0^{++}$ selection rule. For non-zero angle scattering, the production of higher spin and odd parity states is allowed, though

they are strongly suppressed for high enough central masses by the smallness of the final state proton transverse momenta [164]. Given enough statistics one can distinguish the $J = 0$ and higher spin states, by the azimuthal correlations of the protons. Recall that at the ISR (Section 4), one could separate $X = \pi^+\pi^-$ data into S-wave ($J = 0$), P-wave ($J = 1$), and D-wave ($J = 2$) states, mass-bin by mass-bin, from the moments of the angular distributions of the pions, even finding a ρ peak that was too small to see in the raw $M_{\pi^+\pi^-}$ spectrum. This could be done at the ISR thanks to a high level of statistics that is not likely to be available in $p + p \to p + b\bar{b} + p$ data at the LHC, but the principle is the same.

The spin-selection rule also has the advantage that it leads to a leading-order suppression of the $b\bar{b}$ background in the CEP of $H \to b\bar{b}$ (the suppression goes like $\sim m_q^2/M_{JJ}^2$, see Eq.(7.45)). The production of exclusive dijets from light $q\bar{q}$ is likewise negligible, but CEP of gluon pairs receives no such suppression. Exclusive dijets, $X = JJ$, are thus mostly gg jets, with a modest admixture of $b\bar{b}$ jets. The gg dijets can be discriminated against by heavy-flavour tagging, using a combination of displaced vertices and leptons in the jets from both c- and b-quark decays. In the exclusive dijet case one can also profit from the fact that we can have $JJ = b\bar{b}$ or gg, but pairs with net flavour (e.g. bg or bc) are forbidden. Gluon splitting ($g \to b\bar{b}$) can be reduced by requiring both jets to be tagged.

Fig. 15 shows how the cross section for producing a CEP SM Higgs varies with Higgs mass for different gluon distribution functions. The cross section is small and leads to low production rates. In particular, the $b\bar{b}$ channel is very challenging, due to the aforementioned backgrounds and the additional background coming from pile up interactions at high luminosity, which we shall discuss in more detail later. Triggering in this case would certainly benefit from having 220–240 m detectors in place, but even then one relies on optimistic scenarios for the production cross section, detector acceptance and trigger efficiency.

In contrast, the observation of a SM Higgs in the $WW^{(*)}$ channel is more promising. An initial study of the fully leptonic ($l^+l^-\not{E}_T$) and semi-leptonic ($l^-\not{E}_T JJ$) decay modes, with basic experimental cuts, was performed in [165]. The backgrounds considered in this study were $\gamma\gamma$ fusion and exclusive $q\bar{q}$ production with W-strahlung. The contribution of $gg \to W^+W^-$ through a quark loop was also considered, but found to be negligible. In order to bring these backgrounds under control a range of cuts were employed. The rapidities of the W decay products, in the signal case, are mostly central. In contrast, the backgrounds favour a more forward distribution, hence a cut of $|\eta| < 2.5$ was imposed. The $\gamma\gamma$ process is dominated by the region in which the outgoing protons carry very small transverse momenta, and a cut was therefore made to remove this region. Finally, the dijet invariant mass was constrained to lie within a window around the W mass, thus reducing the background from $q\bar{q}$ events not due to W decay. After imposition of these cuts one could expect, for Higgs masses in the range 140 GeV/c^2 $< m_H <$ 200 GeV/c^2, $\sim 2 - 3$ events in 300 fb^{-1} of data, with no appreciable background. One of these would be in the gold-plated fully leptonic channel, producing the striking signature of an event containing two leptons with no other tracks on the vertex and a large missing E_T. A subsequent analysis of the $WW^{(*)}$ channel with a fast detector simulation, taking into account pile-up background and using a more refined triggering strategy, found that the signal should be observable, with signal to background ratio of 1 or better, for $m_H \gtrsim 120$ GeV/c^2 and 300 fb^{-1} of data [2].

Unlike the SM case, the $b\bar{b}$ channel can be rather easier to explore in certain MSSM scenarios. The neutral part of the MSSM Higgs sector consists of one light and one heavy CP-even scalar, the

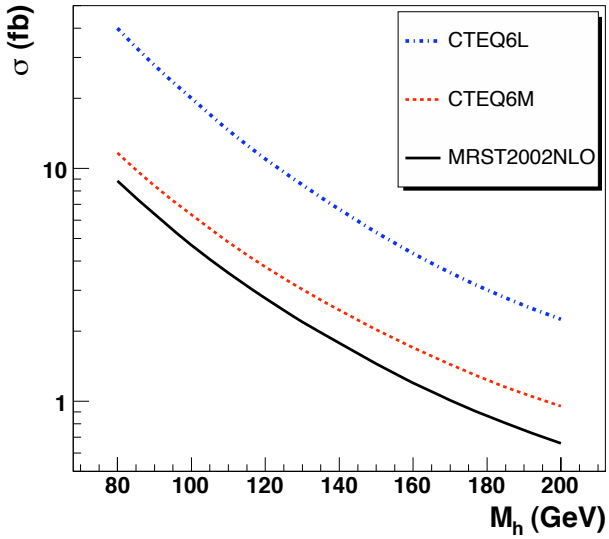

Figure 15: CEP cross section for Standard Model Higgs production. Figure from Ref. [2].

h and H respectively, and one CP-odd scalar, the A. For large $\tan\beta$ and small m_A, the $hb\bar{b}$ coupling is strongly enhanced over the SM case. Fig. 16 shows an example of the region of parameter space[9] in which one could observe $h \to b\bar{b}$ using CEP, for different amounts of integrated luminosity. Fig. 17 shows the result of an in-depth analysis of one particular point in the $m_A - \tan\beta$ plane ($\tan\beta = 40$ and $m_A = 120$ GeV/c^2) [166]. The details of the two analyses can be found in Refs. [2, 166, 167, 168] and they are in broad agreement.

A similar pair of plots for $H \to b\bar{b}$ are shown in Fig 18. In addition to sensitivity in the low m_A region, one can also hope to probe reasonably large values of m_A (at large enough $\tan\beta$). If the MSSM parameters are in this region, an observation using CEP could be critical to understanding the Higgs sector at the LHC. This is because, in the large m_A limit, referred to as the "decoupling limit", the light CP-even Higgs becomes SM-like. In contrast, the coupling of the H and A (which are approximately mass degenerate) to SM gauge bosons is strongly suppressed. As a result, the dominant decay of the H and A is to $b\bar{b}$ ($\tau^+\tau^-$ typically contributes approximately 10%). This leads to the so called "LHC wedge region" [169, 170, 171], where the H and A may escape detection in inclusive searches. Not only that, but current inclusive techniques, proposed to probe the spin and CP properties of the Higgs sector, rely on either the ZZ decay mode at high mass [172] or vector boson fusion at low mass [173, 174, 175], both of which would be suppressed in this case (see also the discussion of this point in Ref. [168]). It should also be noted that this decoupling of higher mass Higgs states from the SM gauge bosons is a common feature of extended Higgs sectors, since such couplings are constrained by the electroweak precision fits. Furthermore, the CEP production of the A boson is strongly suppressed by the parity-even selection rule. This means that any measurement of the H mass and width using the forward proton detectors is unaffected by a nearby A. This is not the case in inclusive production.

[9] In the $M_h^{\max}$ scenario with $\mu = +200$ GeV.

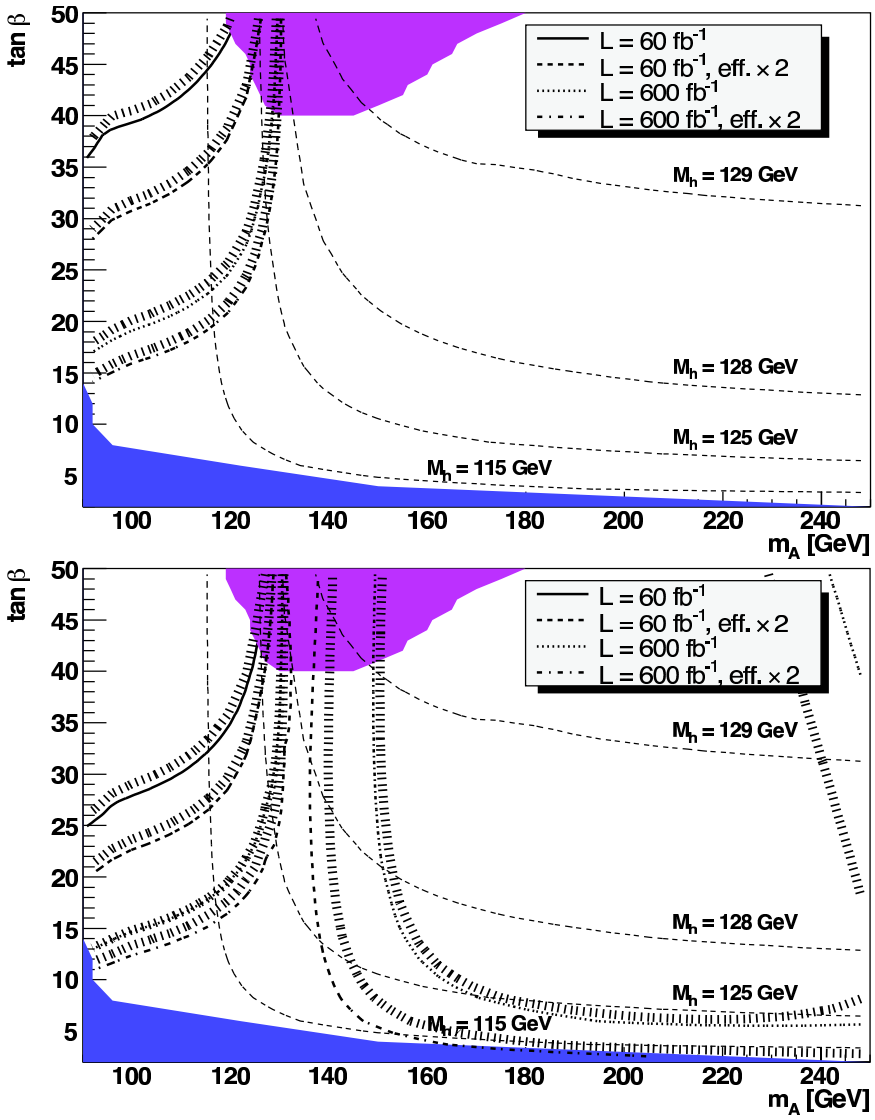

Figure 16: 5σ discovery contours (upper plot) and contours of 3σ statistical significance (lower plot) for the $h \to b\bar{b}$ channel in CEP in the M_A - tanβ plane of the MSSM within the $M_{h,\max}$ benchmark scenario ($\mu = +200$ GeV) for different luminosity scenarios. The values of the mass of the light CP-even Higgs boson, M_h, are indicated by contour lines. The blue shaded region corresponds to the parameter region that is excluded by the LEP Higgs boson searches, while the purple shaded region is that excluded by searches at the Tevatron. Figure from Ref. [168].

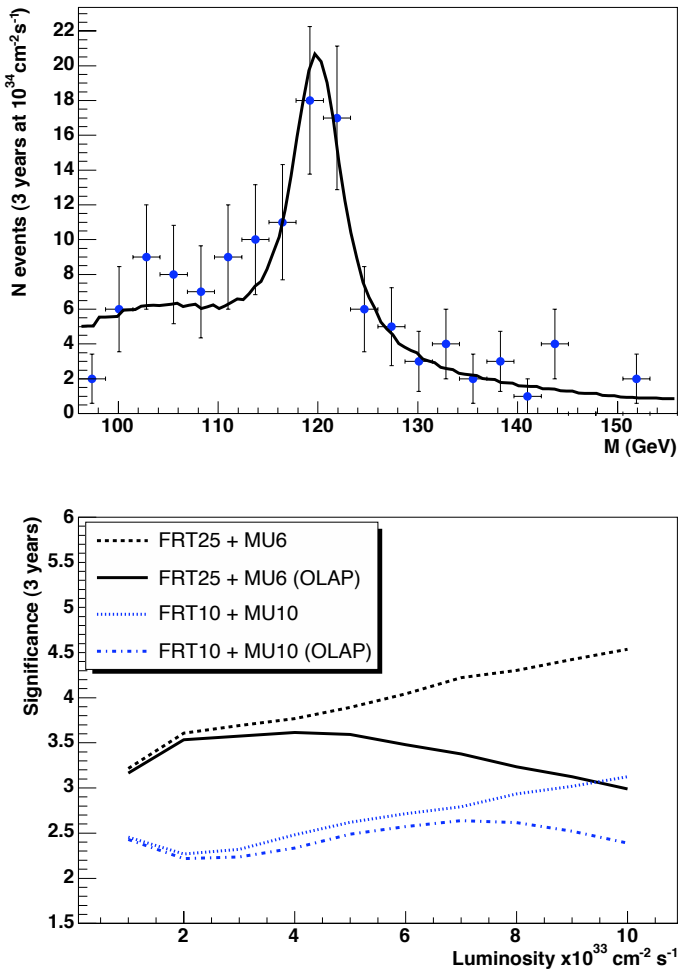

Figure 17: Upper: A typical mass fit for the 120 GeV/c^2 MSSM $h \to b\bar{b}$ after 3 years of data taking at 10^{34} cm^{-2} s^{-1} and after removing the overlap background contribution completely (e.g. using improved timing detectors). The significance is 5σ for these data. Lower: Significance of the measurement of a 120 GeV/c^2 MSSM Higgs boson versus luminosity, for two different combinations of muon (MU6, MU10) and fixed-jet-rate (FRT25, FRT10) triggers. In each case the curves correspond to the baseline (lower) and improved-timing (upper) scenarios, i.e. the curves labelled "OLAP" include pile-up background. Figure from Ref. [2].

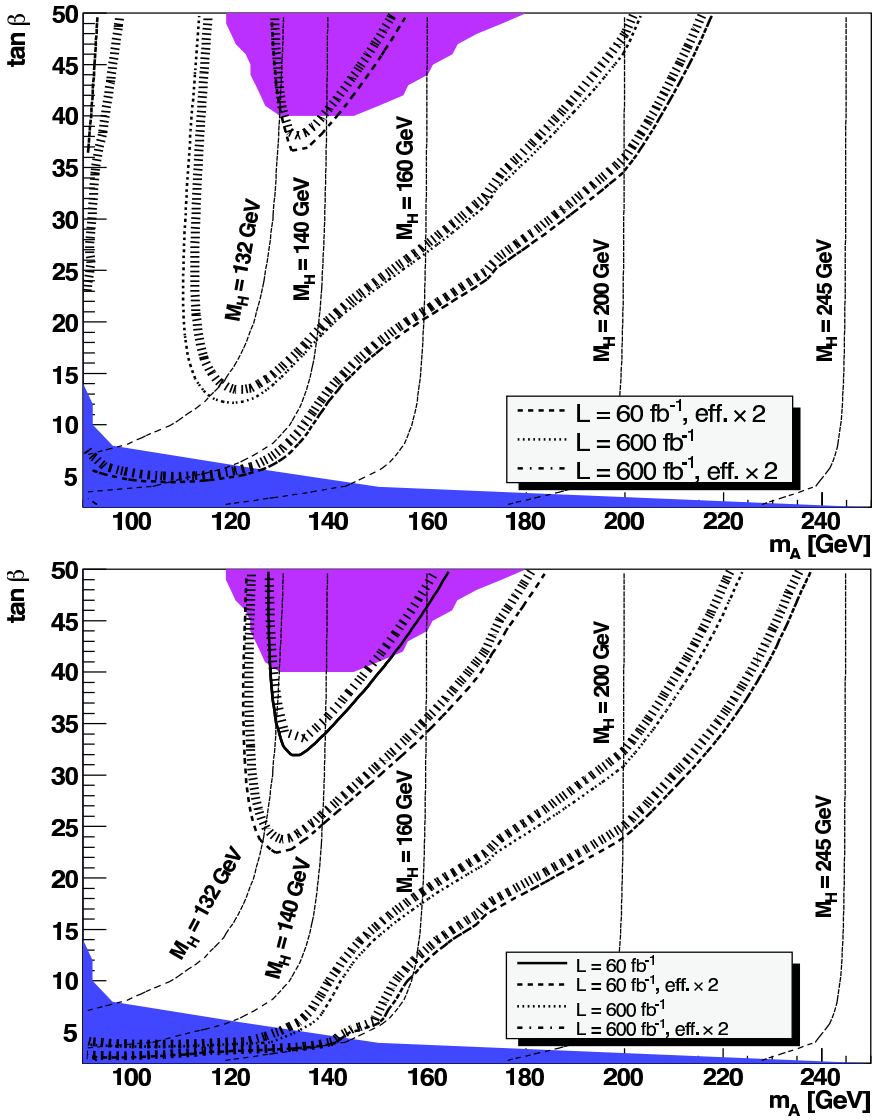

Figure 18: 5σ discovery contours (upper plot) and contours of 3σ statistical significance (lower plot) for the $H \to b\bar{b}$ channel in CEP in the M_A - tanβ plane of the MSSM within the $M_{h,\max}$ benchmark scenario ($\mu = +200$ GeV) for different luminosity scenarios. The values of the mass of the heavy CP-even Higgs boson, M_H, are indicated by contour lines. The blue shaded region corresponds to the parameter region that is excluded by the LEP Higgs boson searches, while the purple shaded region is that excluded by searches at the Tevatron. Figure from Ref. [168].

Returning to Fig. 17, the curves in the lower plot correspond to different trigger scenarios. They also indicate the influence of pile-up background, which is of concern to any CEP analysis. For brevity we denote a signal event with two detected protons and a central state all arising from the same collision as [pXp]. Pile-up backgrounds can originate when one or both protons and the central system originate from different pp collisions. If they originate from three different collisions (triple pile-up) we write [p][X][p] and if they originate from two different collisions (double pile-up) we write [pX][p] or [pp][X]. In the latter case, since there is no acceptance for pure elastic scattering, the central detector will contain particles from both the collision that led to the two measured protons, as well as the particles from the second collision (which has no detected protons). The double and triple pile-up rates both grow strongly with luminosity and at $L \approx 10^{34}$ cm^{-2}s^{-1} [p][X][p] typically dominates [2]. Fortunately there are many ways of reducing the pile-up background to manageable proportions. By measuring the four-momentum of the protons, one can determine the mean rapidity, p_T and invariant mass of the central system. Consistency between these values and those obtained using the central detector then provide a strong constraint. Furthermore, a very large reduction in the pile-up background can come from a precision measurement of the difference in time Δt between the arrival of the two protons in the forward detectors [2]. If they came from the same collision, displaced a distance z_{pp} from the nominal vertex, then $\Delta t = 2z_{pp}/c$ and one can require agreement between the measurements of z_{pp} by the forward proton detectors and as determined from the central tracks. The resolution is $\sigma(z_{pp}) = 2.1$ mm (3 mm/$\sqrt{2}$) for $\sigma(\Delta t) = 10$ ps. As the distribution of interactions has a spread around 60 mm (at 1σ) this leads to a large reduction in pile-up background. Detectors with time resolution ~ 10 ps have been developed for this purpose, and there is hope for further improvement (the spread in arrival times due to different proton trajectories is only ~ 2 ps).

In principle there are two other ways in which pile-up background can be reduced by fast timing. Firstly, additional calibrations could permit the actual collision time to be measured using the forward protons. The collisions in a bunch crossing have a time spread ~ 160 ps. If the individual collision times could also be measured using the detectors in the central region, a match with the collision time from the protons would give additional pile-up rejection. At present the central detectors do not have sufficient time resolution to make this practical. Secondly, one could place arrays of small (~ 1 cm^2) fast-timing detectors in the forward regions, e.g. $3 < |\eta| < 5$. Most inelastic collisions will produce particles in both regions, but central exclusive events will not. One can then veto events that contain extra particles originating from the collision vertex (which is defined by the measured protons). In the limit of the complete elimination of pile-up background, one could make a 5σ discovery of an MSSM Higgs boson with 3 years of high luminosity (10^{34} cm^{-2}s^{-1}) data taking (the mass peak is illustrated in the upper plot in Fig. 17).

8.2 Higgs: NMSSM

We now look at the capabilities for CEP of Higgs boson production in the Next-to-Minimal Supersymmetric Standard Model (NMSSM). More details can be found in [176]. Before discussing the specific details, let us emphasise that this scenario is particularly interesting since it deals with the possibility that a Higgs of mass ~ 100 GeV/c^2 decays predominantly to light particles (in the case we shall review it is four taus). Such a troublesome decay channel should be taken seriously and, as we shall see, CEP can provide an excellent means to study decays of this type.

The NMSSM is an extension of the MSSM that solves the μ-problem, and also the little

hierarchy problem. It achieves this by adding a gauge-singlet superfield, $\hat{S}$, to the MSSM such that the μ term is now dynamical in origin, arising when the scalar member of $\hat{S}$ aquires a vacuum expectation value (VEV). Since μ is no longer fundamental and therefore is no longer naturally of order the GUT scale (as would be the case if it were the only dimensionful parameter in the superpotential), the μ-problem is solved. The little hierarchy problem is also solved because a lighter Higgs is allowed, thereby taking the pressure off the stop mass, $m_{\tilde{t}}$. More specifically, the lightest scalar Higgs can decay predominantly to two pseudoscalar Higgses and the branching ratio to b-quarks is correspondingly suppressed, thereby evading the 114 GeV/c^2 bound from LEP (it drops to 86 GeV/c^2). Having a lighter Higgs means that $m_{\tilde{t}}$ does not need to be so large, and that is preferred by the Z boson mass.

The Higgs sector of the NMSSM extends that of the MSSM by adding an extra pseudoscalar Higgs, the a and an extra scalar Higgs; crucially $\hat{S}$ is a gauge singlet and hence $h \to aa$ can dominate with a light a (i.e. below the threshold for $a \to b\bar{b}$). Freed of the heavy $\tilde{t}$, it is natural to have a light

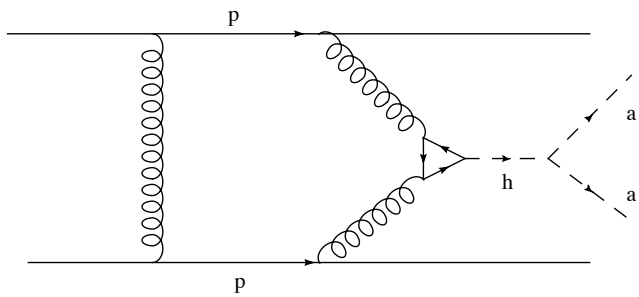

Figure 19: CEP of an NMSSM Higgs.

Higgs with a reducing branching ratio to b-quarks. Masses of the h in the range 85–105 GeV/c^2 are most natural in this scenario and our attention will focus on $m_h = 93$ GeV/c^2 and $m_a = 9.7$ GeV/c^2 with BR($h \to aa$) = 92% and BR($a \to \tau\tau$) = 81% [177]. The lightness of the pseudoscalar a means that the h decays predominantly to 4τ. Should such a decay mode be dominant at the LHC, standard search strategies could fail and, as we shall see, CEP (as illustrated in Fig. 19) could provide the discovery channel. This "natural" scenario of the NMSSM has two additional bonus features that one might draw attention to: (1) A light Higgs is preferred by the precision electroweak data (recall that the best fit value is somewhat below 100 GeV/c^2), and (2) A $\sim$100 GeV/c^2 Higgs with a reduced ($\sim$10%) branching ratio to b-quarks naturally accommodates the existing 2.3 σ LEP excess in $e^+e^- \to Zb\bar{b}$ [178, 179].

To detect the 4τ decay of an NMSSM Higgs using CEP, we need first to trigger on the event. In this regard, we require that at least one of the τs decays to a sufficiently high p_T muon (or two decay to lower p_T muons). The detailed analysis is outlined in [176], here we shall just highlight the key features. Table 2 shows how the signal (CEP) and backgrounds are affected by the cuts imposed. The backgrounds are typical of CEP Higgs studies: DPE refers to the $D\!\!\!\!\mathcal{P}E$ production of a pair of b-quark jets (which is the dominant $D\!\!\!\!\mathcal{P}E$ background after b-tagging both jets) and it was simulated using the POMWIG Monte Carlo [160]; OLAP refers to the background due to pile-up, in particular the three-fold coincidence of two single-diffractive events with an inclusive $pp \to X$ event. The QED background arises from $\gamma\gamma \to 4\tau$ and is easily removed.

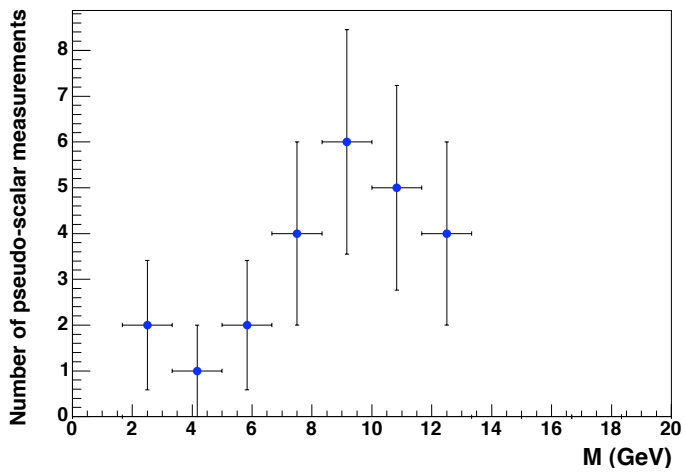

Figure 20: A typical a mass measurement. Figure from Ref. [176].

The top line of the table is the cross section after requiring that there be at least one muon with $p_T > 6$ GeV/c, which is the nominal minimum value to trigger at level 1[10], and the condition that both protons be detected in the 420m detectors. There is also a loose cut on the invariant mass of the central system. Of the remaining cuts, we single out the "$N_{\rm ch} = 4$ or 6" cut for special mention. The charged track ($N_{\rm ch}$) cut is noteworthy because it can be implemented at the highest LHC luminosities: we cut on 4 - 6 charged tracks that point back to the vertex defined by the muon. Pile-up events add extra tracks (to both the signal and background), but they do not often coincide with the primary vertex (e.g. within a 2.5 mm window) and do not spoil the effectiveness of this cut. The ability to make such hard cuts on charged tracks is of much wider utility than in this analysis. The 4–6 track event is then analysed in terms of its topology, exploiting the fact that the charged tracks originate from four taus in the signal, which themselves originate from two heavily boosted pseudoscalars. This analysis is purely track-based with almost no reliance on the calorimeter, which is more affected by pile-up.

Accurate measurements of the proton momenta allow one to constrain the kinematics of the central system (in particular its invariant mass, p_T, and rapidity are known). We can also extract the masses of the h and a on an event-by-event basis. The mass of the h is straightforward (it is measured directly by the forward proton detectors) and a precision below 1 GeV/c^2 can be obtained with just a few events. The measurement of the pseudoscalar mass is more interesting and potentially very important. The proton measurements fix p_z, and $p_{x,y} \approx 0$ for the central system. In addition, the τ pairs are highly boosted, which means they are collinear with their parent pseudoscalars. Thus the four-momentum of each pseudoscalar is approximately proportional to the observed (track) four-momentum. The two unknown proportionality constants (i.e. the missing energy fractions) are overconstrained, since we have three equations from the proton detectors. The result is that we can solve for the pseudoscalar masses, with four measurements per event. Fig. 20 shows a typical distribution of a masses based on 180 fb^{-1} of data collected at 3×10^{33} cm^{-2}s^{-1}.

Although we can expect only a small number of signal events, the background is under

[10] It will turn out that a higher cut of 10 GeV/c is preferred in the subsequent analysis.

	CEP			DPE	OLAP	QED	
Cut	H	$b\bar{b}$	gg	$b\bar{b}$	$b\bar{b}$	4τ	$2\tau\ 2l$
p_{T0}^{μ}, ξ_1, ξ_2, M	0.442	25.14	1.51×10^3	1.29×10^3	1.74×10^6	0.014	0.467
$N_{\rm ch} = 4$ or 6	0.226	1.59	28.84	1.58×10^2	1.44×10^4	0.003	0.056
$Q_h = 0$	0.198	0.207	3.77	18.69	1.29×10^3	5×10^{-4}	0.010
Topology	0.143	0.036	0.432	0.209	1.84	-	<0.001
p_T^{μ}, isolation	0.083	0.001	0.008	0.003	0.082	-	-
$p_T^{1,\mu'}$	0.071	5×10^{-4}	0.004	0.002	0.007	-	-
$m_a > 2m_\tau$	0.066	2×10^{-4}	0.001	0.001	0.005	-	-

Table 2: The table of cross sections for the signal and backgrounds for NMSSM Higgs production. All cross sections are in femtobarns. The pile-up (OLAP) background is computed at a luminosity of 10^{34} cm^{-2} s^{-1}. From Ref. [176].

control. One should be able to collect 4 signal events, on a background of 0.1 events, with 3 years running at an instantaneous luminosity of 5×10^{33} cm^{-2}s^{-1}. Even with these few events, one may extract the masses of both the a and the h, with a resolution below 2-3 GeV/c^2. The statistical significance of any discovery can exceed 5σ in a few years of running at luminosities in excess of 10^{33} cm^{-2}s^{-1}.

8.3 Other new physics

In addition to the MSSM and NMSSM Higgs studies, the CEP of a number of other BSM central systems has been considered in the literature.

For instance, in [180] a CP-violating version of the MSSM was studied. In such a model, the h, H and A may all mix to produce mass eigenstates, H_1, H_2, H_3, of indefinite CP. For large $\tan\beta$, the couplings of the H_i to $b\bar{b}$ and $\tau^+\tau^-$ are enhanced, the states are naturally nearly mass degenerate (separated by a few GeV/c^2) and strong mixing between the states leads to a complicated resonance structure. The CEP of the H_i, with decay to $b\bar{b}$ and $\tau^+\tau^-$ was studied and it was shown that the missing mass distribution could be used to perform a line-shape analysis of the resonance structure, which is probably impossible in inclusive production. Also in the CP-violating MSSM, but in a different parameter region, the LEP bounds on the lightest Higgs mass become much weaker. In [181, 182], CEP of such a light Higgs was studied, though in this case the $b\bar{b}$ channel appears not to be observable and the $\tau^+\tau^-$ channel is marginal.

Another extension of the Higgs sector studied in relation to CEP is a triplet Higgs model in which the Higgs sector consists of one complex Higgs doublet and two triplets (one real and one complex) [183]. In such a model, the neutral Higgs associated with the doublet, H_1^0, has an enhanced coupling to fermions[11]. The observation, using forward proton detectors, in the $H_1^0 \to b\bar{b}$ channel was considered and it was found to be observable, with a significance ranging from $\sim 4\sigma - 14\sigma$ over

[11] The H_1^0 becomes the Standard Model Higgs boson for vanishing doublet-triplet mixing.

much of the parameter space with 60 fb^{-1} of data. With such data, the mass could also be measured very accurately, with an expected error less than 2 GeV/c^2 over a significant region of parameter space (and in some regions better than 0.3 GeV/c^2).

In some extensions of the SM the Higgs decays predominantly to unobservable particles. The CEP of such an "invisible Higgs" has been studied in [184]. However, while a detection in the CEP channel would be especially useful, since it would not rely on the detection of the Higgs decay products, it is not clear that pile-up backgrounds can be brought sufficiently under control.

CEP Higgs production has also been studied in a model where the SM is complemented by a fourth generation of very heavy fermions [168]. The Higgs coupling to gluons in such a model is typically larger than in the SM. In the $H \to b\bar{b}$ channel, it was found that a significance in excess of 3σ could be obtained with 60 fb^{-1} of data over the range 114 GeV/$c^2 \lesssim m_H \lesssim$ 145 GeV/c^2 not excluded by LEP or the Tevatron[12].

Away from the Higgs sector, the production of long-lived gluinos, expected in the "Split Supersymmetry" model [185, 186], was studied in Ref. [187]. Such particles hadronise to produce so-called R-hadrons which look much like slow muons. The CEP process in this case is particularly clean, since cuts on the velocity of the R-hadrons reduce the muon background to a negligible level. It was found that the measurements from the forward proton detectors could in this case give a measurement of the gluino mass to better than 1%, for masses below 350 GeV/c^2 and with 300 fb^{-1} of data. Although not a discovery channel, such a measurement would be highly complementary to any measurement in inclusive production, which suffers from large systematic uncertainties in this mass region [188].

Another model relevant to CEP is White's theory of the critical pomeron [158], which requires the existence of a pair of massive colour sextet quarks, Q_S. Since Q_S loops couple strongly to the pomeron and to weak bosons, processes such as $I\!P I\!P \to W^+W^-$ and ZZ (but not WZ) should occur with a much enhanced cross section. The threshold for this process is above the Tevatron energy but below the LHC energy. The enhanced cross section may even be visible without forward proton tagging, but the latter will be needed to demonstrate that $I\!P I\!P$ interactions are responsible. Photoproduction of Z, $\gamma I\!P \to Z$, should also be enhanced a factor ≥ 10 over the SM, and should be detectable.

8.4 Two photon collisions

So far in this review our attention has focussed mainly on CEP via the strong interaction. At the LHC, high proton luminosities will ensure that the flux of bremsstrahlung photons off the colliding beams is sufficiently large for CEP via $\gamma\gamma \to X$ and $\gamma I\!P \to X$ to be of interest. We focus in this section on the former. The elastic photon flux is shown in Fig. 21, from which the corresponding pp cross section, $\mathrm{d}\sigma_{pp}$, can be obtained:

$$\mathrm{d}\sigma_{pp} = \int \frac{\mathrm{d}L_{\gamma\gamma}}{\mathrm{d}W_{\gamma\gamma}} \mathrm{d}\sigma_{\gamma\gamma}\, \mathrm{d}W_{\gamma\gamma} \ , \tag{8.46}$$

where the integral is over the $\gamma\gamma$ centre-of-mass energy, $W_{\gamma\gamma}$. To put this flux in context, we note that it corresponds to a $\gamma\gamma$ luminosity that is 1% of the pp luminosity for the production of central

[12]The region $m_H \gtrsim 220$ GeV/c^2 is also experimentally allowed, however the CEP rate for $H \to b\bar{b}$ is too low to be accessible in this region.

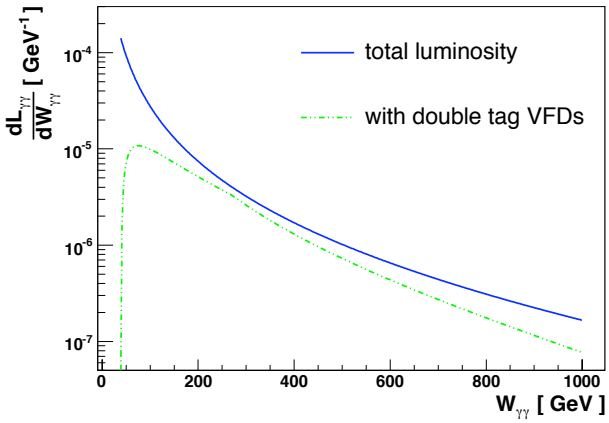

Figure 21: Luminosity spectrum for photon-photon collisions at the LHC in the range $Q^2_{min} < Q^2 < 2$ GeV^2 (solid blue line) compared to the corresponding luminosity if the energy of each photon is restricted to the forward detector tagging range 20 GeV $< E_\gamma <$ 900 GeV (dashed green curve). Figure from Ref. [189].

systems with mass greater than 23 GeV/c^2, falling to 0.1% for masses above 225 GeV/c^2. In addition, the photon virtualities are cut-off sharply by the proton electromagnetic form factor and are small, i.e. $\langle Q^2 \rangle \approx 0.01$ GeV^2; they can usually be assumed to be zero.

Our discussion in this section follows closely the presentation in [2, 189]. In turn, we will consider CEP of: (i) lepton pairs; (ii) weak vector boson pairs; (iii) supersymmetric (SUSY) pairs. The first of these (especially using muon pairs) is a good candidate for measuring the LHC absolute luminosity, the second is an accurate probe of the $\gamma\gamma WW$ coupling and the latter could be used to make accurate mass measurements of the SUSY particles from the forward protons.

Processes		σ (fb)	**Generator**
$\gamma\gamma \to$	$\mu^+\mu^-$ ($p_T^\mu > 2$ GeV/c, $\lvert\eta^\mu\rvert < 3.1$)	72 500	LPAIR [190]
	W^+W^-	108.5	MG/ME [191, 192]
	F^+F^- ($M = 100$ GeV/c^2)	4.06	//
	F^+F^- ($M = 200$ GeV/c^2)	0.40	//
	S^+S^- ($M = 100$ GeV/c^2)	0.68	//
	S^+S^- ($M = 200$ GeV/c^2)	0.07	//
	$H \to b\bar{b}$ ($M = 120$ GeV/c^2)	0.15	MG/ME [191, 192]

Table 3: Production cross sections for $pp \to p + X + p$ (via $\gamma\gamma$ exchange) for various processes (F = fermion, S = scalar). M is the mass of the corresponding particle. Table from Ref. [189].

Using a modified version of MADGRAPH/MADEVENT [191, 192], the Louvain group [189] has computed the production cross sections for the various processes of interest. These are tabulated in Table 3. Since the cross sections for pair production depend only on the charge, spin and mass of the

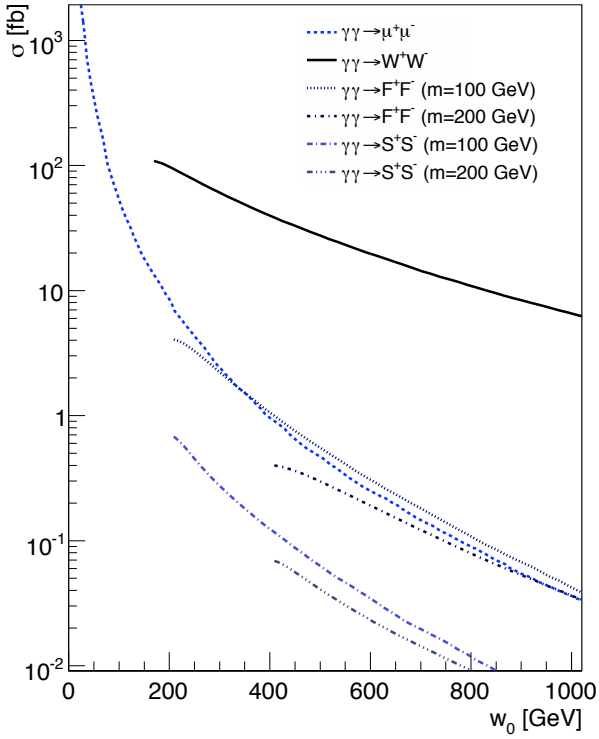

Figure 22: Cross sections for various $\gamma\gamma$ processes at the LHC as a function of the minimal $\gamma\gamma$ centre-of-mass energy W_0. Figure from Ref. [189].

produced particles, the results are shown for singly-charged, colourless fermions and scalars of two different masses. The cross sections are also shown as a function of the minimal $\gamma\gamma$ centre-of-mass energy W_0 in Fig. 22. Note the hierarchy of cross sections, which is driven by the spin of the relevant t-channel exchange. The cross sections are large enough to merit further study. The two-photon production of SUSY pairs was first studied in [193] and the exclusive two-photon production of a SM Higgs was studied in Refs. [194, 195]. The rate is significantly smaller than that arising from strong dynamics (see Fig. 15) but it could become particularly interesting in the case of an enhanced $H\gamma\gamma$ coupling.

Lepton pairs

Two photon collisions can produce exclusive pairs of any charged particles, but it will probably not be possible to observe $\gamma\gamma \to q\bar{q}$ because of overwhelming strong interaction backgrounds ($D\mathbb{P}E$). However, lepton pairs ($e^+e^-, \mu^+\mu^-$ and also, to some extent, $\tau^+\tau^-$) should have very small backgrounds, even in the presence of pile-up. One requires that there are no additional charged particles on the dilepton vertex, and that $p_T(l^+l^-)$ is very small or, equivalently, that the leptons are highly back-to-back ($|\pi - \Delta\phi| \lesssim 1.0$ GeV$/M_{l^+l^-}$ rad) and with similar p_T. The $\Delta\phi$ cut is especially powerful as it is forgiving of poor momentum resolution at high mass. The cross sections, calculated by the LPAIR Monte Carlo [190] at $\sqrt{s} = 14$ TeV, integrated over $M_{\mu\mu} > M_{\mu\mu}(min)$ and for different

η_{max}, are well approximated by the purely empirical fit:

$$\sigma(M_{min}, \eta_{max}) = (480 - 1.25 \times M_{min}) \times \frac{\eta_{max}^{2.2}}{M_{min}^{2.4}} \text{pb} \ . \tag{8.47}$$

This equation agrees with the predictions of LPAIR to within $\pm 4\%$ for M_{min} from 8 GeV/c^2 to 100 GeV/c^2 and out to $\eta_{max} = 3$. This pure QED cross section is so well known that it may provide the most precise measurement of the luminosity of the LHC [195, 196, 197, 198, 199, 200, 201] (integrated over a period), and help calibrate the luminosity monitors, which give a prompt rate measurement. For example the cross section for $M_{\mu^+\mu^-} > 10$ GeV/c^2 and $|\eta| < 2.0$, where one should have excellent and very well-known acceptance, is 8.55 pb. In 500 pb^{-1}, with an unprescaled trigger, one would therefore have ~ 4275 events, which translates into a $\sim 1.5\%$ statistical uncertainty. A knowledge of the acceptance and efficiencies at this level is thus desirable. Without detecting both protons (and no LHC experiments will be able to do that in normal low-β (high luminosity) running at such low masses) a concern is that one or both protons may dissociate. This probability can be measured in shower counters along the beam pipes at low luminosity, when pile-up can be neglected.

Although the QED calculation of the dilepton cross section is accurately known, one still needs to worry about the issue of gap survival S^2. We have already seen that this suppression is large for CEP Higgs production, however $\gamma\gamma$ collisions are much more peripheral and the gap survival factor is much larger. Nevertheless, it must be understood at the percent level if we are to exploit CEP dilepton production as a means to measure the luminosity. Fortunately, studies indicate that the gap survival should be very close to 100% for low-mass dilepton production [201].

How does $\gamma\gamma \to \tau^+\tau^-$ compare with exclusive $p + p \to p + H + p \to p + \tau^+\tau^- + p$? Differentiating the above equation we get $\mathrm{d}\sigma/\mathrm{d}M \approx 0.4$ fb/GeV/c^2 with $|\eta(\tau)| < 2.0$ at 120 GeV/c^2. The branching fraction for a SM Higgs (120) $H \to \tau^+\tau^-$ is ~ 0.07 and so, if $\sigma(p+H+p) \sim 3$ fb [30], the rates will be at least similar. For example, in a 4 GeV/c^2 mass window (which is commensurate with the expected mass resolution of the forward detectors) the cross sections would be around 1.6 fb and 0.2 fb respectively. Even assuming no other backgrounds and 100% detection efficiency, this translates into no more than 2σ evidence of $H \to \tau^+\tau^-$ with 100 fb^{-1} of data. It will therefore be difficult to see a SM Higgs in this decay channel at the LHC, but it may be feasible if the Higgs production rate is enhanced (e.g. see [168]). The $\gamma\gamma$ process is a continuum with well-known cross section on which $H \to \tau^+\tau^-$ would (if the production cross section is sufficiently large) be a narrow peak. By measuring the protons, one could exploit the fact that the background is peaked at smaller values of $|t|$ than the signal to improve the significance of any observation.

As discussed earlier, exclusive $\mu^+\mu^-$ events are also very important for the absolute calibration of the forward proton spectrometers. Note that the two-photon exclusive production of e^+e^- pairs can also be studied at the LHC, though triggering of such events is more difficult, and the $\Delta\phi$ and $p_T(e^+e^-)$ measurements are worsened by bremsstrahlung.

Finally, we note that the prospect of studying so called "unparticles" using the exclusive $\gamma\gamma \to l^+l^-$ channel has been studied in [202].

W and Z boson pairs

As illustrated in Fig. 22, the rate for pair production of W bosons via $\gamma\gamma \to W^+W^-$ is large (around 100 fb) and this can be exploited to investigate the corresponding quartic coupling. The signal is very clean and offers the possibility to study this process out to $M_{WW} \sim 500$ GeV. The cross section for $p_T^\mu > 10$ GeV/c and $|\eta^\mu| < 2.5$ from $p + p \to p + (\gamma\gamma \to W^+W^- \to \mu^+\mu^-\nu\bar{\nu}) + p$ is 0.76 fb [189]. The large reduction comes from the two $W \to \mu\nu$ decays. The cross section is only slightly reduced after adding the requirement of at least one forward proton tag. The unique signature of W pairs in the fully leptonic final state, no additional tracks on the l^+l^- vertex, large lepton acoplanarity and large missing transverse momentum strongly reduces the backgrounds. At low LHC luminosities (i.e. $\ll 10^{33}$ cm^{-2}s^{-1}), pile-up is not a problem and the events can be recognised even without detecting the outgoing protons [189, 203]. However tagging the protons would give improved sensitivity and a M_{WW} measurement. At higher luminosities, proton tagging is needed in order to suppress pile-up backgrounds. The situation is similar for the production of Z boson pairs, assuming fully leptonic, or semi-leptonic decays. In the SM, $\gamma\gamma \to ZZ$ is negligible (it is absent at tree level). Thus any observation would be a direct measurement of an anomalous $\gamma\gamma ZZ$ coupling.

In CEP of W^+W^- and ZZ, the fully leptonic decays (e.g. $WW \to e^-\mu^+\not{E}_T$) have practically no background, but constitute only 4.4% and 0.45% respectively of all decays. However in CEP one may be able to use additional four-momentum constraints to perhaps use about 50% of the events, i.e. all decays except the (six-jet) fully hadronic. For example, in $p+p \to p+WW+p \to p+l\nu JJ+p$, take the four-momenta of all detected objects p, p, l, J, J and calculate the missing mass, which is $m_\nu \sim 0$. Similarly if $X = ZZ \to l^+l^-\nu\bar{\nu}$ the missing mass to p, p, l^+l^- is m_Z (provided the missing $Z \to \nu\bar{\nu}$ is on-shell). CEP can therefore produce a mass peak in $Z \to \nu\bar{\nu}$. With similar 4-momentum constraints as much as 50% of all (on-shell) W^+W^- and ZZ events can be used.

Anomalous $\gamma\gamma WW$ couplings were first studied, within the context of a future e^+e^- collider in [204]. Under the assumptions of electromagnetic gauge invariance, C and P conservation and custodial symmetry (to keep the tree-level $\rho = M_W^2/(M_Z^2 \cos^2\theta_W)$ parameter equal to unity) there are only two relevant couplings to lowest order in an expansion in the inverse of the scale of new physics, Λ, i.e. the lowest non-renormalizable terms occur at dimension 6 in the lagrangian [204]:

$$L_6 = -\frac{e^2}{8}\frac{a_0}{\Lambda^2}F_{\mu\nu}F^{\mu\nu}W^{+\alpha}W^-_\alpha - \frac{e^2}{16}\frac{a_c}{\Lambda^2}F_{\mu\alpha}F^{\mu\beta}(W^{+\alpha}W^-_\beta + W^{-\alpha}W^+_\beta). \tag{8.48}$$

The anomalous couplings are denoted by $a_{0,c}$ and they are zero in the Standard Model. Sensitivity to these anomalous couplings has been investigated by the Louvain group [189]. They focussed upon $\gamma\gamma \to W^+W^- \to l^+l^-\nu\bar{\nu}$ and $\gamma\gamma \to ZZ \to l^+l^-jj$ using the signature of two leptons (e or μ) within the acceptance cuts $|\eta| < 2.5$ and $p_T > 10$ GeV/c. With just a few fb^{-1} of data, the limits are expected to be orders of magnitude better than the best limits established at LEP2 [205] and significantly better than those that would be obtained using the $W\gamma\gamma$ final state at the LHC [206, 207]. Similar conclusions have been reached in the studies presented in [208].

A study of the anomalous triple gauge couplings has also be performed. However, in this case the expected sensitivities are not as impressive [209].

Supersymmetric pairs

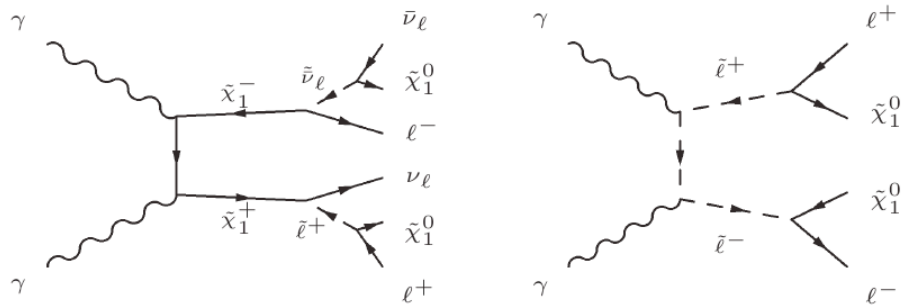

Figure 23: Relevant Feynman diagrams for SUSY pair production with leptons in the final state: chargino pair production (left); slepton pair production (right). Figure from Ref. [189].

The LHC, of course, is geared up to discover and explore low-scale supersymmetric particle production. However, SUSY pair production in $\gamma\gamma$ collisions, with two tagged protons, offers the opportunity to make direct measurements of the sparticle masses [189, 210]. As we shall see, the cross sections are not large and sufficient rate is only possible if the sparticles are light. The two-photon production of supersymmetric particles has been investigated in [193, 211, 212]. For chargino or slepton pair production, the final states are simple, see Fig. 23. Selecting a final state composed of two charged leptons with large missing energy and lepton acoplanarity means that the backgrounds should be under control, and $\gamma\gamma \to W^+W^-$ generates the only irreducible background.

In Ref. [189], three benchmark points in the parameter space of the constrained minimal supersymmetric model (CMSSM) were studied[13]. Here we will present the results for point LM1, which predicts a 97 GeV/c^2 neutralino (the LSP), a $\tilde{l}_R^\pm$ of mass 118 GeV/c^2 ($l = e, \mu$), a $\tilde{l}_L^\pm$ of mass 184 GeV/c^2 and a lightest chargino, $\tilde{\chi}_1^+$, of mass 180 GeV/c^2. Signal and background samples were produced using a modified version of CALCHEP [214] and the following acceptance cuts were applied: two leptons with $p_T > 3$ GeV/c or 10 GeV/c and $|\eta| < 2.5$. Standard high level trigger efficiencies are high for all these types of events.

Measuring the outgoing protons allows one to measure the cross section as a function of $M_{\gamma\gamma}$, and expected event rates with 100 fb^{-1} of data are presented in Fig. 24. The two edges, at twice the mass of the $\tilde{l}_R^\pm$ and at twice the mass of the $\tilde{l}_L^\pm$ are visible. However, the event rates are low and mass measurements with a precision of a few GeV/c^2 will require very high statistics. HECTOR [215] simulations of forward protons from slepton events consistent with the LM1 benchmark point indicate that the 220 m detectors will have both protons tagged for only 30% of events. Addition of detectors at 420 m increases that to 90% of events.

Another attractive feature of two-photon production of SUSY pairs with tagged protons is that both the missing *energy* $\not{E}$ and $\not{E}_T$ are measured, as well as the missing mass (here called $W_{\rm miss}$). For the SUSY signal $W_{\rm miss}$ starts at $2 \times m_{LSP}$[210], as illustrated in Fig. 25, while the background starts at $W_{\rm miss} = 0$

[13]The parameter space is constrained to be in agreement with the latest cosmological data [213].

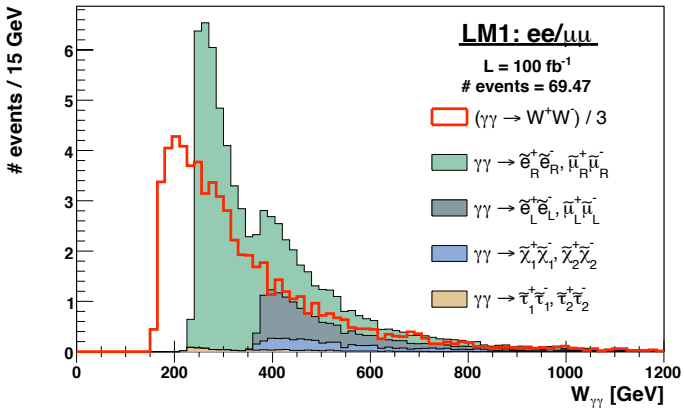

Figure 24: The invariant mass spectrum for SUSY pair production in the LM1 scenario and assuming 100 fb^{-1} of data. The WW background has been down-scaled by the quoted factor. See text for event selection criteria. Figure from Ref. [189].

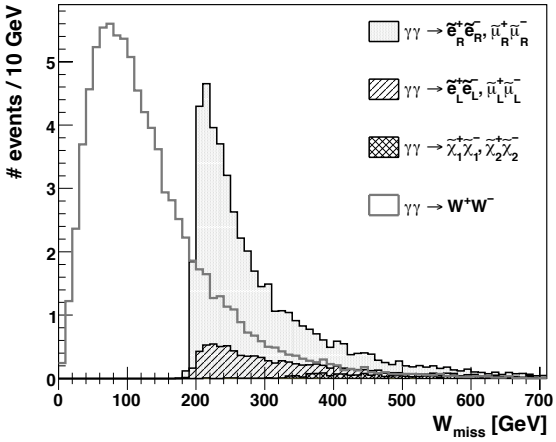

Figure 25: The missing mass distribution for SUSY pair production in the LM1 scenario and assuming 100 fb^{-1} of data. Event selection assumes two isolated opposite charge muons with $p_T > 7$ GeV/c or two electrons with $p_T > 10$ GeV/c, $|\eta_l| < 2.5$ and two tagged protons. Figure from Ref. [210].

8.5 γp collisions

In addition to $D\mathbb{P}E$ and two-photon collisions, it is also possible to study exclusive photoproduction ($\gamma\mathbb{P}$) at the LHC. A quasi-real photon is radiated off one of the protons and fluctuates into a $q\bar{q}$ pair, which scatters diffractively on the other proton. In such a reaction, only states with the same quantum numbers as the photon can be produced (the $\rho, \omega, \phi, J/\psi$ and Υ mesons, their excitations and the Z boson). While vector meson photoproduction has been extensively studied in ep collisions at HERA, it has only recently been observed (for J/ψ and $\psi(2s)$ states) in hadron-hadron collisions at the Tevatron [145] (see section 7.2). It is not our aim here to present a complete survey of the physics which can be studied via exclusive photoproduction at the LHC. Instead, we focus on two examples, Υ production and Z production.

At the LHC, photoproduced $\Upsilon \to \mu^+\mu^-$ may be measurable, with one proton detected (there is no acceptance to measure both). The cross section is sensitive to QCD saturation effects, which arise as a result of non-linear gluon dynamics. The large mass of the Υ offers hope that this effect could be quantified in QCD perturbation theory. Central exclusive Υ production at the LHC has been studied in Refs. [147, 146, 216, 217, 218, 219]. The study in Ref. [219] presented results using a model for diffractive scattering which fits both the existing HERA data, not only for Υ production but also for the total inclusive deep inelastic scattering cross section. The model includes a rudimentary modelling of saturation effects and predicts a cross section of 5.1 pb for 14 TeV pp collisions at the LHC assuming neither proton is detected. This cross section is for $\Upsilon \to \mu^+\mu^-$ with $p_T^\mu > 4$ GeV/c. The cross section falls to 3.0 pb if one proton is detected at 420 m from the interaction point. These are large cross sections and can be measured with early LHC data. Tagging one proton should help control the pile-up background, and proton dissociation e.g. $p \to p\pi^+\pi^-$, thereby making the measurement possible also at high luminosities. The large rates mean that it will also be possible to measure the upsilon rapidity and this should help distinguish between different models of high-energy scattering. Measuring one proton makes possible a direct measurement of the photoproduction cross section, $\sigma(\gamma p \to \Upsilon p)$ since a cut on the transverse momentum (e.g. around $100 - 300$ MeV) of the scattered proton will permit one to divide the event sample into two halves: one in which the detected proton predominantly radiated the photon and one in which it was the undetected proton that radiated the photon. The low p_T sample corresponds to a measurement at higher values of the γp centre-of-mass energy, with sensitivity up to 1 TeV in the γp centre-of-mass energy. The prediction of the photoproduction cross section is, however, complicated by any dependence of gap survival on the scattered proton p_T [220]. On the other hand, the measurement gives information on S^2. It should also not be forgotten that central production of vector mesons can proceed also via odderon exchange, and it would be very interesting to observe that.

Also possible at the LHC is the diffractive photoproduction of Z bosons [157, 147]. As discussed in section 7.2, the Standard Model cross section for Z production is negligibly small at the Tevatron: $\mathrm{d}\sigma/\mathrm{d}y|_{y=0} = 0.077$ fb, compared with an upper limit from CDF of 0.25 pb at 95% C.L. [156]. At the LHC however, the cross section is expected to be about 6 fb for $|y(Z)| < 2$, or 40 exclusive $Z \to e^+e^-$ or $\mu^+\mu^-$ events per 100 fb^{-1} [147]. Clearly one will have to work at high luminosities, which means that pile-up backgrounds need bringing under control. This should be possible by selecting events with only the l^+l^- tracks on the vertex, a dilepton invariant mass matching that of the Z, small $p_T(l^+l^-)$ and $\pi - \Delta\phi(l^+l^-)$, in conjunction with the requirement that the vertex be coincident with that obtained using two measured protons (at 420 m).

9 Concluding remarks

The subject of central exclusive production promises to deliver an entirely new dimension to the physics that will be explored at the LHC. With the installation of forward low-angle proton detectors, central masses can be measured out to a few hundred GeV/c^2 and to a precision at or below 1 GeV/c^2, even in the presence of missing energy, using very few events. Moreover, tagging the protons effectively filters the central system with a strong bias towards $J = 0$, even-parity systems. Such a filter will provide a unique handle on the nature of any new physics that might be produced. It is true to say that this programme constitutes a huge advance over previous studies of CEP performed mainly at the ISR, S$p\bar{p}$S and Tevatron. For the first time (with the exception of the glueball searches), central masses can be produced in a range where interesting new phenomena are expected.

Measurements from CDF at the Tevatron are very encouraging and support the validity of the theoretical calculations based in perturbative QCD: The theory is probably not too far off the mark. A second highlight of the recent past has been the demonstration that high luminosity backgrounds can be brought under control, which opens up the possibility to explore low (i.e. below 1 fb) cross section processes at the LHC.

There are many concrete examples of new physics that may reveal itself in CEP, and we have reviewed many of them here, but it should always be understood that CEP is principally a direct source of glue-glue (or photon-photon) interactions with a filter on the final state quantum numbers. It is thus ideally suited to a study of any new physics that couples to gluons (or photons).

Acknowledgements

We should like to thank the very many of our colleagues who have made our ventures into central exclusive production such a pleasure. Particular thanks are due to Paul Bell, Mike Birse, Frank Close, Brian Cox, Dino Goulianos, Valery Khoze, Krzysztof Piotrzkowski, Andy Pilkington and Misha Ryskin. We should like also to thank the UK's STFC and the U.S. Dept. of Energy for financial support.

References

[1] M. G. Albrow, A. Rostovtsev, Searching for the Higgs at hadron colliders using the missing mass method. arXiv:hep-ph/0009336.

[2] M. G. Albrow, et al., The FP420 R&D Project: Higgs and new physics with forward protons at the LHC, JINST 4 (2009) T10001. arXiv:0806.0302.

[3] J. R. Forshaw, D. A. Ross, Quantum Chromodynamics and the Pomeron, Cambridge Lecture Notes in Physics 9 (1997) 1–248.

[4] S. Donnachie, H. G. Dosch, O. Nachtmann, P. Landshoff, Pomeron Physics and QCD, Camb. Monogr. Part. Phys. Nucl. Phys. Cosmol. 19 (2002) 1–347.

[5] P. D. B. Collins, An Introduction to Regge Theory and High-Energy Physics, Cambridge.

[6] A. B. Kaidalov, Diffractive production mechanisms, Phys. Rept. 50 (1979) 157–226.

[7] S. N. Ganguli, D. P. Roy, Regge phenomenology and inclusive reactions, Phys. Rept. 67 (1980) 201–395.

[8] G. Wolf, Review of high energy diffraction in real and virtual photon proton scattering at HERA, arXiv:0907.1217.

[9] P. Newman, HERA inclusive diffraction and factorisation tests, arXiv:0908.3410.

[10] G. Giacomelli, M. Jacob, Physics at the CERN ISR, Phys. Rept. 55 (1979) 1–132.

[11] A. Donnachie, P. V. Landshoff, pp and $\bar{p}p$ elastic scattering, Nucl. Phys. B231 (1984) 189.

[12] A. Donnachie, P. V. Landshoff, Total cross-sections, Phys. Lett. B296 (1992) 227–232. arXiv:hep-ph/9209205.

[13] E. G. S. Luna, V. A. Khoze, A. D. Martin, M. G. Ryskin, Diffractive dissociation re-visited for predictions at the LHC, Eur. Phys. J. C59 (2009) 1–12. arXiv:0807.4115.

[14] E. Gotsman, E. Levin, U. Maor, J. S. Miller, A QCD motivated model for soft interactions at high energies, Eur. Phys. J. C57 (2008) 689–709. arXiv:0805.2799.

[15] M. G. Ryskin, A. D. Martin, V. A. Khoze, Soft processes at the LHC, I: Multi-component model, Eur. Phys. J. C60 (2009) 249–264. arXiv:0812.2407.

[16] A. H. Mueller, O(2,1) analysis of single particle spectra at high-energy, Phys. Rev. D2 (1970) 2963–2968.

[17] P. D. B. Collins, A. D. Martin, Hadron Interactions, Adam Hilger Ltd. (Graduate Student Series In Physics).

[18] T. W. B. Kibble, Feynman rules for Regge particles, Phys. Rev. 131 (1963) 2282–2291.

[19] R. Lipes, G. Zweig, W. Robertson, Experimental consistency of multi-reggeism in a high-energy reaction, Phys. Rev. Lett. 22 (1969) 433–437.

[20] K. A. Ter-Martirosyan, Y. M. Shabelskii, Particle pair spectra in colliding beams at high energies, Pisma Zh. Eksp. Teor. Fiz. 15 (1972) 164–167.

[21] R. Shankar, Can and does the pomeron occur more than once in a single process?, Nucl. Phys. B70 (1974) 168–188.

[22] A. B. Kaidalov, K. A. Ter-Martirosyan, The pomeron-particle total cross-section and diffractive production of showers at very high energies, Nucl. Phys. B75 (1974) 471–482.

[23] D. M. Chew, G. F. Chew, Prediction of double-pomeron cross-sections from single-diffraction measurements, Phys. Lett. B53 (1974) 191.

[24] Y. I. Azimov, V. A. Khoze, E. M. Levin, M. G. Ryskin, Estimates of the cross-sections for double-reggeon processes, Sov. J. Nucl. Phys. 21 (1975) 215.

[25] J. Pumplin, F. Henyey, Double pomeron exchange in the reaction $pp \to pp\pi^+\pi^-$, Nucl. Phys. B117 (1976) 377.

[26] B. R. Desai, B. C. Shen, M. Jacob, Double pomeron exchange in high-energy pp collisions, Nucl. Phys. B142 (1978) 258.

[27] K. H. Streng, Pomeron-pomeron collisions at collider energies, Phys. Lett. B166 (1986) 443.

[28] V. M. Budnev, I. F. Ginzburg, G. V. Meledin, V. G. Serbo, The two photon particle production mechanism, Phys. Rept. 15 (1974) 181–281.

[29] V. A. Khoze, A. D. Martin, M. G. Ryskin, Double-diffractive processes in high-resolution missing- mass experiments at the Tevatron, Eur. Phys. J. C19 (2001) 477–483, erratum-ibid. C20:599, 2001. arXiv:hep-ph/0011393.

[30] V. A. Khoze, A. D. Martin, M. G. Ryskin, Prospects for new physics observations in diffractive processes at the LHC and Tevatron, Eur. Phys. J. C23 (2002) 311–327. arXiv:hep-ph/0111078.

[31] V. A. Khoze, A. D. Martin, M. G. Ryskin, Can the Higgs be seen in rapidity gap events at the Tevatron or the LHC?, Eur. Phys. J. C14 (2000) 525–534. arXiv:hep-ph/0002072.

[32] V. A. Khoze, A. D. Martin, M. G. Ryskin, The rapidity gap Higgs signal at LHC, Phys. Lett. B401 (1997) 330–336. arXiv:hep-ph/9701419.

[33] A. B. Kaidalov, V. A. Khoze, A. D. Martin, M. G. Ryskin, Extending the study of the Higgs sector at the LHC by proton tagging, Eur. Phys. J. C33 (2004) 261–271. arXiv:hep-ph/0311023.

[34] J. R. Ellis, M. K. Gaillard, D. V. Nanopoulos, A phenomenological profile of the Higgs boson, Nucl. Phys. B106 (1976) 292.

[35] M. B. Voloshin, Once again about the role of gluonic mechanism in interaction of light Higgs boson with hadrons, Sov. J. Nucl. Phys. 44 (1986) 478.

[36] M. A. Shifman, A. I. Vainshtein, M. B. Voloshin, V. I. Zakharov, Low-energy theorems for Higgs boson couplings to photons, Sov. J. Nucl. Phys. 30 (1979) 711–716.

[37] Z. Kunszt, S. Moretti, W. J. Stirling, Higgs production at the LHC: An update on cross sections and branching ratios, Z. Phys. C74 (1997) 479–491. arXiv:hep-ph/9611397.

[38] M. Spira, A. Djouadi, D. Graudenz, P. M. Zerwas, Higgs boson production at the LHC, Nucl. Phys. B453 (1995) 17–82. arXiv:hep-ph/9504378.

[39] A. D. Martin, M. G. Ryskin, Unintegrated generalised parton distributions, Phys. Rev. D64 (2001) 094017. arXiv:hep-ph/0107149.

[40] V. A. Khoze, A. D. Martin, M. G. Ryskin, Soft diffraction and the elastic slope at Tevatron and LHC energies: A multi-pomeron approach, Eur. Phys. J. C18 (2000) 167–179. arXiv:hep-ph/0007359.

[41] A. Levy, Evidence for no shrinkage in elastic photoproduction of J/ψ, Phys. Lett. B424 (1998) 191–194. arXiv:hep-ph/9712519.

[42] A. V. Belitsky, A. V. Radyushkin, Unraveling hadron structure with generalized parton distributions, Phys. Rept. 418 (2005) 1–387. arXiv:hep-ph/0504030.

[43] A. G. Shuvaev, K. J. Golec-Biernat, A. D. Martin, M. G. Ryskin, Off-diagonal distributions fixed by diagonal partons at small x and ξ, Phys. Rev. D60 (1999) 014015. arXiv:hep-ph/9902410.

[44] Y. L. Dokshitzer, D. Diakonov, S. I. Troian, Hard processes in Quantum Chromodynamics, Phys. Rept. 58 (1980) 269–395.

[45] T. D. Coughlin, J. R. Forshaw, Central exclusive production in QCD, JHEP 01 (2010) 121. arXiv:0912.3280.

[46] V. N. Gribov, L. N. Lipatov, Deep inelastic ep scattering in perturbation theory, Sov. J. Nucl. Phys. 15 (1972) 438–450.

[47] G. Altarelli, G. Parisi, Asymptotic freedom in parton language, Nucl. Phys. B126 (1977) 298.

[48] Y. L. Dokshitzer, Calculation of the structure functions for deep inelastic scattering and e^+e^- annihilation by perturbation theory in Quantum Chromodynamics, Sov. Phys. JETP 46 (1977) 641–653.

[49] J. R. Forshaw, Diffractive Higgs production: Theory, arXiv:hep-ph/0508274.

[50] Y. L. Dokshitzer, V. A. Khoze, A. H. Mueller, S. I. Troian, Basics of perturbative QCD, Gif-sur-Yvette, France: Ed. Frontieres (1991) 274 p.

[51] J. D. Bjorken, Rapidity gaps and jets as a new physics signature in very high-energy hadron hadron collisions, Phys. Rev. D47 (1993) 101–113.

[52] Y. L. Dokshitzer, V. A. Khoze, T. Sjöstrand, Rapidity gaps in Higgs production, Phys. Lett. B274 (1992) 116–121.

[53] A. D. Martin, V. A. Khoze, M. G. Ryskin, Rapidity gap survival probability and total cross sections, arXiv:0810.3560.

[54] J. Bartels, S. Bondarenko, K. Kutak, L. Motyka, Exclusive Higgs boson production at the LHC: Hard rescattering corrections, Phys. Rev. D73 (2006) 093004. arXiv:hep-ph/0601128.

[55] M. G. Ryskin, A. D. Martin, V. A. Khoze, Soft processes at the LHC, II: Soft-hard factorization breaking and gap survival, Eur. Phys. J. C60 (2009) 265–272. arXiv:0812.2413.

[56] V. A. Khoze, A. D. Martin, M. G. Ryskin, Diffractive Higgs production: Myths and reality, Eur. Phys. J. C26 (2002) 229–236. arXiv:hep-ph/0207313.

[57] V. A. Khoze, A. D. Martin, M. G. Ryskin, On the role of hard rescattering in exclusive diffractive Higgs production, JHEP 05 (2006) 036. arXiv:hep-ph/0602247.

[58] M. M. Block, F. Halzen, Survival probability of large rapidity gaps in $\bar{p}p$, pp, γp and $\gamma\gamma$ collisions, Phys. Rev. D63 (2001) 114004. arXiv:hep-ph/0101022.

[59] M. Strikman, C. Weiss, Rapidity gap survival in central exclusive diffraction: Dynamical mechanisms and uncertainties, arXiv:0812.1053.

[60] E. Gotsman, E. Levin, U. Maor, J. S. Miller, Soft interactions at high energies: QCD motivated approach, arXiv:0901.1540.

[61] T. Sjöstrand, M. van Zijl, A multiple interaction model for the event structure in hadron collisions, Phys. Rev. D36 (1987) 2019.

[62] R. Corke, T. Sjöstrand, Multiparton interactions and rescattering, arXiv:0911.1909.

[63] J. M. Butterworth, J. R. Forshaw, Photoproduction of multi-jet events at HERA: A Monte Carlo simulation, J. Phys. G19 (1993) 1657–1663.

[64] J. M. Butterworth, J. R. Forshaw, M. H. Seymour, Multiparton interactions in photoproduction at HERA, Z. Phys. C72 (1996) 637–646. arXiv:hep-ph/9601371.

[65] I. Borozan, M. H. Seymour, An eikonal model for multiparticle production in hadron hadron interactions, JHEP 09 (2002) 015. arXiv:hep-ph/0207283.

[66] T. Sjöstrand, P. Z. Skands, Multiple interactions and the structure of beam remnants, JHEP 03 (2004) 053. arXiv:hep-ph/0402078.

[67] M. G. Albrow, et al., Tevatron-for-LHC Report of the QCD Working Group, arXiv:hep-ph/0610012.

[68] P. Z. Skands, D. Wicke, Non-perturbative QCD effects and the top mass at the Tevatron, Eur. Phys. J. C52 (2007) 133–140. arXiv:hep-ph/0703081.

[69] T. Gleisberg, et al., Event generation with SHERPA 1.1, JHEP 02 (2009) 007. arXiv:0811.4622.

[70] M. Bahr, S. Gieseke, M. H. Seymour, Simulation of multiple partonic interactions in Herwig++, JHEP 07 (2008) 076. arXiv:0803.3633.

[71] M. Bahr, J. M. Butterworth, S. Gieseke, M. H. Seymour, Soft interactions in Herwig++, arXiv:0905.4671.

[72] V. A. Khoze, A. D. Martin, M. G. Ryskin, Early LHC measurements to check predictions for central exclusive production, Eur. Phys. J. C55 (2008) 363–375. arXiv:0802.0177.

[73] L. A. Harland-Lang, V. A. Khoze, M. G. Ryskin, W. J. Stirling, Standard candle central exclusive processes at the Tevatron and LHCarXiv:1005.0695.

[74] A. Bialas, P. V. Landshoff, Higgs production in pp collisions by double pomeron exchange, Phys. Lett. B256 (1991) 540–546.

[75] M. Boonekamp, R. B. Peschanski, C. Royon, Popping out the Higgs boson off vacuum at Tevatron and LHC, Nucl. Phys. B669 (2003) 277–305. arXiv:hep-ph/0301244.

[76] A. Schäfer, O. Nachtmann, R. Schopf, Production of Higgs particles in diffractive hadron hadron collisions, Phys. Lett. B249 (1990) 331–335.

[77] B. Muller, A. J. Schramm, Higgs boson production in peripheral heavy ion collisions: Coherent double pomeron exchange, Nucl. Phys. A523 (1991) 677–693.

[78] J.-R. Cudell, O. F. Hernandez, Particle production in a hadron collider rapidity gap: The Higgs case, Nucl. Phys. B471 (1996) 471–502. arXiv:hep-ph/9511252.

[79] H. J. Lu, J. Milana, Exclusive production of Higgs bosons in hadron colliders, Phys. Rev. D51 (1995) 6107–6113. arXiv:hep-ph/9407206.

[80] P. V. Landshoff, O. Nachtmann, Vacuum structure and diffraction scattering, Z. Phys. C35 (1987) 405.

[81] A. Donnachie, P. V. Landshoff, Gluon condensate and pomeron structure, Nucl. Phys. B311 (1989) 509.

[82] A. Bzdak, Exclusive Higgs and dijet production by double pomeron exchange. The CDF upper limits, Phys. Lett. B615 (2005) 240–246. arXiv:hep-ph/0504086.

[83] T. Aaltonen, et al., Observation of exclusive dijet production at the Fermilab Tevatron $p\bar{p}$ collider, Phys. Rev. D77 (2008) 052004. arXiv:0712.0604.

[84] V. A. Petrov, R. A. Ryutin, Exclusive double diffractive Higgs boson production at LHC, Eur. Phys. J. C36 (2004) 509–513. arXiv:hep-ph/0311024.

[85] V. A. Petrov, R. A. Ryutin, Exclusive double diffractive events: Menu for LHC, JHEP 08 (2004) 013. arXiv:hep-ph/0403189.

[86] V. A. Petrov, R. A. Ryutin, Patterns of the exclusive double diffraction, J. Phys. G35 (2008) 065004. arXiv:0711.2370.

[87] A. Szczurek, P. Lebiedowicz, Exclusive scalar $f_0(1500)$ meson production for energy ranges available at the GSI Facility for Antiproton and Ion Research (GSI-FAIR) and at the Japan Proton Accelerator Research Complex (J-PARC), Nucl. Phys. A826 (2009) 101–130. arXiv:0906.0286.

[88] R. S. Pasechnik, A. Szczurek, O. V. Teryaev, Central exclusive production of scalar χ_c meson at the Tevatron, RHIC and LHC energies, Phys. Rev. D78 (2008) 014007. arXiv:0709.0857.

[89] M. G. Albrow, et al., Inelastic diffractive scattering at the CERN ISR, Nucl. Phys. B108 (1976) 1.

[90] D. Denegri, et al., Double pomeron exchange and diffractive dissociation in the reaction $pp \to pp + \pi^+\pi^-$ at 69 GeV/c, Nucl. Phys. B98 (1975) 189.

[91] M. Derrick, B. Musgrave, P. Schreiner, H. Yuta, Double pomeron exchange contribution to the reaction $pp \to pp + \pi^+\pi^-$ at 205-GeV/c, Phys. Rev. Lett. 32 (1974) 80–82.

[92] A. H. Mueller, Multiplicity distributions in Regge pole dominated inclusive reactions., Phys. Rev. D4 (1971) 150–155.

[93] R. D. Field, G. C. Fox, Triple Regge and finite mass sum rule analysis of the inclusive reaction $p + p \to p + X$, Nucl. Phys. B80 (1974) 367.

[94] L. Baksay, et al., Evidence for double pomeron exchange at the CERN ISR, Phys. Lett. B61 (1976) 89.

[95] M. Della Negra, et al., Study of double pomeron exchange in pp collisions at $\sqrt{s} = 31$ GeV, Phys. Lett. B65 (1976) 394–396.

[96] K. L. Au, D. Morgan, M. R. Pennington, Meson Dynamics Beyond the Quark Model: A Study of Final State Interactions, Phys. Rev. D35 (1987) 1633.

[97] H. de Kerret, et al., Experimental evidence for double-pomeron exchange at ISR energies, Phys. Lett. B68 (1977) 385.

[98] D. Drijard, et al., Double pomeron exchange in the reaction $pp \to pp + \pi^+\pi^-$ at ISR energies, Nucl. Phys. B143 (1978) 61.

[99] J. C. M. Armitage, et al., A study of the reaction $pp \to ppX$ at ISR energies, Phys. Lett. B82 (1979) 149.

[100] T. Åkesson, et al., A study of exclusive central hadron production at the ISR as a search for gluonium states, Phys. Lett. B133 (1983) 268.

[101] T. Åkesson, et al., A search for glueballs and a study of double pomeron exchange at the CERN Intersecting Storage Rings, Nucl. Phys. B264 (1986) 154.

[102] E. Klempt, A. Zaitsev, Glueballs, hybrids, multiquarks. Experimental facts versus QCD inspired concepts, Phys. Rept. 454 (2007) 1–202. arXiv:0708.4016.

[103] V. Crede, C. A. Meyer, The experimental status of glueballs, Prog. Part. Nucl. Phys. 63 (2009) 74–116. arXiv:0812.0600.

[104] D. Robson, A basic guide for the glueball spotter, Nucl. Phys. B130 (1977) 328.

[105] R. Waldi, K. r. Schubert, K. Winter, Search for glue balls in a pomeron pomeron scattering experiment, Z. Phys. C18 (1983) 301–306.

[106] D. Barberis, et al., A partial wave analysis of the centrally produced $\pi^+\pi^-$ system in pp interactions at 450 GeV/c, Phys. Lett. B453 (1999) 316–324. arXiv:hep-ex/9903043.

[107] C. Amsler, et al., Review of Particle Physics, Phys. Lett. B667 (2008) 1.

[108] S. Narison, Scalar mesons in QCD and tests of the gluon content of the sigma, Nucl. Phys. Proc. Suppl. 121 (2003) 131–134. arXiv:hep-ph/0208081.

[109] G. Mennessier, P. Minkowski, S. Narison, W. Ochs, Can the $\gamma\gamma$ processes reveal the nature of the σ?, arXiv:0707.4511.

[110] Y. Nambu, G. Jona-Lasinio, Dynamical model of elementary particles based on an analogy with superconductivity. I, Phys. Rev. 122 (1961) 345–358.

[111] P. Minkowski, W. Ochs, Identification of the glueballs and the scalar meson nonet of lowest mass, Eur. Phys. J. C9 (1999) 283–312. arXiv:hep-ph/9811518.

[112] F. E. Close, The end of the constituent quark model?, AIP Conf. Proc. 717 (2004) 919–936. arXiv:hep-ph/0311087.

[113] L. Camilleri, Proton anti-proton physics at the CERN Intersecting Storage Rings, Phys. Rept. 144 (1987) 51–115.

[114] D. Barberis, et al., Observation of vertex factorisation breaking in central pp interactions, Phys. Lett. B388 (1996) 853–858.

[115] A. Kirk, Resonance production in central pp collisions at the CERN Omega Spectrometer, Phys. Lett. B489 (2000) 29–37. arXiv:hep-ph/0008053.

[116] A. Breakstone, et al., The reaction pomeron-pomeron $\to \pi^+\pi^-$ and an unusual production mechanism for the $f_2(1270)$, Z. Phys. C48 (1990) 569–576.

[117] F. E. Close, A. Kirk, A glueball- $q\bar{q}$ filter in central hadron production, Phys. Lett. B397 (1997) 333–338. arXiv:hep-ph/9701222.

[118] F. E. Close, A. Kirk, G. Schuler, Dynamics of glueball and $q\bar{q}$ production in the central region of pp collisions, Phys. Lett. B477 (2000) 13–18. arXiv:hep-ph/0001158.

[119] N. M. Agababyan, et al., Pomeron-pomeron cross-section from inclusive production of a central cluster in quasielastic π^+p and K^+p scattering at 250 GeV/c, Z. Phys. C60 (1993) 229–234.

[120] M. A. Reyes, et al., Partial wave analysis of the centrally produced $K^0_S K^0_S$ system at 8 GeV/c, Phys. Rev. Lett. 81 (19) (1998) 4079–4082.

[121] R. Bonino, et al., Evidence for transverse jets in high mass diffraction, Phys. Lett. B211 (1988) 239.

[122] G. Ingelman, P. E. Schlein, Jet structure in high mass diffractive scattering, Phys. Lett. B152 (1985) 256.

[123] A. Brandt, et al., A study of inclusive double pomeron exchange in $p\bar{p} \to pX\bar{p}$ at $\sqrt{s} =$ 630 GeV, Eur. Phys. J. C25 (2002) 361–377. arXiv:hep-ex/0205037.

[124] D. Joyce, et al., Double pomeron exchange studies in $p\bar{p}$ interactions at 0.63 TeV, Phys. Rev. D48 (1993) 1943–1948.

[125] F. Abe, et al., Measurement of small angle antiproton-proton elastic scattering at $\sqrt{s} = 546$ and 1800 GeV, Phys. Rev. D 50 (9) (1994) 5518–5534.

[126] F. Abe, et al., Measurement of the $\bar{p}p$ total cross-section at $\sqrt{s} = 546$ GeV and 1800 GeV, Phys. Rev. D50 (1994) 5550–5561.

[127] N. A. Amos, et al., $\bar{p}p$ elastic scattering at $\sqrt{s} = 1.8$ TeV from $|t| = 0.034$ GeV/c^2 to 0.65 GeV/c^2, Phys. Lett. B247 (1990) 127–130.

[128] C. Avila, et al., The ratio, ρ, of the real to the imaginary part of the $\bar{p}p$ forward elastic scattering amplitude at $\sqrt{s} = 1.8$-TeV, Phys. Lett. B537 (2002) 41–44.

[129] H. Stenzel, Total cross section and elastic scattering from Tevatron to LHC, arXiv:0907.3033.

[130] F. Abe, et al., Measurement of $\bar{p}p$ single diffraction dissociation at $\sqrt{s} = 546$ GeV and 1800 GeV, Phys. Rev. D50 (1994) 5535–5549.

[131] K. Goulianos, J. Montanha, Factorization and scaling in hadronic diffraction, Phys. Rev. D59 (1999) 114017. arXiv:hep-ph/9805496.

[132] B. Abbott, et al., Hard single diffraction in $\bar{p}p$ collisions at $\sqrt{s} = 630$ GeV and 1800 GeV, Phys. Lett. B531 (2002) 52–60. arXiv:hep-ex/9912061.

[133] A. A. Affolder, et al., Diffractive dijet production at $\sqrt{s} = 630$ GeV and 1800 GeV at the Fermilab Tevatron, Phys. Rev. Lett. 88 (2002) 151802. arXiv:hep-ex/0109025.

[134] F. Abe, et al., Observation of diffractive W boson production at the Tevatron, Phys. Rev. Lett. 78 (1997) 2698–2703. arXiv:hep-ex/9703010.

[135] V. M. Abazov, et al., Observation of diffractively produced W and Z bosons in $\bar{p}p$ collisions at $\sqrt{s} = 1800$ GeV, Phys. Lett. B574 (2003) 169–179. arXiv:hep-ex/0308032.

[136] K. Goulianos, Diffractive W and Z Production at Tevatron, arXiv:0905.4281.

[137] T. Affolder, et al., Dijet production by double pomeron exchange at the Fermilab Tevatron, Phys. Rev. Lett. 85 (20) (2000) 4215–4220.

[138] R. B. Appleby, J. R. Forshaw, Diffractive dijet production, Phys. Lett. B541 (2002) 108–114. arXiv:hep-ph/0111077.

[139] B. E. Cox, A. Pilkington, Central exclusive di-jet production at the Tevatron, Phys. Rev. D72 (2005) 094024. arXiv:hep-ph/0508249.

[140] F. Abe, et al., Observation of rapidity gaps in $\bar{p}p$ collisions at 1.8 TeV, Phys. Rev. Lett. 74 (1995) 855–859.

[141] M. G. Albrow, et al., A search for the Higgs boson using very forward tracking detectors with CDF. arXiv:hep-ex/0511057.

[142] V. A. Khoze, A. D. Martin, M. G. Ryskin, W. J. Stirling, Diffractive $\gamma\gamma$ production at hadron colliders, Eur. Phys. J. C38 (2005) 475–482. arXiv:hep-ph/0409037.

[143] T. Aaltonen, et al., Search for exclusive $\gamma\gamma$ production in hadron-hadron collisions, Phys. Rev. Lett. 99 (2007) 242002. arXiv:0707.2374.

[144] A. Abulencia, et al., Observation of exclusive electron positron production in hadron hadron collisions, Phys. Rev. Lett. 98 (2007) 112001. arXiv:hep-ex/0611040.

[145] T. Aaltonen, et al., Observation of exclusive charmonium production and $\gamma + \gamma \to \mu^+\mu^-$ in $p\bar{p}$ collisions at $\sqrt{s} = 1.96$ TeV, Phys. Rev. Lett. 102 (2009) 242001. arXiv:0902.1271.

[146] S. R. Klein, J. Nystrand, Photoproduction of quarkonium in proton proton and nucleus nucleus collisions, Phys. Rev. Lett. 92 (2004) 142003. arXiv:hep-ph/0311164.

[147] L. Motyka, G. Watt, Exclusive photoproduction at the Tevatron and LHC within the dipole picture, Phys. Rev. D78 (2008) 014023. arXiv:0805.2113.

[148] W. Schäfer, A. Szczurek, Exclusive photoproduction of J/ψ in proton-proton and proton-antiproton scattering, Phys. Rev. D76 (2007) 094014. arXiv:0705.2887.

[149] C. Ewerz, The odderon: Theoretical status and experimental tests, arXiv:hep-ph/0511196.

[150] V. A. Khoze, A. D. Martin, M. G. Ryskin, W. J. Stirling, Double-diffractive χ meson production at the hadron colliders, Eur. Phys. J. C35 (2004) 211–220. arXiv:hep-ph/0403218.

[151] F. Yuan, Heavy quarkonium production in double pomeron exchange processes in perturbative QCD, Phys. Lett. B510 (2001) 155–160. arXiv:hep-ph/0103213.

[152] A. Bzdak, Remark on double diffractive χ meson production, Phys. Lett. B619 (2005) 288–292. arXiv:hep-ph/0506101.

[153] L. A. Harland-Lang, V. A. Khoze, M. G. Ryskin, W. J. Stirling, Central exclusive χ_c meson production at the Tevatron revisited. arXiv:0909.4748.

[154] http://projects.hepforge.org/superchic/.

[155] M. Albrow, et al., Forward physics with rapidity gaps at the LHC, JINST 4 (2009) P10001. arXiv:0811.0120.

[156] T. Aaltonen, et al., Search for exclusive Z boson production and observation of high mass $p\bar{p} \to \gamma\gamma \to p + \ell\ell + \bar{p}$ events in $p\bar{p}$ collisions at $\sqrt{s} = 1.96$ TeV, Phys. Rev. Lett. 102 (2009) 222002. arXiv:0902.2816.

[157] V. P. Goncalves, M. V. T. Machado, Diffractive photoproduction of Z^0 bosons in coherent interactions at CERN-LHC, Eur. Phys. J. C56 (2008) 33–38, erratum-ibid C **61**, 351 (2009). arXiv:0710.4287.

[158] A. R. White, The physics of a sextet quark sector, Phys. Rev. D72 (2005) 036007. arXiv:hep-ph/0412062.

[159] M. Albrow, Exclusive high mass di-leptons in CDF, arXiv:0909.3471.

[160] B. E. Cox, J. R. Forshaw, Pomwig: Herwig for diffractive interactions, Comput. Phys. Commun. 144 (2002) 104–110. arXiv:hep-ph/0010303.

[161] J. Monk, A. Pilkington, ExHuME: A Monte Carlo event generator for exclusive diffraction, Comput. Phys. Commun. 175 (2006) 232–239. arXiv:hep-ph/0502077.

[162] M. Boonekamp, T. Kucs, Pomwig v2.0: Updates for double diffraction, Comput. Phys. Commun. 167 (2005) 217. arXiv:hep-ph/0312273.

[163] V. A. Khoze, A. D. Martin, M. G. Ryskin, New physics with tagged forward protons at the LHC, Frascati Phys. Ser. 44 (2007) 147–160. arXiv:0705.2314.

[164] A. B. Kaidalov, V. A. Khoze, A. D. Martin, M. G. Ryskin, Central exclusive diffractive production as a spin parity analyser: From hadrons to Higgs, Eur. Phys. J. C31 (2003) 387–396. arXiv:hep-ph/0307064.

[165] B. E. Cox, et al., Detecting the standard model Higgs boson in the WW decay channel using forward proton tagging at the LHC, Eur. Phys. J. C45 (2006) 401–407. arXiv:hep-ph/0505240.

[166] B. E. Cox, F. K. Loebinger, A. D. Pilkington, Detecting Higgs bosons in the $b\bar{b}$ decay channel using forward proton tagging at the LHC, JHEP 10 (2007) 090. arXiv:0709.3035.

[167] S. Heinemeyer, et al., Studying the MSSM Higgs sector by forward proton tagging at the LHC, Eur. Phys. J. C53 (2008) 231–256. arXiv:0708.3052.

[168] S. Heinemeyer, V. A. Khoze, M. G. Ryskin, M. Tasevsky, G. Weiglein, BSM Higgs studies at the LHC in the forward proton mode, arXiv:0909.4665.

[169] ATLAS detector and physics performance. Technical design report. Vol. 2, CERN-LHCC-99-15.

[170] G. L. Bayatian, et al., CMS technical design report, volume II: Physics performance, J. Phys. G34 (2007) 995–1579.

[171] S. Gennai, et al., Search for heavy neutral MSSM Higgs bosons with CMS: Reach and Higgs-mass precision, Eur. Phys. J. C52 (2007) 383–395. arXiv:0704.0619.

[172] V. Buescher, K. Jakobs, Higgs boson searches at hadron colliders, Int. J. Mod. Phys. A20 (2005) 2523–2602. arXiv:hep-ph/0504099.

[173] T. Plehn, D. L. Rainwater, D. Zeppenfeld, Determining the structure of Higgs couplings at the LHC, Phys. Rev. Lett. 88 (2002) 051801. arXiv:hep-ph/0105325.

[174] V. Hankele, G. Klamke, D. Zeppenfeld, T. Figy, Anomalous Higgs boson couplings in vector boson fusion at the CERN LHC, Phys. Rev. D74 (2006) 095001. arXiv:hep-ph/0609075.

[175] C. Ruwiedel, N. Wermes, M. Schumacher, Prospects for the measurement of the structure of the coupling of a Higgs boson to weak gauge bosons in weak boson fusion with the ATLAS detector, Eur. Phys. J. C51 (2007) 385–414.

[176] J. R. Forshaw, J. F. Gunion, L. Hodgkinson, A. Papaefstathiou, A. D. Pilkington, Reinstating the 'no-lose' theorem for NMSSM Higgs discovery at the LHC, JHEP 04 (2008) 090. arXiv:0712.3510.

[177] U. Ellwanger, C. Hugonie, NMHDECAY 2.0: An updated program for sparticle masses, Higgs masses, couplings and decay widths in the NMSSM, Comput. Phys. Commun. 175 (2006) 290–303. arXiv:hep-ph/0508022.

[178] R. Dermisek, J. F. Gunion, Escaping the large fine tuning and little hierarchy problems in the next to minimal supersymmetric model and $h \to aa$ decays, Phys. Rev. Lett. 95 (2005) 041801. arXiv:hep-ph/0502105.

[179] R. Dermisek, J. F. Gunion, Consistency of LEP event excesses with an $h \to aa$ decay scenario and low-fine-tuning NMSSM models, Phys. Rev. D73 (2006) 111701. arXiv:hep-ph/0510322.

[180] J. R. Ellis, J. S. Lee, A. Pilaftsis, Diffraction as a CP and lineshape analyzer for MSSM Higgs bosons at the LHC, Phys. Rev. D71 (2005) 075007. arXiv:hep-ph/0502251.

[181] V. A. Khoze, A. D. Martin, M. G. Ryskin, Hunting a light CP-violating Higgs via diffraction at the LHC, Eur. Phys. J. C34 (2004) 327–334. arXiv:hep-ph/0401078.

[182] B. E. Cox, J. R. Forshaw, J. S. Lee, J. Monk, A. Pilaftsis, Observing a light CP-violating Higgs boson in diffraction, Phys. Rev. D68 (2003) 075004. arXiv:hep-ph/0303206.

[183] M. Chaichian, P. Hoyer, K. Huitu, V. A. Khoze, A. D. Pilkington, Searching for the triplet Higgs sector via central exclusive production at the LHC, JHEP 05 (2009) 011. arXiv:0901.3746.

[184] K. Belotsky, V. A. Khoze, A. D. Martin, M. G. Ryskin, Can an invisible Higgs boson be seen via diffraction at the LHC?, Eur. Phys. J. C36 (2004) 503–507. arXiv:hep-ph/0406037.

[185] N. Arkani-Hamed, S. Dimopoulos, Supersymmetric unification without low energy supersymmetry and signatures for fine-tuning at the LHC, JHEP 06 (2005) 073. arXiv:hep-th/0405159.

[186] G. F. Giudice, A. Romanino, Split supersymmetry, Nucl. Phys. B699 (2004) 65–89. arXiv:hep-ph/0406088.

[187] P. J. Bussey, T. D. Coughlin, J. R. Forshaw, A. D. Pilkington, Central exclusive production of longlived gluinos at the LHC, JHEP 11 (2006) 027. arXiv:hep-ph/0607264.

[188] W. Kilian, T. Plehn, P. Richardson, E. Schmidt, Split supersymmetry at colliders, Eur. Phys. J. C39 (2005) 229–243. arXiv:hep-ph/0408088.

[189] J. de Favereau de Jeneret, et al., High energy photon interactions at the LHC, arXiv:0908.2020.

[190] S. P. Baranov, O. Duenger, H. Shooshtari, J. A. M. Vermaseren, LPAIR: A generator for lepton pair production. In Proceedings, Physics at HERA, vol. 3, 1478-1482 (1991).

[191] F. Maltoni, T. Stelzer, MadEvent: Automatic event generation with MadGraph, JHEP 02 (2003) 027. arXiv:hep-ph/0208156.

[192] T. Stelzer, W. F. Long, Automatic generation of tree level helicity amplitudes, Comput. Phys. Commun. 81 (1994) 357–371. arXiv:hep-ph/9401258.

[193] J. Ohnemus, T. F. Walsh, P. M. Zerwas, Gamma gamma production of non-strongly interacting SUSY particles at hadron colliders, Phys. Lett. B328 (1994) 369–373. arXiv:hep-ph/9402302.

[194] J. F. Gunion, H. E. Haber, Higgs boson production in the photon-photon collider mode of a high-energy e^+e^- linear collider, Phys. Rev. D48 (1993) 5109–5120.

[195] K. Piotrzkowski, Tagging two-photon production at the LHC, Phys. Rev. D63 (2001) 071502. arXiv:hep-ex/0009065.

[196] V. M. Budnev, I. F. Ginzburg, G. V. Meledin, V. G. Serbo, The process $pp \to ppe^+e^-$ and the possibility of its calculation by means of quantum electrodynamics only, Nucl. Phys. B63 (1973) 519–541.

[197] A. G. Shamov, V. I. Telnov, Precision luminosity measurement at LHC using two-photon production of $\mu^+\mu^-$ pairs, Nucl. Instrum. Meth. A494 (2002) 51–56. arXiv:hep-ex/0207095.

[198] D. Bocian, K. Piotrzkowski, Very forward two-photon e^+e^- production and luminosity measurement for ion collisions at the LHC, Acta Phys. Polon. B35 (2004) 2417–2424.

[199] M. W. Krasny, J. Chwastowski, K. Slowikowski, Luminosity measurement method for LHC: The theoretical precision and the experimental challenges, Nucl. Instrum. Meth. A584 (2008) 42–52. arXiv:hep-ex/0610052.

[200] J. A. M. Vermaseren, Two photon processes at very high-energies, Nucl. Phys. B229 (1983) 347.

[201] V. A. Khoze, A. D. Martin, R. Orava, M. G. Ryskin, Luminosity monitors at the LHC, Eur. Phys. J. C19 (2001) 313–322. arXiv:hep-ph/0010163.

[202] I. Sahin, S. C. Inan, Probe of unparticles at the LHC in exclusive two lepton and two photon production via photon-photon fusion, JHEP 09 (2009) 069. arXiv:0907.3290.

[203] E. Chapon, C. Royon, O. Kepka, Probing $WW\gamma\gamma$ and $ZZ\gamma\gamma$ quartic anomalous couplings with 10 pb^{-1} at the LHC, arXiv:0908.1061.

[204] G. Belanger, F. Boudjema, $\gamma\gamma \to W^+W^-$ and $\gamma\gamma \to ZZ$ as tests of novel quartic couplings, Phys. Lett. B288 (1992) 210–220.

[205] G. Abbiendi, et al., Constraints on anomalous quartic gauge boson couplings from $\nu\bar{\nu}\gamma\gamma$ and $q\bar{q}\gamma\gamma$ events at LEP2, Phys. Rev. D70 (2004) 032005. arXiv:hep-ex/0402021.

[206] O. J. P. Eboli, M. C. Gonzalez-Garcia, S. M. Lietti, S. F. Novaes, Anomalous quartic gauge boson couplings at hadron colliders, Phys. Rev. D63 (2001) 075008. arXiv:hep-ph/0009262.

[207] P. J. Bell, Quartic gauge couplings and the radiation zero in $pp \to l\nu\gamma\gamma$ events at the LHC, Eur. Phys. J. C64 (2009) 25–33. arXiv:0907.5299.

[208] E. Chapon, O. Kepka, C. Royon, Anomalous $WW\gamma$ couplings in two-photon processes at high luminosity at the LHC, arXiv:0912.5161.

[209] O. Kepka, C. Royon, Anomalous $WW\gamma$ coupling in photon-induced processes using forward detectors at the LHC, Phys. Rev. D78 (2008) 073005. arXiv:0808.0322.

[210] K. Piotrzkowski, N. Schul, Two-photon exclusive production of supersymmetric pairs at the LHC. arXiv:0910.0202.

[211] G. Bhattacharya, P. Kalyniak, K. A. Peterson, Photon and Z induced heavy charged lepton pair production at a hadron supercollider, Phys. Rev. D53 (1996) 2371–2379. arXiv:hep-ph/9512255.

[212] M. Drees, R. M. Godbole, M. Nowakowski, S. D. Rindani, $\gamma\gamma$ processes at high-energy pp colliders, Phys. Rev. D50 (1994) 2335–2338. arXiv:hep-ph/9403368.

[213] M. Battaglia, et al., Updated post-WMAP benchmarks for supersymmetry, Eur. Phys. J. C33 (2004) 273–296. arXiv:hep-ph/0306219.

[214] A. Pukhov, Calchep 2.3: MSSM, structure functions, event generation, batches, and generation of matrix elements for other packages, arXiv:hep-ph/0412191.

[215] J. de Favereau, X. Rouby, K. Piotrzkowski, Hector, a fast simulator for the transport of particles in beamlines, JINST 2 (2007) P09005. arXiv:0707.1198.

[216] A. Rybarska, W. Schäfer, A. Szczurek, Exclusive photoproduction of upsilon: From HERA to Tevatron, Phys. Lett. B668 (2008) 126–132. arXiv:0805.0717.

[217] A. Bzdak, L. Motyka, L. Szymanowski, J. R. Cudell, Exclusive J/psi and Upsilon hadroproduction and the QCD odderon, Phys. Rev. D75 (2007) 094023. arXiv:hep-ph/0702134.

[218] V. P. Goncalves, M. V. T. Machado, Quarkonium production in coherent hadron-hadron interactions at the LHC, Phys. Rev. D77 (2008) 014037. arXiv:0707.2523.

[219] B. E. Cox, J. R. Forshaw, R. Sandapen, Diffractive Υ production at the LHC, JHEP 06 (2009) 034. arXiv:0905.0102.

[220] V. A. Khoze, A. D. Martin, M. G. Ryskin, Photon exchange processes at hadron colliders as a probe of the dynamics of diffraction, Eur. Phys. J. C24 (2002) 459–468. arXiv:hep-ph/0201301.